

QM for AMOP

Chapter 24

Angular Momentum Coupling and Tensor Operators

W. G. Harter

The quantum mechanics of coupled angular momentum states are developed. The development begins with the simplest example of two spin-1/2 particles and spin-spin interaction for atomic hydrogen hyperfine states obtained by Clebsch-Gordan coupling and their 21-centimeter resonance used by astronomers to gauge free H-atom population. Non-relativistic electron spin-spin and spin-orbit coupling models are introduced. The boson algebraic derivation in Chapter 23 of Wigner-D functions is extended to derive CG and Wigner 3j coefficients as we continue to develop Clebsch-Gordan-Wigner angular momentum calculus. Examples of R(3) subgroup CG coefficients are also derived .

Chapter 24. Angular Momentum Coupling and Tensor Operators 1

24.1 Angular Momentum States and Atomic Level Structure	1
a. Spin-spin $(1/2)_2$ product states: Hydrogen hyperfine structure	1
Spin-spin interaction reduces symmetry $R(3)_p \times R(3)_e$ to $R(3)_p \otimes R(3)_e$	2
Reduced symmetry reduces representation $D_{1/2} \otimes D_{1/2}$ to $D_1 \oplus D_0$	3
Reduced representation $D_1 \oplus D_0$ implies singlet-triplet splitting	6
Comparing singlet-triplet and NMR-ESR states: Entanglement	9
b. Two-Electron Atomic Configurations	14
Orbital states $p \otimes p = D \oplus P \oplus S$	14
Spin-S states to match orbital-L states: Pauli-Fermi-Dirac exclusion-symmetry rules	15
c. Spin-Orbital Coupling	17
d. Angular-momentum cones and vector coupling models	21
Anomalous magnetic moments and g-factors	23
24.2 Symmetry Properties of CGC and Wigner 3j Coefficients	25
a. Scalars, Vectors, and Tensors	25
b. The general R_3 scalar coupling	27
c. CGC Definitions and Symmetry Relations: The Wigner 3j Coefficient	29
Point symmetry group coupling coefficients	32
24.3 Clebsch-Gordon and Wigner Coefficient Formulas	37
a. The A-and-B-Boson states	37
b. Scalar “no-count” states	41
c. N-Boson coupled momentum states	41
Appendix 24A Classical theory for spin-interactions and fine structure	1
Electronic-nuclear-orbit-spin interaction	2
Electronic-nuclear spin-spin interaction	2
Electronic-spin-orbit interaction	5

Chapter 24. Angular Momentum Coupling and Tensor Operators

24.1 Angular Momentum States and Atomic Level Structure

The electron and the proton each have a spin-1/2 and a magnetic moment. As has become customary in this text, we begin by describing the finest spectral details first, namely, electron-proton spin-spin interaction as an example of coupling and symmetry and the simplest example of *hyperfine* spectra. Then atomic orbit-orbit and spin-orbit coupling and atomic *fine structure* is introduced

Proton-electron spin-spin interaction is very weak compared to other atomic forces such as the Coulomb attraction that binds the lowest energy states of H. This allows us to focus on just the spin states of the proton nucleus and electron fixed in a zero-orbit (1s) ground state. Details of H-orbital states $1s, 2s, 2p, 3s, 3p, 3d, \dots$ are treated in Chapter 26 but are not needed for the approximations used here.

a. Spin-spin (1/2)² product states: Hydrogen hyperfine structure

Without spin-spin interaction the following four outer \otimes -product “ket-ket” states would be degenerate eigenstates. Such products were introduced in Section 21.1 equation (21.1.12) as a 2D harmonic oscillator basis. The relevant ket-kets are listed below just for the fundamental spin-up and spin-down states.

$$|\uparrow\rangle|\uparrow\rangle = \begin{pmatrix} \frac{1}{2} \\ \frac{1}{2} \end{pmatrix}^{\text{proton}} \begin{pmatrix} \frac{1}{2} \\ \frac{1}{2} \end{pmatrix}^{\text{electron}}, \quad |\uparrow\rangle|\downarrow\rangle = \begin{pmatrix} \frac{1}{2} \\ \frac{1}{2} \end{pmatrix}^{\text{proton}} \begin{pmatrix} \frac{1}{2} \\ -\frac{1}{2} \end{pmatrix}^{\text{electron}}, \quad |\downarrow\rangle|\uparrow\rangle = \begin{pmatrix} \frac{1}{2} \\ -\frac{1}{2} \end{pmatrix}^{\text{proton}} \begin{pmatrix} \frac{1}{2} \\ \frac{1}{2} \end{pmatrix}^{\text{electron}}, \quad |\downarrow\rangle|\downarrow\rangle = \begin{pmatrix} \frac{1}{2} \\ -\frac{1}{2} \end{pmatrix}^{\text{proton}} \begin{pmatrix} \frac{1}{2} \\ -\frac{1}{2} \end{pmatrix}^{\text{electron}}$$

The column matrix representations of each ket-ket are the following.

$$\begin{pmatrix} 1 \\ 0 \end{pmatrix} \otimes \begin{pmatrix} 1 \\ 0 \end{pmatrix} = \begin{pmatrix} 1 \\ 0 \\ 0 \\ 0 \end{pmatrix}, \quad \begin{pmatrix} 1 \\ 0 \end{pmatrix} \otimes \begin{pmatrix} 0 \\ 1 \end{pmatrix} = \begin{pmatrix} 0 \\ 1 \\ 0 \\ 0 \end{pmatrix}, \quad \begin{pmatrix} 0 \\ 1 \end{pmatrix} \otimes \begin{pmatrix} 1 \\ 0 \end{pmatrix} = \begin{pmatrix} 0 \\ 0 \\ 1 \\ 0 \end{pmatrix}, \quad \begin{pmatrix} 0 \\ 1 \end{pmatrix} \otimes \begin{pmatrix} 0 \\ 1 \end{pmatrix} = \begin{pmatrix} 0 \\ 0 \\ 0 \\ 1 \end{pmatrix}.$$

For zero interaction we may rotate either spin independently without varying energy. This is done using spin-1/2 representation $D_{m,n}^{1/2}(\alpha\beta\gamma) = \langle \frac{1}{2} \mathbf{R}(\alpha\beta\gamma) | \frac{1}{2} \rangle$ applied in turn to proton and electron kets.

$$D^{1/2}(\alpha\beta\gamma) = \begin{pmatrix} D_{+1/2,+1/2}^{1/2} & D_{+1/2,-1/2}^{1/2} \\ D_{-1/2,+1/2}^{1/2} & D_{-1/2,-1/2}^{1/2} \end{pmatrix} = \begin{pmatrix} e^{-\frac{i(\alpha+\gamma)}{2}} \cos \frac{\beta}{2} & -e^{-\frac{i(\alpha-\gamma)}{2}} \sin \frac{\beta}{2} \\ e^{\frac{i(\alpha-\gamma)}{2}} \sin \frac{\beta}{2} & e^{\frac{i(\alpha+\gamma)}{2}} \cos \frac{\beta}{2} \end{pmatrix} \quad (10.A.1)_{\text{repeated}}$$

$$\begin{aligned}
\mathbf{R}(\alpha_p \beta_p \gamma_p) \begin{vmatrix} \frac{1}{2} \\ +\frac{1}{2} \end{vmatrix}^p &= D_{+1/2,+1/2}^{1/2} \begin{vmatrix} \frac{1}{2} \\ +\frac{1}{2} \end{vmatrix}^p + D_{-1/2,+1/2}^{1/2} \begin{vmatrix} \frac{1}{2} \\ -\frac{1}{2} \end{vmatrix}^p & \mathbf{R}(\alpha_e \beta_e \gamma_e) \begin{vmatrix} \frac{1}{2} \\ +\frac{1}{2} \end{vmatrix}^e &= D_{+1/2,+1/2}^{1/2} \begin{vmatrix} \frac{1}{2} \\ +\frac{1}{2} \end{vmatrix}^e + D_{-1/2,+1/2}^{1/2} \begin{vmatrix} \frac{1}{2} \\ -\frac{1}{2} \end{vmatrix}^e \\
\mathbf{R}(\alpha_p \beta_p \gamma_p) \begin{vmatrix} \frac{1}{2} \\ -\frac{1}{2} \end{vmatrix}^p &= D_{+1/2,-1/2}^{1/2} \begin{vmatrix} \frac{1}{2} \\ +\frac{1}{2} \end{vmatrix}^p + D_{-1/2,-1/2}^{1/2} \begin{vmatrix} \frac{1}{2} \\ -\frac{1}{2} \end{vmatrix}^p & \mathbf{R}(\alpha_e \beta_e \gamma_e) \begin{vmatrix} \frac{1}{2} \\ -\frac{1}{2} \end{vmatrix}^e &= D_{+1/2,-1/2}^{1/2} \begin{vmatrix} \frac{1}{2} \\ +\frac{1}{2} \end{vmatrix}^e + D_{-1/2,-1/2}^{1/2} \begin{vmatrix} \frac{1}{2} \\ -\frac{1}{2} \end{vmatrix}^e
\end{aligned} \quad \text{Each}$$

rotation uses the same $U(2)$ representation matrix of equation (10.A.1) but proton angles $(\alpha_p, \beta_p, \gamma_p)$ may differ from $(\alpha_e, \beta_e, \gamma_e)$ for the electron. The result is an *outer product symmetry* $U(2)^{\text{proton}} \times U(2)^{\text{electron}}$.

Each operator ($\mathbf{R}^{\text{proton}}$, $\mathbf{R}^{\text{electron}}$) is a \times -product of two parts: $\mathbf{R}^{\text{proton}}$ operates only on proton kets while $\mathbf{R}^{\text{electron}}$ operates only on electron kets. This makes a *Kronecker product* $D^{\frac{1}{2}} \otimes D^{\frac{1}{2}}$ matrix representation. Kronecker

product components are $D_{m'_p m_p}^{\frac{1}{2}}(0 \beta_p 0) D_{m'_e m_e}^{\frac{1}{2}}(0 \beta_e 0) = D_{m'_p m_p}^{\frac{1}{2}} \otimes D_{m'_e m_e}^{\frac{1}{2}}$.

$$D^{\frac{1}{2}} \otimes D^{\frac{1}{2}} = \quad (24.1.2)$$

$$\begin{pmatrix} D_{\frac{1}{2} \frac{1}{2}}^{\frac{1}{2}}(\beta_p) & D_{\frac{1}{2} -\frac{1}{2}}^{\frac{1}{2}}(\beta_p) \\ D_{-\frac{1}{2} \frac{1}{2}}^{\frac{1}{2}}(\beta_p) & D_{-\frac{1}{2} -\frac{1}{2}}^{\frac{1}{2}}(\beta_p) \end{pmatrix} \otimes \begin{pmatrix} D_{\frac{1}{2} \frac{1}{2}}^{\frac{1}{2}}(\beta_e) & D_{\frac{1}{2} -\frac{1}{2}}^{\frac{1}{2}}(\beta_e) \\ D_{-\frac{1}{2} \frac{1}{2}}^{\frac{1}{2}}(\beta_e) & D_{-\frac{1}{2} -\frac{1}{2}}^{\frac{1}{2}}(\beta_e) \end{pmatrix} = \begin{pmatrix} D_{\frac{1}{2} \frac{1}{2}}^{\frac{1}{2}} D_{\frac{1}{2} \frac{1}{2}}^{\frac{1}{2}} & D_{\frac{1}{2} \frac{1}{2}}^{\frac{1}{2}} D_{\frac{1}{2} -\frac{1}{2}}^{\frac{1}{2}} & D_{\frac{1}{2} -\frac{1}{2}}^{\frac{1}{2}} D_{\frac{1}{2} \frac{1}{2}}^{\frac{1}{2}} & D_{\frac{1}{2} -\frac{1}{2}}^{\frac{1}{2}} D_{\frac{1}{2} -\frac{1}{2}}^{\frac{1}{2}} \\ D_{\frac{1}{2} \frac{1}{2}}^{\frac{1}{2}} D_{\frac{1}{2} \frac{1}{2}}^{\frac{1}{2}} & D_{\frac{1}{2} \frac{1}{2}}^{\frac{1}{2}} D_{\frac{1}{2} -\frac{1}{2}}^{\frac{1}{2}} & D_{\frac{1}{2} -\frac{1}{2}}^{\frac{1}{2}} D_{\frac{1}{2} \frac{1}{2}}^{\frac{1}{2}} & D_{\frac{1}{2} -\frac{1}{2}}^{\frac{1}{2}} D_{\frac{1}{2} -\frac{1}{2}}^{\frac{1}{2}} \\ D_{-\frac{1}{2} \frac{1}{2}}^{\frac{1}{2}} D_{\frac{1}{2} \frac{1}{2}}^{\frac{1}{2}} & D_{-\frac{1}{2} \frac{1}{2}}^{\frac{1}{2}} D_{\frac{1}{2} -\frac{1}{2}}^{\frac{1}{2}} & D_{-\frac{1}{2} -\frac{1}{2}}^{\frac{1}{2}} D_{\frac{1}{2} \frac{1}{2}}^{\frac{1}{2}} & D_{-\frac{1}{2} -\frac{1}{2}}^{\frac{1}{2}} D_{\frac{1}{2} -\frac{1}{2}}^{\frac{1}{2}} \\ D_{-\frac{1}{2} \frac{1}{2}}^{\frac{1}{2}} D_{-\frac{1}{2} \frac{1}{2}}^{\frac{1}{2}} & D_{-\frac{1}{2} \frac{1}{2}}^{\frac{1}{2}} D_{-\frac{1}{2} -\frac{1}{2}}^{\frac{1}{2}} & D_{-\frac{1}{2} -\frac{1}{2}}^{\frac{1}{2}} D_{-\frac{1}{2} \frac{1}{2}}^{\frac{1}{2}} & D_{-\frac{1}{2} -\frac{1}{2}}^{\frac{1}{2}} D_{-\frac{1}{2} -\frac{1}{2}}^{\frac{1}{2}} \end{pmatrix}$$

For example, with just the y-rotation Euler angles β_p and β_e , the Kronecker matrix is as follows.

$$\begin{pmatrix} \cos \frac{\beta_p}{2} & -\sin \frac{\beta_p}{2} \\ \sin \frac{\beta_p}{2} & \cos \frac{\beta_p}{2} \end{pmatrix} \otimes \begin{pmatrix} \cos \frac{\beta_e}{2} & -\sin \frac{\beta_e}{2} \\ \sin \frac{\beta_e}{2} & \cos \frac{\beta_e}{2} \end{pmatrix} = \begin{pmatrix} \cos \frac{\beta_p}{2} \cos \frac{\beta_e}{2} & -\cos \frac{\beta_p}{2} \sin \frac{\beta_e}{2} & -\sin \frac{\beta_p}{2} \cos \frac{\beta_e}{2} & \sin \frac{\beta_p}{2} \sin \frac{\beta_e}{2} \\ \cos \frac{\beta_p}{2} \sin \frac{\beta_e}{2} & \cos \frac{\beta_p}{2} \cos \frac{\beta_e}{2} & -\sin \frac{\beta_p}{2} \sin \frac{\beta_e}{2} & -\sin \frac{\beta_p}{2} \cos \frac{\beta_e}{2} \\ \sin \frac{\beta_p}{2} \cos \frac{\beta_e}{2} & -\sin \frac{\beta_p}{2} \sin \frac{\beta_e}{2} & \cos \frac{\beta_p}{2} \cos \frac{\beta_e}{2} & -\cos \frac{\beta_p}{2} \sin \frac{\beta_e}{2} \\ \sin \frac{\beta_p}{2} \sin \frac{\beta_e}{2} & \sin \frac{\beta_p}{2} \cos \frac{\beta_e}{2} & \cos \frac{\beta_p}{2} \sin \frac{\beta_e}{2} & \cos \frac{\beta_p}{2} \cos \frac{\beta_e}{2} \end{pmatrix}$$

The cross-product matrix (24.12) is an irreducible representation of the cross-product $R_3 \times R_3$ group.

Spin-spin interaction reduces symmetry $R(3)_p \times R(3)_e$ to $R(3)_{pe}$

If electron and proton spins are coupled then operator $[\mathbf{R}(\alpha_p \beta_p \gamma_p), \mathbf{R}(\alpha_e \beta_e \gamma_e)]$ is no longer a symmetry operator unless $\alpha_p = \alpha_e$, $\beta_p = \beta_e$, and $\gamma_p = \gamma_e$ because only “rigid” rotations preserve the *relative* orientation of the two spins and are still symmetry operators. Rotation operators such as

$$\left(\mathbf{R}(0\beta_p 0), \mathbf{R}(0\beta_e 0)\right) = e^{-i\beta_p \mathbf{J}_y^{\text{proton}}} e^{-i\beta_e \mathbf{J}_y^{\text{electron}}} \quad (24.1.3)$$

are generated by individual angular-momentum operators J_y^{proton} and J_y^{electron} but now must be multiplied by equal angles ($\beta_p = \beta_e \equiv \beta_{ep}$). With equal angles the rigid rotation about the y -axis simplifies as follows.

$$\left(\mathbf{R}(0\beta_{ep} 0), \mathbf{R}(0\beta_{ep} 0)\right) = e^{-i\beta_{ep} \mathbf{J}_y^{\text{proton}}} e^{-i\beta_{ep} \mathbf{J}_y^{\text{electron}}} = e^{-i\beta_{ep} (\mathbf{J}_y^{\text{proton}} + \mathbf{J}_y^{\text{electron}})} = e^{-i\beta_{ep} (\mathbf{J}_y^{\text{total}})} \quad (24.1.4)$$

The *total* angular momentum is a symmetry operator generator. Individual spin momentum of each proton or electron may no longer be conserved by an interaction, but total momentum is still constant.

$$\mathbf{J}^{\text{total}} = \mathbf{J}^{\text{proton}} + \mathbf{J}^{\text{electron}} \quad (24.1.5)$$

By total momentum we mean here total spin angular momentum $\mathbf{J} = \mathbf{S}$. The orbital momentum of the H s -state electron is zero here. Spin-orbit and orbit-orbit interactions will be introduced later.

Reduced symmetry reduces representation $D^{1/2} \otimes D^{1/2}$ to $D^1 \oplus D^0$

The Kronecker product $D^{\frac{1}{2}} \otimes D^{\frac{1}{2}}$ (Recall (24.1.2).) is an irreducible representation (irrep) of $R_3 \times R_3$, but it is a reducible representation of the reduced symmetry generated by J^{total} operators. The following transformation (which we derive shortly) of the matrix $D^{\frac{1}{2}} \otimes D^{\frac{1}{2}}$ shows how (24.1.2) reduces when only rigid rotations ($(\beta_p = \beta_e \equiv \beta)$, etc.) are allowed.

$$\begin{pmatrix} 1 & 0 & 0 & 0 \\ 0 & \frac{1}{\sqrt{2}} & \frac{1}{\sqrt{2}} & 0 \\ 0 & 0 & 0 & 1 \\ 0 & \frac{1}{\sqrt{2}} & -\frac{1}{\sqrt{2}} & 0 \end{pmatrix} \begin{pmatrix} \cos^2 \frac{\beta}{2} & -\sin \frac{\beta}{2} \cos \frac{\beta}{2} & -\sin \frac{\beta}{2} \cos \frac{\beta}{2} & \sin^2 \frac{\beta}{2} \\ \sin \frac{\beta}{2} \cos \frac{\beta}{2} & \cos^2 \frac{\beta}{2} & -\sin^2 \frac{\beta}{2} & -\sin \frac{\beta}{2} \cos \frac{\beta}{2} \\ \sin \frac{\beta}{2} \cos \frac{\beta}{2} & -\sin^2 \frac{\beta}{2} & \cos^2 \frac{\beta}{2} & -\sin \frac{\beta}{2} \cos \frac{\beta}{2} \\ \sin^2 \frac{\beta}{2} & \sin \frac{\beta}{2} \cos \frac{\beta}{2} & \sin \frac{\beta}{2} \cos \frac{\beta}{2} & \cos^2 \frac{\beta}{2} \end{pmatrix} \begin{pmatrix} 1 & 0 & 0 & 0 \\ 0 & \frac{1}{\sqrt{2}} & 0 & \frac{1}{\sqrt{2}} \\ 0 & \frac{1}{\sqrt{2}} & 0 & -\frac{1}{\sqrt{2}} \\ 0 & 0 & 1 & 0 \end{pmatrix} \\ = \begin{pmatrix} \sin^2 \frac{\beta}{2} & \frac{-\sin \beta}{\sqrt{2}} & \sin^2 \frac{\beta}{2} & 0 \\ \frac{\sin \beta}{\sqrt{2}} & \cos \beta & \frac{-\sin \beta}{\sqrt{2}} & 0 \\ \sin^2 \frac{\beta}{2} & \frac{\sin \beta}{\sqrt{2}} & \cos^2 \frac{\beta}{2} & 0 \\ 0 & 0 & 0 & 1 \end{pmatrix} \quad (24.1.6a)$$

In matrix notation this is the following. Note that the D^I above agrees with D^I in (23.1.15c).

$$C \cdot D^{\frac{1}{2}}(0\beta 0) \otimes D^{\frac{1}{2}}(0\beta 0) \cdot C = \left(\begin{array}{c|c} D^1(0\beta 0) & \begin{matrix} 0 \\ 0 \\ 0 \end{matrix} \\ \hline \begin{matrix} 0 & 0 & 0 \end{matrix} & D^0 \end{array} \right) = D^1 \oplus D^0. \quad (24.1.6b)$$

Standard index notation for this block transformation is shown below.

$$\sum_{m_1 m_1' m_2 m_2'} C_{m_1 m_1' M}^{\frac{1}{2} \frac{1}{2} J} D_{m_1 m_2}^{\frac{1}{2}} D_{m_1' m_2'}^{\frac{1}{2}} C_{m_2 m_2' M'}^{\frac{1}{2} \frac{1}{2} J'} = \delta^{JJ'} D_{M M'}^J \quad (24.1.6c)$$

Here the transformation matrix components are called *Clebsch-Gordan (CG) coefficients* or *CGC*.

$$C_{m_p m_e M}^{\frac{1}{2} \frac{1}{2} J} \equiv \left\langle \begin{array}{c} \frac{1}{2} \quad \frac{1}{2} \\ m_p \quad m_e \end{array} \middle| \begin{array}{c} J \\ M \end{array} \right\rangle \quad (24.1.6d)$$

CGC combine ket-kets into single kets of definite total-momentum quantum J and z -component M .

$$\left| \begin{array}{c} J \\ M \end{array} \right\rangle^{\left(\frac{1}{2} \otimes \frac{1}{2}\right)} = \sum_{m_p, m_e} \left| \begin{array}{c} \frac{1}{2} \quad \frac{1}{2} \\ m_p \quad m_e \end{array} \right\rangle \left\langle \begin{array}{c} \frac{1}{2} \quad \frac{1}{2} \\ m_p \quad m_e \end{array} \middle| \begin{array}{c} J \\ M \end{array} \right\rangle = \sum_{m_p, m_e} C_{m_p m_e M}^{\frac{1}{2} \frac{1}{2} J} \left| \begin{array}{c} \frac{1}{2} \quad \frac{1}{2} \\ m_p \quad m_e \end{array} \right\rangle \quad (24.1.6e)$$

Also, CGC reduce the product representation $D^{\frac{1}{2}} \otimes D^{\frac{1}{2}}$ of R_3^{Rigid} symmetry as shown in (24.1.6). CGC are tabulated just as they appear in their transformation matrix. For example, (24.1.6a) is tabulated below.

$$\left\langle \begin{array}{c} \frac{1}{2} \quad \frac{1}{2} \\ \cdot \quad \cdot \end{array} \middle| \cdot \right\rangle = \begin{array}{|c|c|c|c|} \hline j_1 = \frac{1}{2} & \otimes & j_2 = \frac{1}{2} & \begin{array}{c} J=1 \\ M=1 \end{array} \\ \hline m_1 = \frac{1}{2} & & m_2 = \frac{1}{2} & \begin{array}{ccc} 1 & 1 & 1 \\ 0 & 0 & -1 \end{array} \\ \hline +\frac{1}{2} & & -\frac{1}{2} & \begin{array}{ccc} \cdot & \frac{1}{\sqrt{2}} & \cdot \\ \cdot & \frac{1}{\sqrt{2}} & \cdot \\ \cdot & \cdot & 1 \end{array} \\ \hline -\frac{1}{2} & & +\frac{1}{2} & \begin{array}{ccc} \cdot & \frac{1}{\sqrt{2}} & \cdot \\ \cdot & \cdot & 1 \end{array} \\ \hline -\frac{1}{2} & & -\frac{1}{2} & \begin{array}{ccc} \cdot & \cdot & 1 \\ \cdot & \cdot & 1 \end{array} \\ \hline \end{array} \quad (24.1.7)$$

More general derivation of coupling coefficients can be done by appealing to the generators

$J_z^{\text{total}} = J_z^{\text{particle 1}} + J_z^{\text{particle 2}}$ and $J_{\pm}^{\text{total}} = J_{\pm}^{\text{particle 1}} + J_{\pm}^{\text{particle 2}}$. First, J_z^{total} is applied to a general coupled ket made of

particle-1 of spin j_1 and particle-2 of spin j_2 , that is, like (24.1.6) but with general spin values j_1 and j_2 .

$$\left| \begin{matrix} J \\ M \end{matrix} \begin{matrix} (j_1 \otimes j_2) \end{matrix} \right\rangle = \sum_{m_1, m_2} C_{m_1 m_2 M}^{j_1 j_2 J} \left| \begin{matrix} j_1 j_2 \\ m_1 m_2 \end{matrix} \right\rangle \quad (24.1.8a)$$

Each z -component operator sidles up to its respective eigenstate and yields its m -eigenvalue.

$$\begin{aligned} J_z^{total} \left| \begin{matrix} J \\ M \end{matrix} \begin{matrix} (j_1 \otimes j_2) \end{matrix} \right\rangle &= \sum_{m_1, m_2} C_{m_1 m_2 M}^{j_1 j_2 J} J_z^{total} \left| \begin{matrix} j_1 j_2 \\ m_1 m_2 \end{matrix} \right\rangle = M \left| \begin{matrix} J \\ M \end{matrix} \begin{matrix} (j_1 \otimes j_2) \end{matrix} \right\rangle = M \sum_{m_1, m_2} C_{m_1 m_2 M}^{j_1 j_2 J} \left| \begin{matrix} j_1 j_2 \\ m_1 m_2 \end{matrix} \right\rangle \\ \sum_{m_1, m_2} C_{m_1 m_2 M}^{j_1 j_2 J} \left(J_z^{particle1} \left| \begin{matrix} j_1 \\ m_1 \end{matrix} \right\rangle \left| \begin{matrix} j_2 \\ m_2 \end{matrix} \right\rangle + \left| \begin{matrix} j_1 \\ m_1 \end{matrix} \right\rangle J_z^{particle2} \left| \begin{matrix} j_2 \\ m_2 \end{matrix} \right\rangle \right) &= \sum_{m_1, m_2} C_{m_1 m_2 M}^{j_1 j_2 J} (m_1 + m_2) \left| \begin{matrix} j_1 j_2 \\ m_1 m_2 \end{matrix} \right\rangle \end{aligned} \quad (24.1.8b)$$

Product states are orthonormal and so (24.1.8) implies $C_{m_1 m_2 M}^{j_1 j_2 J} = 0$ unless $M = m_1 + m_2$.

$$\left\langle \begin{matrix} j_1 j_2 \\ m_1' m_2' \end{matrix} \left| \begin{matrix} j_1 j_2 \\ m_1 m_2 \end{matrix} \right\rangle = \left\langle \begin{matrix} j_1 \\ m_1' \end{matrix} \left| \begin{matrix} j_1 \\ m_1 \end{matrix} \right\rangle \left\langle \begin{matrix} j_2 \\ m_2' \end{matrix} \left| \begin{matrix} j_2 \\ m_2 \end{matrix} \right\rangle = \delta_{m_1' m_1} \delta_{m_2' m_2} \quad (24.1.8c)$$

The total z component M must be the sum of the z components of the factor states. The state with the highest momentum $M = m_1 + m_2 = J$ is made from factors j_1 and j_2 each of which has its highest possible m -value, namely,

$m_1 = j_1$ and $m_2 = j_2$, that is, if $M = j_1 + j_2 = J$, then we have $C_{j_1 j_2 j_1+j_2}^{j_1 j_2 J} = 1$.

$$\left| \begin{matrix} j_1 j_2 \\ j_1 j_2 \end{matrix} \right\rangle = \left| \begin{matrix} J=j_1+j_2 \\ M=j_1+j_2 \end{matrix} \begin{matrix} (j_1 \otimes j_2) \end{matrix} \right\rangle. \quad (24.1.9)$$

The total lowering operator J_-^{total} is then applied to this highest state using relations (23.1.5c-d).

$$\begin{aligned} J_-^{total} \left| \begin{matrix} J \\ J \end{matrix} \begin{matrix} (j_1 \otimes j_2) \end{matrix} \right\rangle &= J_-^{particle1} \left| \begin{matrix} j_1 \\ j_1 \end{matrix} \right\rangle J_-^{particle2} \left| \begin{matrix} j_2 \\ j_2 \end{matrix} \right\rangle, \\ \sqrt{2(j_1 + j_2)} \left| \begin{matrix} J \\ J-1 \end{matrix} \begin{matrix} (j_1 \otimes j_2) \end{matrix} \right\rangle &= \sqrt{2j_1} \left| \begin{matrix} j_1 \\ j_1-1 \end{matrix} \right\rangle \left| \begin{matrix} j_2 \\ j_2 \end{matrix} \right\rangle + \sqrt{2j_2} \left| \begin{matrix} j_1 \\ j_1 \end{matrix} \right\rangle \left| \begin{matrix} j_2 \\ j_2-1 \end{matrix} \right\rangle, \\ \left| \begin{matrix} J \\ J-1 \end{matrix} \begin{matrix} (j_1 \otimes j_2) \end{matrix} \right\rangle &= \sqrt{\frac{j_1}{j_1+j_2}} \left| \begin{matrix} j_1 \\ j_1-1 \end{matrix} \right\rangle \left| \begin{matrix} j_2 \\ j_2 \end{matrix} \right\rangle + \sqrt{\frac{j_2}{j_1+j_2}} \left| \begin{matrix} j_1 \\ j_1 \end{matrix} \right\rangle \left| \begin{matrix} j_2 \\ j_2-1 \end{matrix} \right\rangle, \end{aligned} \quad (24.1.10)$$

For example, the proton-electron problem has $j_1 = \frac{1}{2} = j_2$ and that yields the following.

$$\left| \begin{array}{c} J = 1 \\ \\ M = 0 \end{array} \left(\frac{1}{2} \otimes \frac{1}{2} \right) \right\rangle = \sqrt{\frac{1}{2}} \left| \begin{array}{c} \frac{1}{2} \quad \frac{1}{2} \\ -\frac{1}{2} \quad +\frac{1}{2} \end{array} \right\rangle + \sqrt{\frac{1}{2}} \left| \begin{array}{c} \frac{1}{2} \quad \frac{1}{2} \\ +\frac{1}{2} \quad -\frac{1}{2} \end{array} \right\rangle \quad (24.1.10) \text{ example}$$

This is in the 2nd-column of the table of (24.1.7). Applying J_-^{total} again gives the 3rd-column state

$$\left| \begin{array}{c} J = 1 \\ \\ M = -1 \end{array} \left(\frac{1}{2} \otimes \frac{1}{2} \right) \right\rangle = \left| \begin{array}{c} \frac{1}{2} \quad \frac{1}{2} \\ -\frac{1}{2} \quad -\frac{1}{2} \end{array} \right\rangle.$$

Finally, the 4th-column state results by making it normal to the 2nd-column ($J=1, M=0$) state (24.1.10)_{ex}. The result is the ($J=0, M=0$)-*singlet* state of the Hydrogen hyperfine level spectrum.

$$\left| \begin{array}{c} J = 0 \\ \\ M = 0 \end{array} \left(\frac{1}{2} \otimes \frac{1}{2} \right) \right\rangle = e^{i\phi} \left(\sqrt{\frac{1}{2}} \left| \begin{array}{c} \frac{1}{2} \quad \frac{1}{2} \\ -\frac{1}{2} \quad +\frac{1}{2} \end{array} \right\rangle - \sqrt{\frac{1}{2}} \left| \begin{array}{c} \frac{1}{2} \quad \frac{1}{2} \\ +\frac{1}{2} \quad -\frac{1}{2} \end{array} \right\rangle \right) \quad (24.1.11)$$

The result is defined only up to an overall phase factor $e^{i\phi}$. In this case the phase is conventionally chosen to be $e^{i\pi} = -1$. At first, phase conventions for CGC seem arbitrary and capricious. In Sec. 24.2 we make them seem less arbitrary by deriving relations between $C_{m_1 m_2 M}^{j_1 j_2 J}$, $C_M^{j_1 j_2}$ and $C_{m_1 M m_2}^{j_1 j_2}$.

Reduced representation $D^1 \oplus D^0$ implies singlet-triplet splitting

This reduction of a four-by-four representation $D^{\frac{1}{2}} \otimes D^{\frac{1}{2}}$ to a three-by-three “vector” irrep D^1 and a one-by-one “scalar” irrep D^0 implies a splitting of the four spin energy levels of Hydrogen into a ($J=1$) “triplet” and a ($J=0$) “singlet,” as shown in Figure 24.1.1 on the following page.

The observed magnitude of this splitting is small, but very important to radio astronomers. It is one of the more precisely measured quantities: $1,420,405,751.8 \pm 0.03$ Hz or approximate equivalents 5.88×10^{-5} eV; 0.0474 cm⁻¹, or $1/(21.2$ cm). It is the well-known 21-cm line that is used to locate atomic Hydrogen in intergalactic space. This is described by the *Fermi spin-spin contact interaction* Hamiltonian.

$$H_{contact} = a_{ep} \mathbf{J}^{proton} \bullet \mathbf{J}^{electron} \quad (24.1.12a)$$

The name “contact” refers to a $\delta(0)$ -function interaction based on the value $\psi(0)$ of the electronic wave function at the location of the proton at origin. The classical theory is reviewed in Appendix 24A.

$$a_{ep} = (2\mu_0 / 3)g_e\beta_e g_p\beta_p |\psi(0)^2| \quad (\mu_0 = 4\pi \cdot 10^{-7} \text{N/Amp}^2) \quad (24.1.12b)$$

The electron Compton wavelength $\lambda_{Compton} = \hbar / 2m_e c = 2r_{Dirac}$ is greater than that of the proton by a factor of $m_p/m_e=1836$. As sketched in Fig. 5.4.2 and Appendix 24A, the electron “engulfs” the tiny proton. But, all that matters is Hydrogen (1s) wave function probability $|\psi_{1s}(0)|^2$ at the origin inside the tiny “belly” of the proton where the proton B-field is most monstrous. Hydrogen waves are described in Chapter 26.

$$|\psi_{1s}(0)|^2 = 1 / (\pi a_0^3) \quad (24.1.12c)$$

Potential energy of a magnetic dipole \mathbf{m} in a B-field has the form $-\mathbf{m} \cdot \mathbf{B}$. The proton’s dipole $\mathbf{m}=a_p\mathbf{J}$ points along its spin angular momentum vector \mathbf{J}^{proton} that then tends to line up with B. The electron’s dipole $\mathbf{m}=-a_e\mathbf{J}$ is opposite its spin $\mathbf{J}^{electron}$ so it tends to anti-align to B, which in this case is the proton’s B-field.

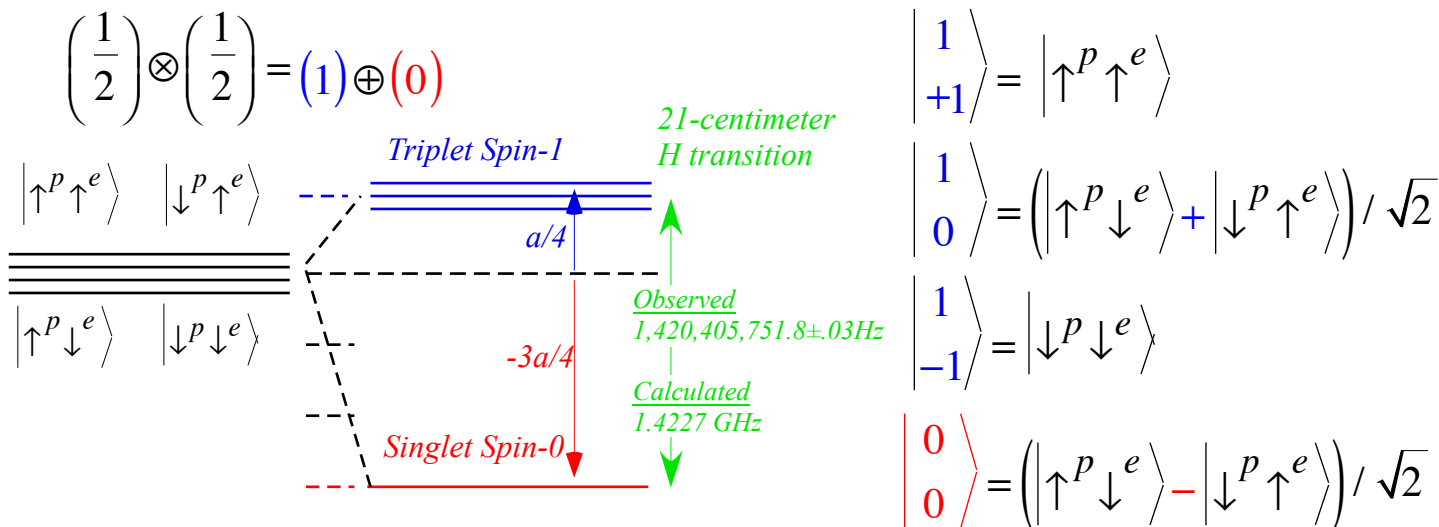


Fig. 24.1.1 21-cm Singlet-triplet splitting of levels for interacting spin-1/2 electron and proton.

The Bohr radius as given by (5.4.3) is $a_0 = \hbar^2 / m_e^2 = 0.5292 \times 10^{-10}$ m. The *g-factors* g_e ($=2.0023$) and g_p ($=5.585$) depend on internal structure of the electron and proton, respectively. Gyro-magnetic constants μ_e ($= \hbar / 2m_e = 9.27401 \cdot 10^{-24}$ Joule / Tesla) and μ_p ($= \hbar / 2m_p = 5.05078 \times 10^{-27}$ J / T) are *magneton moments* for the electron and proton, respectively, and vary inversely with rest mass. Classical development of the g and μ

constants is presented in Appendix 24A. (See Tables after (24.1.18). More rigorous derivation of spin interaction involves the Dirac algebra and will be discussed in later units.)

The eigenvalues of the contact interaction are easy to find if it is rewritten in terms of operators that are diagonal in the bases of triplet and singlet states (24.1.10)_x and (24.1.11):

$$\begin{aligned} a_{ep} \mathbf{J}^{proton} \cdot \mathbf{J}^{electron} &= \frac{a_{ep}}{2} \left[(\mathbf{J}^{proton} + \mathbf{J}^{electron})^2 - (\mathbf{J}^{proton})^2 - (\mathbf{J}^{electron})^2 \right] \\ &= \frac{a_{ep}}{2} \left[(\mathbf{J}^{total})^2 - (\mathbf{J}^{proton})^2 - (\mathbf{J}^{electron})^2 \right]. \end{aligned} \quad (24.1.13)$$

This trick is often used to evaluate the eigenvalues of interaction operators as in the example here.

$$\begin{aligned} \left\langle \begin{matrix} J \\ M \end{matrix} \left(\frac{1}{2} \otimes \frac{1}{2} \right) \middle| H_{contact} \middle| \begin{matrix} J \\ M \end{matrix} \left(\frac{1}{2} \otimes \frac{1}{2} \right) \right\rangle &= \frac{a_{ep}}{2} \left[J(J+1) - \frac{1}{2} \left(\frac{1}{2} + 1 \right) - \frac{1}{2} \left(\frac{1}{2} + 1 \right) \right] \\ &= \begin{cases} a_{ep} / 4 & \text{for the } (J = 1) \text{ triplet state,} \\ -3a_{ep} / 4 & \text{for the } (J = 0) \text{ singlet state.} \end{cases} \end{aligned} \quad (24.1.14)$$

Note that the magnitude of the singlet-triplet splitting is equal to that of the interaction constant (a_{ep}). Substituting the magnetic constants given with Eq. (24.1.12) yields the following approximate value.

$$a_{ep} (\text{calculated}) = 1.4227 \text{ GHz.} \quad (24.1.15)$$

This agrees with the observed value up to the third decimal place. Further theory of relativistic spin- $\frac{1}{2}$ particles is needed to get more accuracy. However, no theory so far can honestly be said to have the 10- or 11-place accuracy of the experiment since that is so far beyond our present accuracy of knowledge of fundamental constants other than c .

To continue the coupling analysis for more general values of angular momentum, one needs to finish the lowering job started in Eq. (24.1.10). After N lowering steps the result is

$$(J_-)^N \left| \begin{matrix} J = j_1 + j_2 \\ M = j_1 + j_2 \end{matrix} \right\rangle = \sum_{n_1, n_2=0}^N \frac{N!}{n_1! n_2!} (\mathbf{J}^{proton})^{n_1} \left| \begin{matrix} j_1 \\ j_1 \end{matrix} \right\rangle (\mathbf{J}^{electron})^{n_2} \left| \begin{matrix} j_2 \\ j_2 \end{matrix} \right\rangle,$$

where $N = n_1 + n_2$. Using Eq. (5.4.23b) repeatedly one obtains

$$(J_-)^n \left| \begin{matrix} j \\ m \end{matrix} \right\rangle = \sqrt{\frac{(j+m)!(j-m+n)!}{(j-m)!(j+m-n)!}} \left| \begin{matrix} j \\ m-n \end{matrix} \right\rangle. \quad (24.1.16)$$

This gives the desired result

$$\left| \begin{matrix} J = j_1 + j_2 \\ M = m_1 + m_2 \end{matrix} \right\rangle = \sum_{m_1, m_2} C_{m_1, m_2}^{j_1, j_2, J} \left| \begin{matrix} j_1, j_2 \\ m_1, m_2 \end{matrix} \right\rangle,$$

where the total momentum $J = j_1 + j_2$ and z-component $M = m_1 + m_2$ are maximal.

$$C_{m_1, m_2}^{j_1, j_2, j_1+j_2} = \sqrt{\frac{(J-M)!}{(j_1-m_1)!(j_2+m_2)!} \frac{(J+M)!}{((j_1+m_1)!(j_2+m_2)!)} \frac{(2j_1)!(2j_2)!}{(2J)!}}. \quad (24.1.17)$$

These are the coupling coefficients for the cases of highest total momentum $J = j_1 + j_2$. The coefficients for the other possibilities, $J = j_1 + j_2 - 1, j_1 + j_2 - 2, \dots, |j_1 - j_2|$ are obtained by orthogonalization, or by a generalization of Eq. (24.1.17) and derived in the following Section 24.2.

Comparing singlet-triplet and NMR-ESR states: Entanglement

Before considering more general coupling theory let us consider the quantum mechanics of the coupling process and the physical difference between “primitive” product states $|\uparrow\rangle|\uparrow\rangle, |\uparrow\rangle|\downarrow\rangle, |\downarrow\rangle|\uparrow\rangle, \text{ or } |\downarrow\rangle|\downarrow\rangle$ and the “coupled” product states, such as $(|\uparrow\rangle|\downarrow\rangle + |\downarrow\rangle|\uparrow\rangle) / \sqrt{2}$, that are *correlated* or *entangled* by Clebsch-Gordan coefficients. To do this we imagine an experiment in which correlated or coupled states are gradually transformed into primitive ones (or vice-versa) by changing an externally applied B-field. This could be done by a Hamiltonian that has Zeeman-Larmour magnetic moment interactions with an external B-field. Terms $a_p J^{proton}$ and $a_e J^{electron}$ are added to Fermi-contact interaction operator (24.1.2).

$$H_{1s-B\text{-field}} = -a_p B_z J_z^{proton} + a_e B_z J_z^{electron} + a_{ep} J^{proton} \bullet J^{electron} \quad (24.1.18)$$

The constants are repeated in the tables below and discussed in Appendix 24A.

	<i>g</i> – factor	Bohr – magneton	gyromagnetic factor	Fermi – contact factor	
<i>electron</i>	g_e $= 2.0023$	$\mu_e = \frac{e\hbar}{2m_e}$ $= 9.27401 \cdot 10^{-24} \frac{J}{T}$	$a_e = g_e \mu_e$ $= 1.8570 \cdot 10^{-23} \frac{J}{T}$	$a_{ep} = \mu_0 \frac{2}{3} \frac{1}{\pi a_0^3} a_e a_p = 9.427 \cdot 10^{-25} J$	
<i>proton</i>	g_p $= 5.585$	$\mu_p = \frac{e\hbar}{2m_p}$ $= 5.05078 \cdot 10^{-27} \frac{J}{T}$	$a_p = g_p \mu_p$ $= 2.8209 \cdot 10^{-26} \frac{J}{T}$	$\mu_0 \frac{2}{3} \frac{1}{\pi a_0^3} \frac{a_e a_p}{h} = 1.4227 \cdot 10^9 Hz$	
				$\mu_0 \frac{2}{3} \frac{1}{\pi a_0^3} \frac{a_e a_p}{hc} = 4.746 m^{-1}$	
				$= \frac{1}{21.1} cm^{-1}$	

Magnetic constant : $\mu_0 / 4\pi = 10^{-7} N / A^2$

The $H(l_s)$ -B-field energy (24.1.18) has Zeeman $-\mathbf{m} \cdot \mathbf{B} = g\mu B_z J_z$ interactions with an external B-field in the z direction. Primitive product states are eigenvectors of external $\mathbf{m} \cdot \mathbf{B}$ interactions while coupled states are eigenvectors of the internal Fermi-contact interaction.

The in-line-spin states $|^1_1\rangle = |\uparrow\rangle|\uparrow\rangle$ and $|^1_{-1}\rangle = |\downarrow\rangle|\downarrow\rangle$ are eigenvectors of both interactions so their eigenvalues are calculated immediately in either basis as shown below. But, a conflict exists between the anti-aligned $M=0$ states $|\uparrow\rangle|\downarrow\rangle$ or $|\downarrow\rangle|\uparrow\rangle$ versus correlated $|^1_0\rangle$ or $|^0_0\rangle$ states. As seen in the left hand matrix in the primitive $\{|\uparrow\rangle|\uparrow\rangle, |\uparrow\rangle|\downarrow\rangle, |\downarrow\rangle|\uparrow\rangle, |\downarrow\rangle|\downarrow\rangle\}$ representation below, the states $|\uparrow\rangle|\downarrow\rangle$ and $|\downarrow\rangle|\uparrow\rangle$ are eigenstates of the Zeeman operator, but $|\uparrow\rangle|\downarrow\rangle$ and $|\downarrow\rangle|\uparrow\rangle$ are not eigenstates of the Fermi-contact operator. The latter is diagonal in the representation that uses correlated bases $\{|^1_1\rangle, |^1_0\rangle, |^0_0\rangle, |^1_{-1}\rangle\}$ as shown below.

$$\langle -a_p B_z J_z^{proton} + a_e B_z J_z^{electron} \rangle =$$

	$ \uparrow^p \uparrow^e\rangle$	$ \uparrow^p \downarrow^e\rangle$	$ \downarrow^p \uparrow^e\rangle$	$ \downarrow^p \downarrow^e\rangle$
$\langle \uparrow^p \uparrow^e $	$\frac{1}{2}(a_e - a_p)B_z$.	.	.
$\langle \uparrow^p \downarrow^e $.	$\frac{-1}{2}(a_e + a_p)B_z$	0	.
$\langle \downarrow^p \uparrow^e $.	0	$\frac{1}{2}(a_e + a_p)B_z$.
$\langle \downarrow^p \downarrow^e $.	.	.	$\frac{-1}{2}(a_e - a_p)B_z$

$$\langle a_{ep} J^{proton} \bullet J^{electron} \rangle =$$

	$ \uparrow^p \uparrow^e\rangle$	$ \uparrow^p \downarrow^e\rangle$	$ \downarrow^p \uparrow^e\rangle$	$ \downarrow^p \downarrow^e\rangle$
$\langle \uparrow^p \uparrow^e $	$\frac{a_{ep}}{4}$.	.	.
$\langle \uparrow^p \downarrow^e $.	$\frac{-a_{ep}}{4}$	$\frac{a_{ep}}{2}$.
$\langle \downarrow^p \uparrow^e $.	$\frac{a_{ep}}{2}$	$\frac{-a_{ep}}{4}$.
$\langle \downarrow^p \downarrow^e $.	.	.	$\frac{a_{ep}}{4}$

Correlated $\{|^1_0\rangle, |^0_0\rangle\}$ are not Zeeman eigenstates but they do diagonalize the Fermi-contact operator.

$$\langle -a_p B_z J_z^{proton} + a_e B_z J_z^{electron} \rangle =$$

	$ 1\rangle$	$ 0\rangle$	$ 0\rangle$	$ 1\rangle$
$\langle 1 $	$\frac{1}{2}(a_e - a_p)B_z$.	.	.
$\langle 0 $.	0	$\frac{-1}{2}(a_e + a_p)B_z$.
$\langle 0 $.	$\frac{-1}{2}(a_e + a_p)B_z$	0	.
$\langle 1 $.	.	.	$\frac{-1}{2}(a_e - a_p)B_z$

$$\langle a_{ep} J^{proton} \bullet J^{electron} \rangle =$$

	$ 1\rangle$	$ 0\rangle$	$ 0\rangle$	$ 1\rangle$
$\langle 1 $	$\frac{a_{ep}}{4}$.	.	.
$\langle 0 $.	$\frac{a_{ep}}{4}$	0	.
$\langle 0 $.	0	$\frac{-3a_{ep}}{4}$.
$\langle 1 $.	.	.	$\frac{a_{ep}}{4}$

The Hamiltonian is a sum of Zeeman and Fermi-contact operators, and so energy states lie somewhere between the two extremes depending on the relative strength of the Zeeman $a_e B_z$ or $a_p B_z$ and Fermi a_{ep} . Note the following Clebsch-Gordan transformation (24.1.7) between the two extremes. It transforms the Zeeman 2-by-2 matrix from AD-symmetry to B-symmetry and vice-versa for the Fermi 2-by-2 matrix.

$$\begin{pmatrix} \frac{1}{\sqrt{2}} & \frac{1}{\sqrt{2}} \\ \frac{1}{\sqrt{2}} & \frac{-1}{\sqrt{2}} \end{pmatrix} \begin{pmatrix} -\frac{a_e + a_p}{2} B & 0 \\ 0 & \frac{a_e + a_p}{2} B \end{pmatrix} \begin{pmatrix} \frac{1}{\sqrt{2}} & \frac{1}{\sqrt{2}} \\ \frac{1}{\sqrt{2}} & \frac{-1}{\sqrt{2}} \end{pmatrix} = \begin{pmatrix} 0 & -\frac{a_e + a_p}{2} B \\ -\frac{a_e + a_p}{2} B & 0 \end{pmatrix}$$

$$\begin{pmatrix} \frac{1}{\sqrt{2}} & \frac{1}{\sqrt{2}} \\ \frac{1}{\sqrt{2}} & \frac{-1}{\sqrt{2}} \end{pmatrix} \begin{pmatrix} -\frac{a_{ep}}{4} & \frac{a_{ep}}{2} \\ \frac{a_{ep}}{2} & -\frac{a_{ep}}{4} \end{pmatrix} \begin{pmatrix} \frac{1}{\sqrt{2}} & \frac{1}{\sqrt{2}} \\ \frac{1}{\sqrt{2}} & \frac{-1}{\sqrt{2}} \end{pmatrix} = \begin{pmatrix} \frac{a_{ep}}{4} & 0 \\ 0 & -\frac{3a_{ep}}{4} \end{pmatrix}$$

We know the eigenvalues of each operator in its preferred basis, that is, the Zeeman values in the product basis $\{|\uparrow\rangle|\downarrow\rangle, |\downarrow\rangle|\uparrow\rangle\}$ and Fermi values (24.1.14) in the coupled basis $\{|0\rangle, |0\rangle\}$. A CGC transformation (24.1.7) then provides a simple way to evaluate each operator in the other basis. (Nevertheless, you should develop your raising-operator skills by evaluating each operator representation directly.)

We write the H-matrix in convenient form by defining a sum S and a difference D of moments.

$$S = 2(a_e + a_p) / a_{ep} \qquad D = 2(a_e - a_p) / a_{ep}$$

Then the eigenvalues take a form convenient for plotting in Fig. 24.1 2. The straight-line eigenvalues are

$$E(\uparrow^p \uparrow^e) = E_1^1 = \frac{a_{ep}}{4} (1 + DB_z), \qquad E(\downarrow^p \downarrow^e) = E_{-1}^1 = \frac{a_{ep}}{4} (1 - DB_z).$$

The hyperbolas are eigenvalues of the 2-by-2 matrix here rewritten in $a_{ep} / 4$ units.

$$\langle H(\uparrow\downarrow) \rangle = \begin{pmatrix} \frac{a_{ep}}{4} & -\frac{a_e + a_p}{2} B_z \\ -\frac{a_e + a_p}{2} B_z & -\frac{3a_{ep}}{4} \end{pmatrix} = \frac{a_{ep}}{4} \begin{pmatrix} 1 & -SB_z \\ -SB_z & -3 \end{pmatrix}$$

Low- B_z eigenvalues split like B_z^2 . Then they approach straight-line asymptotes as the B_z -field increases.

$$E_{\pm} = \frac{a_{ep}}{4} \left(-1 \pm \sqrt{4 + S^2 B_z^2} \right) \xrightarrow{|B_z| \rightarrow 0} \frac{a_{ep}}{4} \begin{cases} 1 + S^2 B_z^2 / 2 \\ -3 - S^2 B_z^2 / 2 \end{cases} \xrightarrow{|B_z| \rightarrow \infty} \frac{a_{ep}}{4} \begin{cases} -1 + SB_z \\ -1 - SB_z \end{cases}$$

Eigenstates are transformed if field B_z varies. For low field they are singlet-triplet states $|\downarrow\rangle$ or $|\uparrow\rangle$ with H -eigenvalues 1 and -3 , respectively, in $a_{ep}/4$ units. For higher B_z -field they gradually morph into primitive $|\uparrow\rangle|\downarrow\rangle$ or $|\downarrow\rangle|\uparrow\rangle$ product states. This is a B-to-A-type symmetry change similar to the Ch. 10 description of the NH_3 maser levels in Fig. 10.3.1. Levels in Fig. 24.1.2(a) support H-maser transitions.

Level plots straighten out as the transformations finish. The absolutely straight level lines belong to states that do not transform at all. The levels cross if there is a difference, however slight, between the sum S and difference D between the two magnetic moments. The asymptotes $-I \pm SB_z$ will cross one of the straight-line levels $+I \pm DB_z$ at certain B_z -values $B_z = \pm 2/(S-D) = \pm 8a_{ep}/a_p$, which for the H-atom in Fig. 24.1.2(a), happens well off the plot at $B_z = \pm 16 T$. In Fig. 24.1.2(b), where a_p is assumed to be 10 times larger, asymptote crossings occur at much smaller field values $B_z = \pm 1.6 T$. However, the level crossings are just inside that value since the symmetry transformation pulls the hyperbola off the asymptote.

A classical electron model has rotating negative charge and a magnetic moment \mathbf{m} opposite to its spin \mathbf{S} or \mathbf{J} . Such a model would find its lowest magnetic potential energy $-\mathbf{m} \cdot \mathbf{B}$ with spin anti-aligned to the B-field, while the proton wants to align its \mathbf{J} with \mathbf{B} . So, it is not surprising that the lowest state for positive B_z -field is proton-up and electron-down $|\uparrow^p \downarrow^e\rangle$ in the lower right hand side of Fig. 24.1.2(a).

However, the highest state is not the reverse spin state $|\downarrow^p \uparrow^e\rangle$ until after the $2/(S-D)$ -level crossing.

(Compare the upper right hand sides of parts (a) and (b) of Fig. 24.1.2.) Later we will describe transitions between these levels. Generally, transitions that flip nuclear spins give *nuclear magnetic resonance NMR* spectra while flipping electronic spins give *electron spin resonance ESR* spectra. Level crossing spectra, such as 21-cm lines at $B=0$, involve both *NMR* and *ESR*. (Do we need another acronym like *NMESS*?)

b. Two-Electron Atomic Configurations

Consider the elementary electronic structure of the Carbon atom which has six electrons in a configuration $(1s)^2(2s)^2(2p)^2$. An approximate model ignores, at first, the two pairs of electrons in the “closed” $1s$ and $2s$ shells, and treats the atom as though it had only a pair of $2p$ ($\ell=1$)-electrons. The orbital basis of this model has nine $(2p)^2$ bases $|^1_{m_1}\rangle|^1_{m_2}\rangle$ made from products of individual $2p$ orbital $|^1_{m_1}\rangle$ and $|^1_{m_2}\rangle$ states.

Orbital states $p \otimes p = D \oplus P \oplus S$

If no electrostatic repulsion or interaction of any kind existed between the electrons, then these nine states would be degenerate in energy. However, in the presence of interaction the following coupled states are model eigenstates whose energy depends on values of total orbit momentum L , *but not* M .

$$\left| (2p)^2 \begin{matrix} L \\ M \end{matrix} \right\rangle = \sum_{m_1, m_2} C_{m_1 m_2 M}^{1 1 L} \left| \begin{matrix} 1 \\ m_1 \end{matrix} \right\rangle \left| \begin{matrix} 1 \\ m_2 \end{matrix} \right\rangle \tag{24.1.19a}$$

Formula (24.1.17) gives the $L=2$ coefficients $C_{m_1 m_2 M}^{1 1 2}$ in the left-hand block of the following table. Applying orthogonalization and lowering to the $L=2$ entries gives the $L=1$ and $L=0$ states.

		2	2	2	2	2	1	1	1	0
	$1 \otimes 1$	2	1	0	-1	-2	1	0	-1	0
$\left C_{m_1 m_2 M}^{1 1 L} \right\rangle =$	1	1	1
	1	0	.	$\frac{1}{\sqrt{2}}$.	.	.	$\frac{1}{\sqrt{2}}$.	.
	1	-1	.	.	$\frac{1}{\sqrt{6}}$.	.	.	$\frac{1}{\sqrt{2}}$	$\frac{1}{\sqrt{3}}$
	0	1	.	$\frac{1}{\sqrt{2}}$.	.	.	$-\frac{1}{\sqrt{2}}$.	.
	0	0	.	.	$\sqrt{\frac{2}{3}}$	$-\frac{1}{\sqrt{3}}$
	0	-1	.	.	.	$\frac{1}{\sqrt{2}}$.	.	$\frac{1}{\sqrt{2}}$.
	-1	1	.	.	$\frac{1}{\sqrt{6}}$.	.	.	$-\frac{1}{\sqrt{2}}$	$\frac{1}{\sqrt{3}}$
	-1	0	.	.	.	$\frac{1}{\sqrt{2}}$.	.	$-\frac{1}{\sqrt{2}}$.
	-1	-1	1	.	.	.

The electrostatic interaction causes a splitting of the nine $|^1_{m_1}\rangle|^1_{m_2}\rangle$ levels and it results in $L=2, 1,$ and 0 levels, labeled $D, P,$ and $S,$ respectively, in Figure 24.1.3(a) that shows the three lowest levels for carbon.

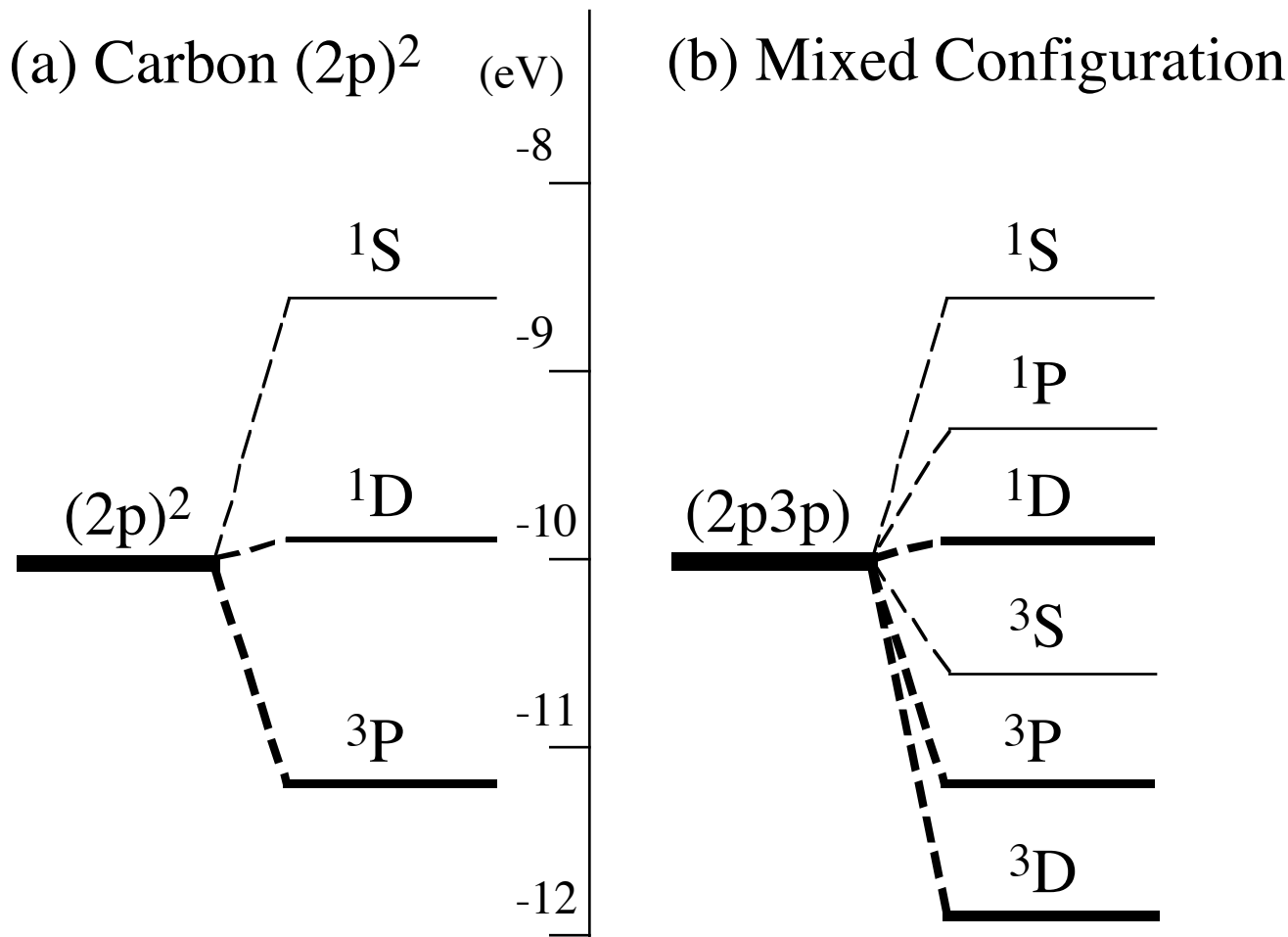


Figure 24.1.3 Atomic ^{2S+1}L multiplet levels for two ($l = 1$) p electrons. (a) Two equivalent electrons. Pauli exclusion principle allows only 1S , 1D , and 3P levels for two p-electrons with the same radial quantum number. (b) Two inequivalent electrons. All combinations of spin and orbit states are allowed.

Spin-S states to match orbital-L states: Pauli-Fermi-Dirac exclusion-symmetry rules

Each 2p electron also has a spin-1/2 and total spin states make triplets and singlet of Figure 24.1.1. First there is a triplet set from (24.1.10) followed by a singlet state from (24.1.11).

$$\left| \begin{smallmatrix} S=1 \\ M_s=+1 \end{smallmatrix} \right\rangle = \left| \begin{smallmatrix} 1/2 \\ +1/2 \end{smallmatrix} \right\rangle \left| \begin{smallmatrix} 1/2 \\ +1/2 \end{smallmatrix} \right\rangle, \quad \left| \begin{smallmatrix} S=1 \\ M_s=0 \end{smallmatrix} \right\rangle = \left(\left| \begin{smallmatrix} 1/2 \\ +1/2 \end{smallmatrix} \right\rangle \left| \begin{smallmatrix} 1/2 \\ -1/2 \end{smallmatrix} \right\rangle + \left| \begin{smallmatrix} 1/2 \\ -1/2 \end{smallmatrix} \right\rangle \left| \begin{smallmatrix} 1/2 \\ +1/2 \end{smallmatrix} \right\rangle \right) / \sqrt{2}, \quad \left| \begin{smallmatrix} S=1 \\ M_s=-1 \end{smallmatrix} \right\rangle = \left| \begin{smallmatrix} 1/2 \\ -1/2 \end{smallmatrix} \right\rangle \left| \begin{smallmatrix} 1/2 \\ -1/2 \end{smallmatrix} \right\rangle.$$

(24.1.20a)

$$\left| \begin{matrix} S=0 \\ M_S=0 \end{matrix} \right\rangle = \left(\left| \begin{matrix} 1/2 \\ +1/2 \end{matrix} \right\rangle \left| \begin{matrix} 1/2 \\ -1/2 \end{matrix} \right\rangle - \left| \begin{matrix} 1/2 \\ -1/2 \end{matrix} \right\rangle \left| \begin{matrix} 1/2 \\ +1/2 \end{matrix} \right\rangle \right) / \sqrt{2} \quad (24.1.20b)$$

The triplet atomic 3L -states are ket-ket products of an $\left| \begin{matrix} L \\ M \end{matrix} \right\rangle$ orbital state with a triplet spin state $\left| \begin{matrix} S=1 \\ M_S \end{matrix} \right\rangle$.

$$\left| {}^3LM_L M_S \right\rangle \equiv \left| \begin{matrix} L \\ M_L \end{matrix} \right\rangle \left| \begin{matrix} S=1 \\ M_S \end{matrix} \right\rangle \quad (24.1.21a)$$

A singlet atomic 1L -state is a ket-ket product of an $\left| \begin{matrix} L \\ M \end{matrix} \right\rangle$ orbital state with a singlet spin state $\left| \begin{matrix} S=0 \\ 0 \end{matrix} \right\rangle$.

$$\left| {}^1LM_L 0 \right\rangle \equiv \left| \begin{matrix} L \\ M_L \end{matrix} \right\rangle \left| \begin{matrix} S=0 \\ 0 \end{matrix} \right\rangle \quad (24.1.21b)$$

But, the *Pauli Exclusion Principle* rules out some states due to *Fermi-Dirac*-anti-symmetry.

The Pauli principle requires $\left| {}^{2S+1}L \right\rangle$ states be anti-symmetric to permutation of electrons. Even- L orbital states $\left| \begin{matrix} L=2 \\ M \end{matrix} \right\rangle$ and $\left| \begin{matrix} L=0 \\ 0 \end{matrix} \right\rangle$ in the table of (24.1.19) are symmetric to the interchange $\left| \begin{matrix} 1 \\ m_1 \end{matrix} \right\rangle \left| \begin{matrix} 1 \\ m_2 \end{matrix} \right\rangle \rightarrow \left| \begin{matrix} 1 \\ m_2 \end{matrix} \right\rangle \left| \begin{matrix} 1 \\ m_1 \end{matrix} \right\rangle$ of the *orbital* states of the electrons and can only “marry” an *anti*-symmetric $S = 0$ singlet *spin* state. So, states $\left| {}^1L = 2 \right\rangle$ or (1D) and $\left| {}^1L = 0 \right\rangle$ or (1S) obey the Pauli principle and exist in Figure 24.1.3(a). Similarly, odd- L orbital state $\left| \begin{matrix} L=1 \\ M \end{matrix} \right\rangle$ is *anti*-symmetric and can only marry all symmetric ($S=1$)-triplet spin states to give the one (3P) triplet term containing *nine* states $\left| {}^3P \begin{matrix} L=1 \\ M_L \\ S=1 \\ M_S \end{matrix} \right\rangle$ in the ground $(2p)^2$ configuration.

In excited configurations like $(2p)(3p)$ shown in Figure 24.1.3(b), the terms (3D), (1P), and (3S) missing from $(2p)^2$ are no longer excluded since, for example an anti-symmetric $(2p)(3p)$ - 3D -orbital state such as $\left| (2p3p) {}^3D \begin{matrix} 2 \\ 2 \end{matrix} \right\rangle = \left| 2p \begin{matrix} 1 \\ 1 \end{matrix} \right\rangle \left| 3p \begin{matrix} 1 \\ 1 \end{matrix} \right\rangle - \left| 3p \begin{matrix} 1 \\ 1 \end{matrix} \right\rangle \left| 2p \begin{matrix} 1 \\ 1 \end{matrix} \right\rangle$ exists, but $\left| (2p)^2 {}^3D \begin{matrix} 2 \\ 2 \end{matrix} \right\rangle = \left| 2p \begin{matrix} 1 \\ 1 \end{matrix} \right\rangle \left| 2p \begin{matrix} 1 \\ 1 \end{matrix} \right\rangle - \left| 2p \begin{matrix} 1 \\ 1 \end{matrix} \right\rangle \left| 2p \begin{matrix} 1 \\ 1 \end{matrix} \right\rangle = 0$ vanishes for $(2p)^2$.

It is sometimes possible to estimate the ordering of ${}^{2S+1}L$ terms. Because of its anti-symmetry the $\left| {}^3P \begin{matrix} L=1 \\ M_L \end{matrix} \right\rangle$ orbital wave function must go to zero as its two electrons approach each other. ($x_1 \rightarrow x_2$)

$$\langle x_1 x_2 \left| (2p)^2 {}^3P \begin{matrix} L=1 \\ M_L \end{matrix} \right\rangle = -\langle x_2 x_1 \left| (2p)^2 {}^3P \begin{matrix} L=1 \\ M_L \end{matrix} \right\rangle \xrightarrow{x_2 \rightarrow x_1} 0$$

Therefore, the two electrons in this triplet spin state are never at the same point, and seldom near each other, thus making electrostatic repulsion energy less for triplet spin-states than for singlet ($S=0$) total spin. Indeed 3P is the ground state of carbon.

Now a classical argument can be made to tell which ${}^{2S+1}L$ for a given total spin S should be lowest. One may imagine that to make the greatest L the electrons must orbit in more or less the same direction so they have

less chance of colliding and raising the electrostatic energy. Indeed, 1D is lower than 1S . Together, these arguments about symmetry of S and L states give what are known as *Hund's rule* for atomic $(\ell)^n$ ground states ${}^{2S+1}L$. The ground configuration has the highest possible spin S and orbital momentum L allowed by the Pauli principle. They are followed throughout the Periodic chart of atoms wherever S and L are good quantum state labels.

c. Spin-Orbital Coupling

The Clebsch-Gordan outer product is used to describe states corresponding to two properties of a single electron, such as spin and orbit. The ℓs -ket-kets of a single electron in hydrogen are written as follows.

$$\left| \ell \right\rangle_{m_1} \left| \frac{1}{2} \right\rangle_{m_2} \equiv \left| \ell \frac{1}{2} \right\rangle_{m_1 m_2}, \quad (24.1.22)$$

Then Clebsch-Gordan coefficients (CGC) give states of definite total angular momentum j .

$$\left| \left(\ell \otimes \frac{1}{2} \right)^j \right\rangle_m = \sum_{m_1 m_2} C_{m_1 m_2 m}^{\ell \frac{1}{2} j} \left| \ell \frac{1}{2} \right\rangle_{m_1 m_2} \quad (24.1.23)$$

Before discussing the spin-orbit interaction, one may predict the form of the splitting of ℓ -levels. Several $n\ell_j$ levels of hydrogen are plotted in Figure 24.1.4 according to the following CGC reduction.

$$C^{\dagger} D^{\ell} \otimes D^{\frac{1}{2}} C = D^{\ell+\frac{1}{2}} \oplus D^{\ell-\frac{1}{2}} \quad (\ell > 0) \quad (24.1.24)$$

The fine-structure constant is $\alpha = e^2 / \hbar c \sim \frac{1}{137}$. (Recall (5.6.3). Atomic units are used here.

$\epsilon = e^2 / a_0 = me^4 / \hbar c \sim 27.21 \text{ eV}$) The expectation values for the spin-orbit splitting are as follows.

$$\left\langle \begin{matrix} j \\ m \end{matrix} \left(\ell \otimes \frac{1}{2} \right) \middle| H_{s.o.} \middle| \begin{matrix} j \\ m \end{matrix} \left(\ell \otimes \frac{1}{2} \right) \right\rangle = a_{s.o.} \left[j(j+1) - \ell(\ell+1) - \frac{3}{4} \right] \quad (j = \ell \pm \frac{1}{2}), \quad (24.1.26)$$

The total angular momentum $j = \ell + s$ has been used in the same manner as in the preceding section.

The spin-orbit effects, like most spin interactions, are derived most elegantly using the Dirac equation.

This includes all relativistic effects and leads to a very simple expression for energy eigenvalues:

$$\epsilon_{n,j} = -\frac{Z^2}{2n^2} - \frac{\alpha^2 Z^4}{2n^3} \left(\frac{1}{j + \frac{1}{2}} - \frac{3}{4n} \right). \quad (24.1.27)$$

The Dirac formula predicts that a degeneracy remains between pairs of fine levels such as ($2s_{1/2}$ - $2p_{1/2}$) and ($3p_{3/2}$ - $3d_{3/2}$). This degeneracy is lifted by a small quantum electrodynamic (QED) perturbation and the splitting is called the *Lamb shift*. The degeneracy between $n\ell_j$ and $n\ell'_j$ states can also be understood in terms of a relativistic generalization of Coulomb symmetry discussed later.

Fine structure is more easily observed in multi-electron configurations. In fact, it dominates the electrostatic energies in some larger atoms since the spin-orbit term in (24.1.25) varies as the 4th power Z^4 of the atomic number. Model states such as those for carbon can be spin-orbit or *LS coupled* as follows.

$$\left| {}^{2S+1}L_J \quad M \right\rangle = \sum_{M_S, M_L} C_{M_S, M_L}^{S, L, J} \left| \begin{matrix} S \\ M_S \end{matrix} \right\rangle \left| \begin{matrix} L \\ M_L \end{matrix} \right\rangle. \quad (24.1.28)$$

This gives, finally, states of definite total electronic angular momentum J . In general, a given ${}^{2S+1}L$ term will split into a number $2S + 1$ of J -states for each $S \leq L$. For example, the triplet levels of carbon split into three, as shown in the lower left-hand side Fig. 24.1.5(a) and on the lower right-hand side of Fig. 24.1.5(a). The problem is that, while the fine-structure label J is a good quantum number (in absence of hyperfine effects), strong spin-orbit coupling mixes J -states (24.1.28) of different spin S and orbit L quanta.

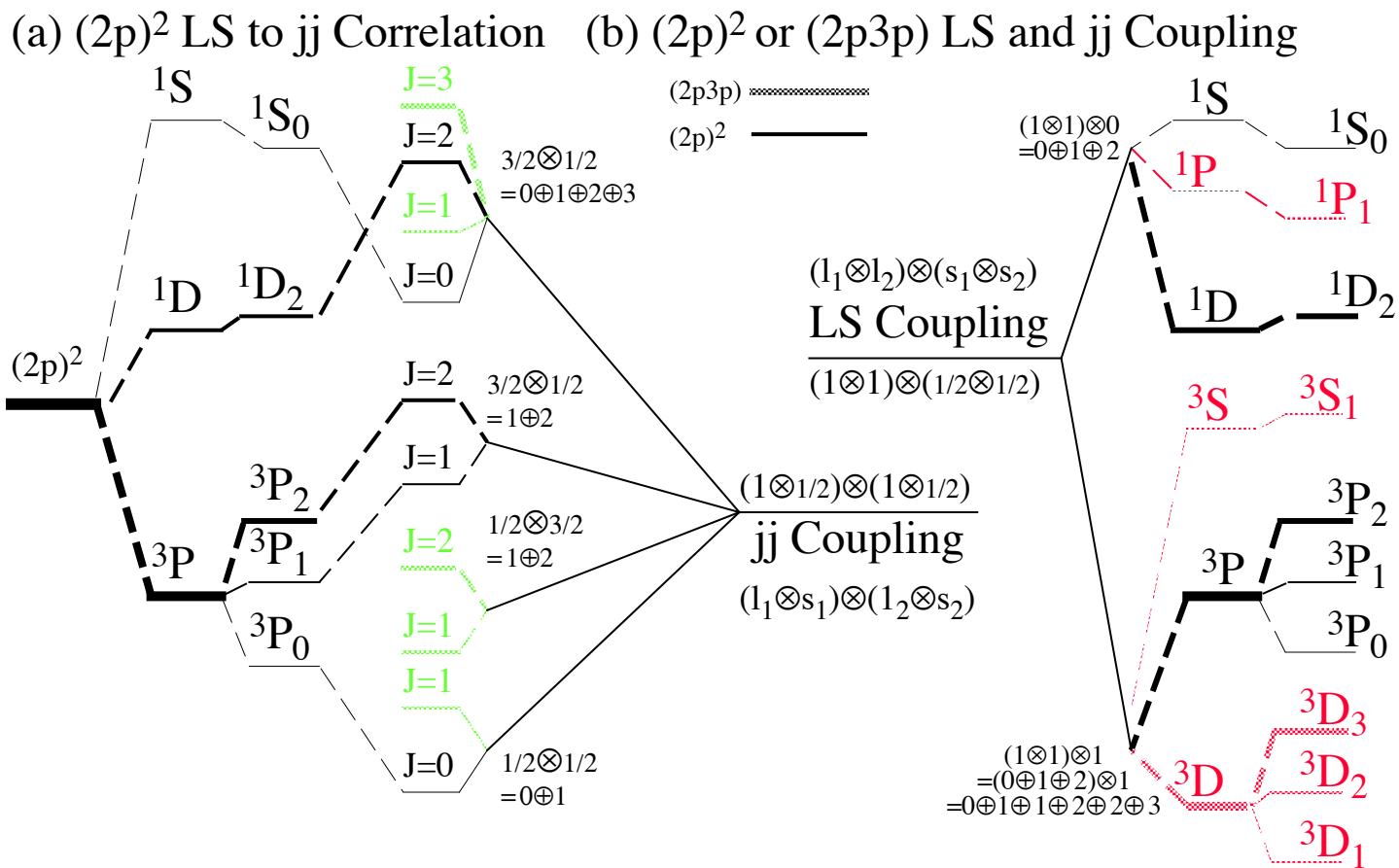


Figure 24.1.5 Fine-structure levels for configurations involving two p electrons. (a) $(2p)^2$ configuration in coupling case. (b) Comparison between jj - and LS -coupling cases. In the LS case L and S are good approximate quantum labels and the splitting between levels of different J and the same (L,S) is relatively small. In the jj case j and j' are good approximate quantum labels.

The four angular-momentum factors $(1 \otimes \frac{1}{2} \otimes 1 \otimes \frac{1}{2})$ for two p electrons may be *associated* differently. The following association corresponds to what is called *LS coupling*.

$$(1 \otimes 1) \otimes (\frac{1}{2} \otimes \frac{1}{2}) = (2 \otimes 1 \otimes 0) \otimes (1 \otimes 0) = (\dots \otimes L \dots) \otimes (\dots \otimes S \dots) = (\dots \otimes J \otimes \dots)$$

The LS levels appear on the outside of Figures 24.1.5(a and b). The gray lines in Fig. 24.1.5(b) indicate levels allowed in mixed- n ($n_1 p n_2 p$) configurations but Pauli-excluded from pure $(np)^2$ configurations. The LS scheme provides useful quantum labels if spin-orbit energy is smaller than that of electron repulsion.

A strong spin-orbit perturbation makes the following *jj coupling* association more appropriate.

$$(1 \otimes \frac{1}{2}) \otimes (1 \otimes \frac{1}{2}) = (\frac{3}{2} \otimes \frac{1}{2}) \otimes (\frac{3}{2} \otimes \frac{1}{2}) = (\dots \otimes j \dots) \otimes (\dots \otimes j' \dots) = (\dots \otimes J \otimes \dots)$$

The resulting levels are indicated in the center of Fig. 24.1.4(b). For each J term that comes out of the jj association, there must be a corresponding term with the same J in the LS association. Figures 24.1.5(a) and 24.1.5(b) show the connection by “avoided-crossing” lines between the levels of the same J .

d. Angular-momentum cones and vector coupling models

Two states of angular momentum j_1 and j_2 couple to make a total momentum $j_3 = j_1 + j_2, j_1 + j_2 - 1, \dots$, or $[j_1 - j_2]$. The corresponding level diagram shown in Figure 24.1.6 is a generic version of Fig. 24.1.1. A vector triangle with sides j_1, j_2 , and j_3 is sketched at each level. A Clebsch-Gordan $C_{m_1 m_2 m_3}^{j_1 j_2 j_3}$ coefficient (CGC) is zero unless the *triangular condition* $j_1 + j_2 \geq j_3 \geq |j_1 - j_2|$ holds and $\langle \mathbf{J}_z \rangle$ adds up $m_1 + m_2 = m_3$.

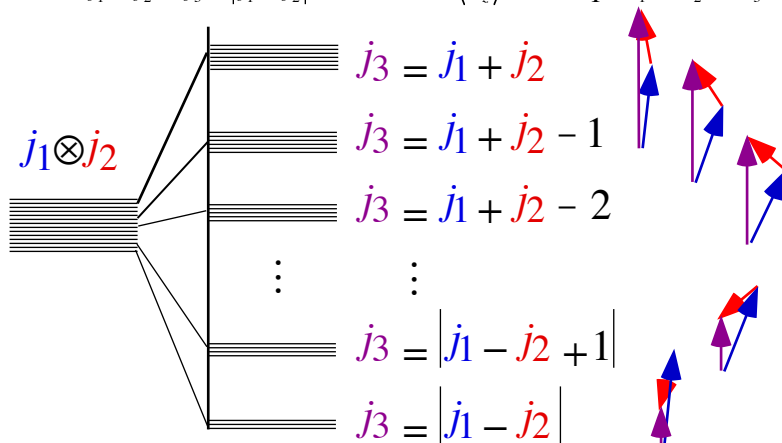


Figure 24.1.6 Level-splitting and vector-addition picture of angular-momentum coupling.

Vector addition models of CGC become semi-quantitative if each vector is drawn with its quantum length $|j_1| = \sqrt{j_1(j_1 + 1)}$, $|j_2| = \sqrt{j_2(j_2 + 1)}$ and $|j_3| = \sqrt{j_3(j_3 + 1)}$ with quantum z -components $m_1 + m_2 = m_3$. The resulting *angular-momentum cones* were used to quantify $D_{mn}^j(\beta)$ amplitudes in Figures 23.1.2 and 23.2.2. A similar view of CGC amplitudes uses the angular-momentum cone and vector arrangement in Figure 24.1.7. Since z -component conservation requires that $m_1 + m_2 = m_3$, we may plot $C_{m m_3 - m m_3}^{j_1 j_2 j_3}$, as a function of a single variable $m_1 = m$ for fixed j_1, j_2, j_3 and m_3 . This is done in Figure 24.1.8 for $j_1 = j_2 = 9$ and select values of j_3 and m_3 . The plots remind one of $D_{mn}^j(\beta)$ plots in Figure 23.2.2 of the earlier chapter.

For one thing, the projection of angular-momentum cone rims on the m or z -axis defines “classical” limits and inflection points of a discrete wave. Outside the rims CGC or D values drops exponentially. Inside its rims $C_{m m_3 - m m_3}^{j_1 j_2 j_3}$ has $j_1 + j_2 - j_3$ nodes where it changes sign, while $D_{mn}^j(\beta)$ has $j - n$ nodes. The discrete quantum number m_3 plays a role for the CGC waves that the continuous rotation angle β plays for $D_{mn}^j(\beta)$ in Figure 23.2.2. Note that “nodes” are only rarely exact zeros of $D_{mn}^j(\beta)$ or $C_{m m_3 - m m_3}^{j_1 j_2 j_3}$ since they generally fall between the integer values of the quantum number m defining $D_{mn}^j(\beta)$ or $C_{m m_3 - m m_3}^{j_1 j_2 j_3}$.

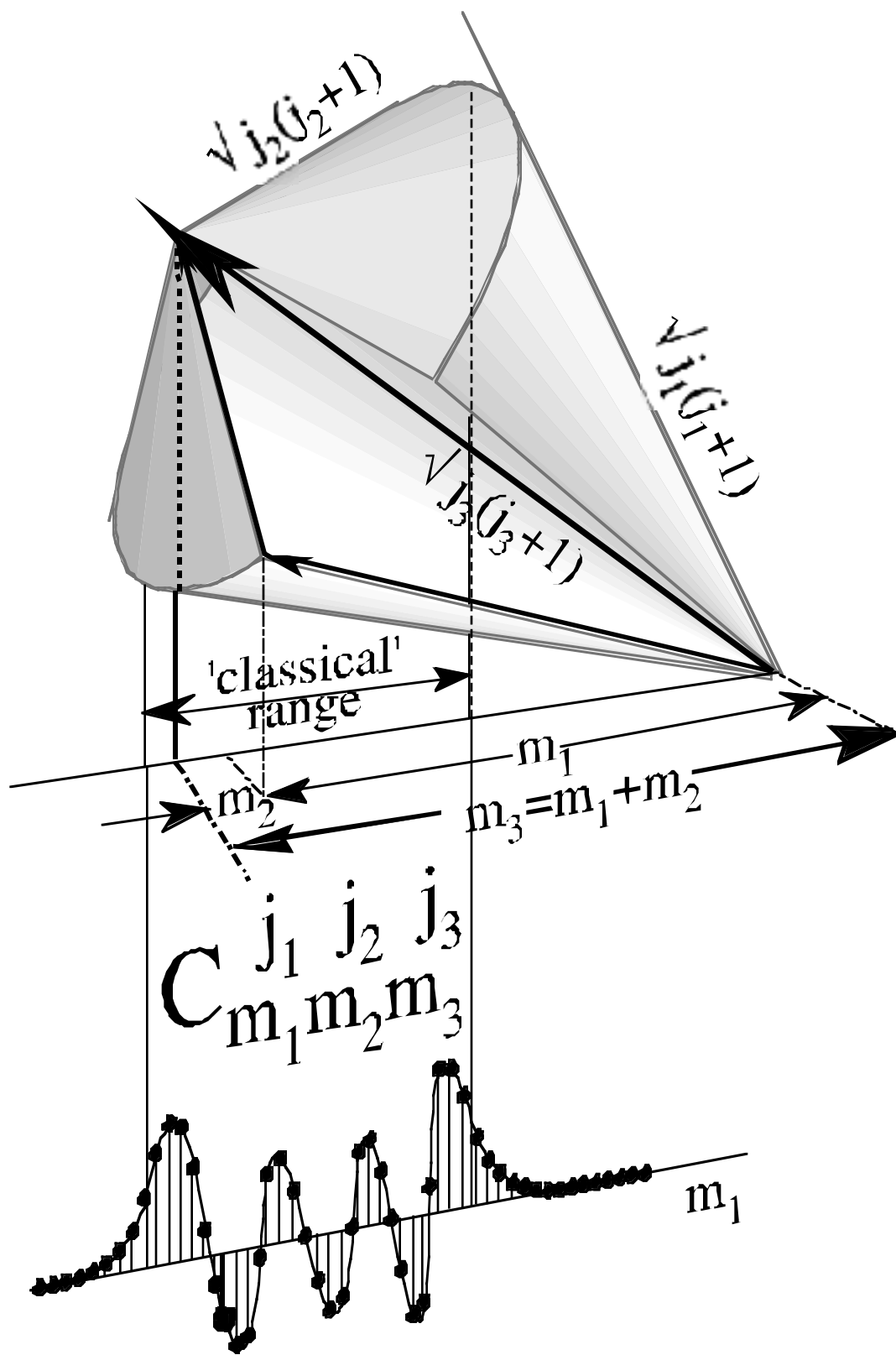


Figure 24.1.7 Angular-momentum cone picture of Clebsch-Gordan coupling amplitudes.

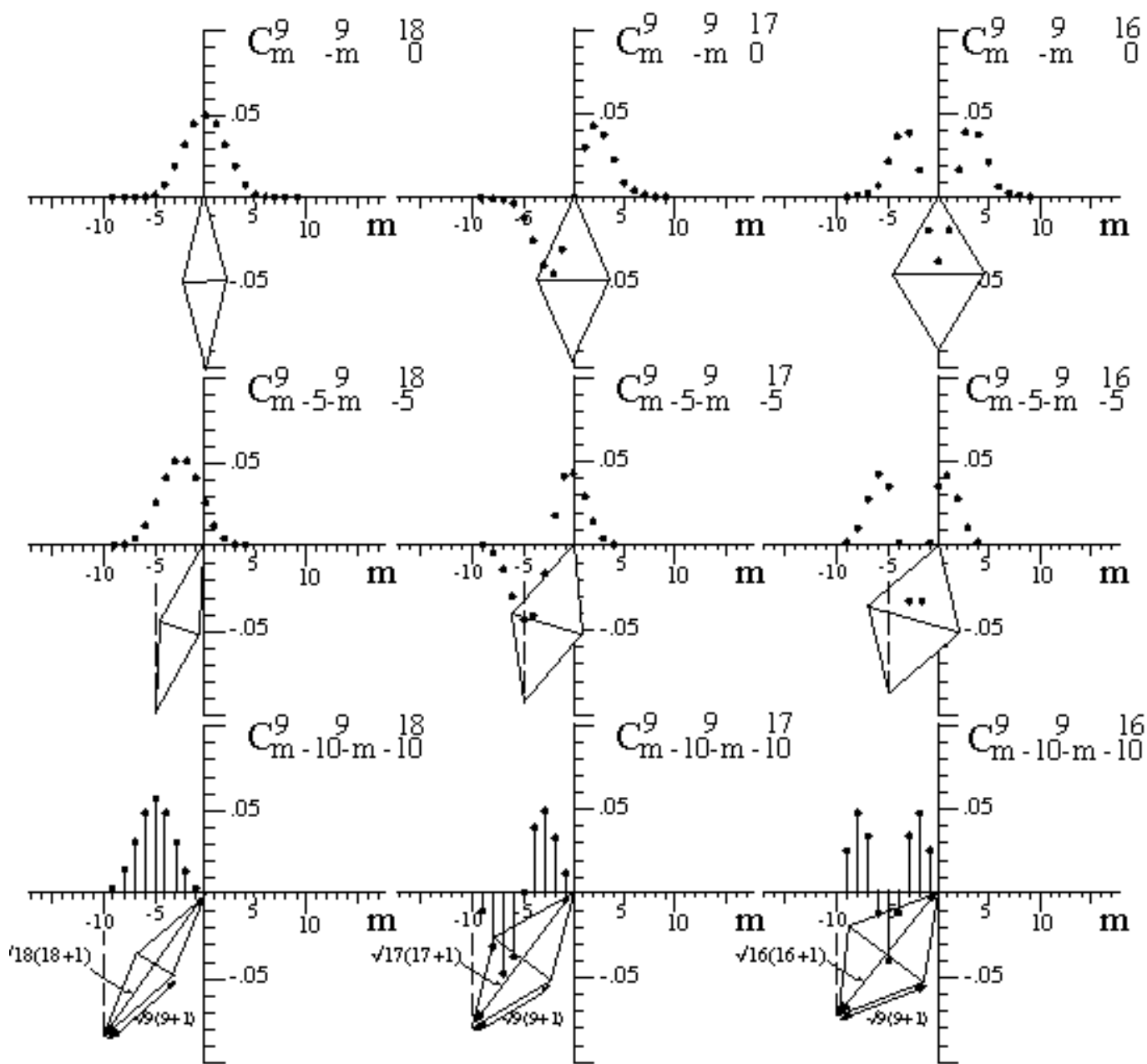


Figure 24.1.8 Clebsch-Gordan coefficients plotted next to their angular-momentum cones.

Anomalous magnetic moments and g-factors

An uncoupled angular momentum state $|j_1, m_1\rangle |j_2, m_2\rangle$ in a magnetic \mathbf{B} -field has each magnetic moment $\mathbf{m}_1 = g_1 \mu_1 \mathbf{j}_1 \equiv \beta_1 \mathbf{j}_1$ and $\mathbf{m}_2 = g_2 \mu_2 \mathbf{j}_2 \equiv \beta_2 \mathbf{j}_2$ precess according to Zeeman $\mathbf{m} \cdot \mathbf{B}$ energy eigenvalues that are a product of a gyromagnetic coefficient (24.1.18_{Table}) with its z -momentum quantum number m_1 or m_2 .

$$E_1 = \hbar g_1 \mu_1 B_z m_1 \equiv \hbar \beta_1 B_z m_1 \quad (24.1.29a)$$

$$E_2 = \hbar g_2 \mu_2 B_z m_2 \equiv \hbar \beta_2 B_z m_2 \quad (24.1.29b)$$

Independent z -precessional motion is indicated in Fig. 24.1.9(a). Fig. 24.1(b) shows the effect of coupling.

In a coupled angular momentum state $|j_3=J, m_3=M\rangle$ \mathbf{j}_1 and \mathbf{j}_2 swivel about $\mathbf{j}_3 = \mathbf{j}_1 + \mathbf{j}_2$ instead of \hat{z} . A B_z -field disfavors rigid swiveling about internal \mathbf{j}_3 but favors independent swiveling about external \hat{z} axes. The result is level splitting and crossing. (Recall B_z -field splitting of $e-p$ -levels in Fig. 24.1.2.) If the B_z -field is less than that of interaction, a vector-coupling picture will approximate the Zeeman energy of $|j_3=J, m_3=M\rangle$.

An estimate of $\mathbf{m} \cdot \mathbf{B}$ energy in the situation depicted in Fig. 24.1.9(b) assumes fast precession of vectors of moment \mathbf{m}_1 and \mathbf{m}_2 and momentum \mathbf{j}_1 and \mathbf{j}_2 *in unison* around the sum-total momentum vector $\mathbf{J} \equiv \mathbf{j}_3 = \mathbf{j}_1 + \mathbf{j}_2$ so that components of \mathbf{m}_1 and \mathbf{m}_2 transverse to $\mathbf{j}_3 \equiv \mathbf{J}$ average to zero. So, only longitudinal components $\mathbf{m}_1 \cdot \hat{\mathbf{j}}_3$ and $\mathbf{m}_2 \cdot \hat{\mathbf{j}}_3$ contribute, on the average, to Zeeman- z -components $\mathbf{j}_3 \cdot \hat{z}$.

$$\begin{aligned} \mathbf{m}_{TOTAL} \cdot \hat{z} &= \mathbf{m}_1 \cdot \hat{z} + \mathbf{m}_2 \cdot \hat{z} = \beta_1 \mathbf{j}_1 \cdot \hat{z} + \beta_2 \mathbf{j}_2 \cdot \hat{z} \\ &\cong (\beta_1 \mathbf{j}_1 \cdot \hat{\mathbf{j}}_3 + \beta_2 \mathbf{j}_2 \cdot \hat{\mathbf{j}}_3) \hat{\mathbf{j}}_3 \cdot \hat{z} = \frac{(\beta_1 \mathbf{j}_1 \cdot \mathbf{j}_3 + \beta_2 \mathbf{j}_2 \cdot \mathbf{j}_3) \mathbf{j}_3 \cdot \hat{z}}{|\mathbf{j}_3|^2} \end{aligned}$$

The second line approximation ignores all but \mathbf{j}_3 -components of \mathbf{m}_1 and \mathbf{m}_2 . Sum \mathbf{j}_3 -vector is made of fast $\mathbf{j}_1 + \mathbf{j}_2$ but z -precesses slowly according to its Zeeman B_z -field projection. The $\mathbf{j} \cdot \mathbf{j}$ trick of (24.1.13) is used.

$$\begin{aligned} \langle m_{TOTAL-z} B_z \rangle &\cong \frac{(\beta_1 \mathbf{j}_1 \cdot \mathbf{j}_3 + \beta_2 \mathbf{j}_2 \cdot \mathbf{j}_3) \langle \mathbf{j}_3 \cdot \hat{z} \rangle}{\langle |\mathbf{j}_3|^2 \rangle} B_z = \frac{\beta_1 \mathbf{j}_1 \cdot \mathbf{j}_3 + \beta_2 \mathbf{j}_2 \cdot \mathbf{j}_3}{j_3(j_3+1)} m_3 B_z \\ &= \frac{\beta_1 (j_3(j_3+1) + j_1(j_1+1) - j_2(j_2+1)) + \beta_2 (j_3(j_3+1) - j_1(j_1+1) + j_2(j_2+1))}{2j_3(j_3+1)} m_3 B_z \end{aligned} \tag{24.1.30a}$$

This gives the Lande' formula for effective magnetic moment.

$$\beta_{Lande'} = \frac{(\beta_1 + \beta_2) j_3(j_3+1) + (\beta_1 - \beta_2)(j_1(j_1+1) - j_2(j_2+1))}{2j_3(j_3+1)} \quad \text{where: } \langle m_{TOTAL} B_z \rangle = \beta_{Lande'} m_3 B_z \tag{24.1.30b}$$

Electrons are a special case. Orbit $j_1 \equiv L$ has $\beta_1 = g_1 \mu_1 \equiv \mu_B$. Spin $j_2 = S$ is twice that with $\beta_2 = g_2 \mu_2 = 2\mu_B$.

$$g_{Lande'} = \frac{3J(J+1) - L(L+1) + S(S+1)}{2J(J+1)} \quad \text{where: } \langle m_{TOTAL} B_z \rangle = g_{Lande'} \mu_{Bohr} m_3 B_z \tag{24.1.30c}$$

Equal factors ($\beta_1 = \beta_2$) give $g=I$. Spin g_s is called *anomalous* since it is twice that of orbit ($g_s = 2g_L = 2$).

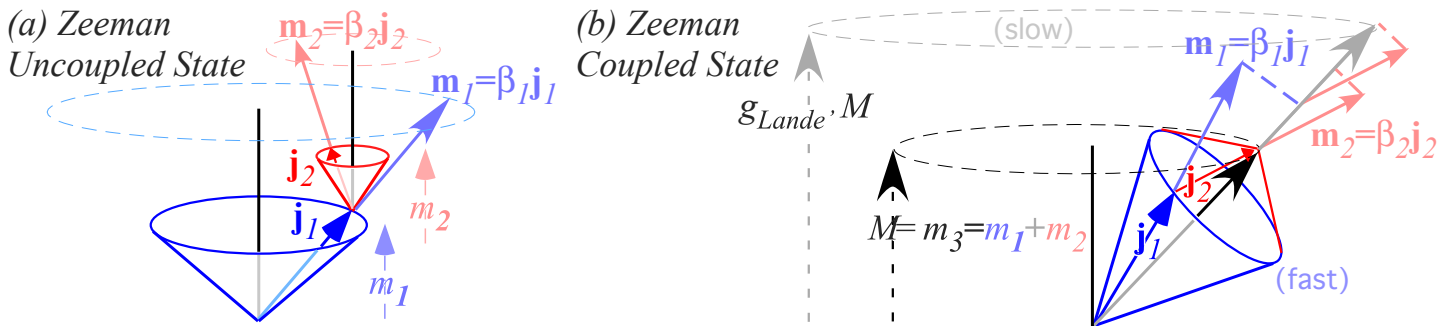


Fig. 24.1.9 Zeeman effect on momenta j_1 and j_2 . (a) Uncoupled state $|j_1, m_1\rangle |j_2, m_2\rangle$, (b) Coupled state $|j_3=J, m_3=M\rangle$.

24.2 Symmetry Properties of CGC and Wigner 3j Coefficients

We now discuss mathematical properties and applications of Clebsch-Gordan coefficients (CGC) beginning with their relation to common products in vector analysis. Then the fundamental relations between the CGC coefficients and the D irreps will be derived and used to define symmetry relations. This will lead naturally to the definition of the Wigner 3j coefficients.

a. Scalars, Vectors, and Tensors

Consider two ordinary three-dimensional vectors.

$$\mathbf{A} = \begin{pmatrix} A_x \\ A_y \\ A_z \end{pmatrix} \quad \text{and} \quad \mathbf{B} = \begin{pmatrix} B_x \\ B_y \\ B_z \end{pmatrix} \quad (24.2.1)$$

From the theory of vector analysis there are three different types of products between them. There is a *scalar*, dot, or Gibbs inner product

$$\mathbf{A} \bullet \mathbf{B} = A_x B_x + A_y B_y + A_z B_z, \quad (24.2.2a)$$

a *vector*, or Gibbs cross-product

$$\mathbf{A} \times \mathbf{B} = \begin{pmatrix} A_y B_z - A_z B_y \\ A_z B_x - A_x B_z \\ A_x B_y - A_y B_x \end{pmatrix}, \quad (24.2.2b)$$

and a *tensor*, dyadic, or Kronecker outer product

$$\mathbf{AB} = \mathbf{A} \otimes \mathbf{B} = \begin{pmatrix} A_x B_x & A_x B_y & A_x B_z \\ A_y B_x & A_y B_y & A_y B_z \\ A_z B_x & A_z B_y & A_z B_z \end{pmatrix}. \quad (24.2.2c)$$

It is instructive to note that these three products correspond directly with the three reductions of products between $\ell = 1$ or (p)-states which give total $L = 0, 1,$ and 2 states, respectively.

To make this correspondence we recall having two different types of coordinates, namely, Cartesian or *plane-polarization* components (A_x, A_y, A_z) on one hand, and R_3 symmetry-defined or *circular-polarization* components A_1^1, A_0^1, A_{-1}^1 on the other. An earlier eq. (23.3.3) relates the sets.

$$\begin{aligned} A_1^1 &= -(A_x + iA_y)/\sqrt{2}, & A_x &= (A_{-1}^1 - A_1^1)/\sqrt{2}, & A_z &= A_0^1, \\ A_{-1}^1 &= (A_x - iA_y)/\sqrt{2}, & A_y &= i(A_{-1}^1 + A_1^1)/\sqrt{2}, & A_0^1 &= A_z. \end{aligned} \quad (24.2.3)$$

(x, y, z) relates to spherical harmonics (Y_1^1, Y_0^1, Y_{-1}^1) or multipole functions ($rY_1^1, rY_0^1, rY_{-1}^1$) in (23.3.3).

We use the CGC in the $1 \otimes 1$ table (24.1.15) to make *L-symmetry-defined products* of A^1 and B^1 .

$$\left[A^1 \otimes B^1 \right]_M^L \equiv \sum_{m_1, m_2} C_{m_1 m_2}^1 \quad {}^1 \quad {}^L \quad M \quad A_{m_1}^1 \quad B_{m_2}^1 \quad (24.2.4a)$$

The ($L=0$)-case is proportional to the scalar product in Eq. (24.2.2a).

$$\begin{aligned}
\left[A^1 \otimes B^1 \right]_0^0 &= \frac{1}{\sqrt{3}} A_1^1 B_{-1}^1 - \frac{1}{\sqrt{3}} A_0^1 B_0^1 + \frac{1}{\sqrt{3}} A_{-1}^1 B_1^1 \\
&= \frac{(-A_x - iA_y)(B_x - iB_y)}{2\sqrt{3}} - \frac{A_z B_z}{\sqrt{3}} + \frac{(A_x - iA_y)(-B_x - iB_y)}{2\sqrt{3}} \\
&= -(A_x B_x + A_y B_y + A_z B_z) / \sqrt{3} = -\mathbf{A} \cdot \mathbf{B} / \sqrt{3}.
\end{aligned} \tag{24.2.4}$$

The product for $L=1$ and $M=0$ is proportional to the ${}_0^1$ or z -component of the cross product (24.2.2b).

$$\begin{aligned}
\left[A^1 \otimes B^1 \right]_0^1 &\equiv \sum_{m_1, m_2} C_{m_1 m_2 0}^{1 1 1} A_{m_1}^1 B_{m_2}^1 = \frac{1}{\sqrt{2}} A_1^1 B_{-1}^1 - \frac{1}{\sqrt{2}} A_{-1}^1 B_1^1 \\
&= i \frac{(-A_y B_x + A_x B_y)}{\sqrt{2}} = \frac{i}{\sqrt{2}} (\mathbf{A} \times \mathbf{B})_z
\end{aligned} \tag{24.2.5}$$

Finally, the $L = 2$ products are made of second-rank tensor components.

$$\left[A^1 \otimes B^1 \right]_m^2 = \sum_{m_1, m_2} C_{m_1 m_2 m}^{1 1 2} A_{m_1}^1 B_{m_2}^1, \tag{24.2.6a}$$

$$\begin{aligned}
\left[A^1 \otimes B^1 \right]_2^2 &= (A_x B_x - A_y B_y + iA_x B_y + iA_y B_x) / 2, \\
\left[A^1 \otimes B^1 \right]_1^2 &= -(A_x B_z + A_z B_x + iA_y B_z + iA_z B_y) / 2, \\
\left[A^1 \otimes B^1 \right]_0^2 &= (-A_x B_x - A_y B_y + 2A_z B_z) / \sqrt{6}.
\end{aligned} \tag{24.2.6b}$$

The above products are summarized in the following matrix that is a unitary transformation between Cartesian components $T_{ij} = A_i B_j$ and symmetry-defined components $T_q^k = [A \times B]_q^k$ of a second-rank tensor:

$$\ddot{\mathbf{T}} = \sum_{ij} T_{ij} \hat{x}_i \hat{x}_j = \sum_{kg} T_q^k [xx]_q^k \tag{24.2.7a}$$

If the two vectors \mathbf{A} and \mathbf{B} are the radius vector ($\mathbf{A}=\mathbf{B}=\mathbf{r}$) in (24.2.4-11), then one obtains *elementary multipole functions* $X_q^k = r^k Y_q^k \sqrt{4\pi / 2k + 1}$. Here we get quadrupole X_q^2 functions shown in (23.3.8).

$$\begin{aligned}
\left[r^1 r^1 \right]_2^2 &= (x^2 - y^2 + 2ixy) / 2, & \left[r^1 r^1 \right]_1^2 &= -(x + iy)z, & \left[r^1 r^1 \right]_0^2 &= -(x^2 + y^2 - 2z^2) / \sqrt{6}, \\
&= \sqrt{\frac{2}{3}} X_2^2 & &= \sqrt{\frac{2}{3}} X_1^2 & &= \sqrt{\frac{2}{3}} X_0^2
\end{aligned} \tag{24.2.8}$$

Tensor or polynomial algebra may be continued up to arbitrary rank or order k , by attaching k vector factors. The new tensor or polynomial at each stage, i.e., the one which has the highest $L = k$, is made by the following coupling formulas using the CGC formulas (24.2.9) to (24.2.11) derived using (24.1.17).

$\langle xyz ^k_q \rangle =$	$A \otimes B$	2	2	2	2	2	1	1	1	0
		2	1	0	-1	-2	1	0	-1	0
	$x \quad x$	$\frac{1}{2}$	\cdot	$\frac{-1}{\sqrt{6}}$	\cdot	$\frac{1}{2}$	\cdot	\cdot	\cdot	$\frac{-1}{\sqrt{3}}$
	$x \quad y$	$\frac{i}{2}$	\cdot	\cdot	\cdot	$\frac{-i}{2}$	\cdot	$\frac{i}{\sqrt{2}}$	\cdot	\cdot
	$x \quad z$	\cdot	$\frac{-1}{2}$	\cdot	$\frac{1}{2}$	\cdot	$\frac{-1}{2}$	\cdot	$\frac{-1}{2}$	\cdot
	$y \quad x$	$\frac{i}{2}$	\cdot	\cdot	\cdot	$\frac{-i}{2}$	\cdot	$\frac{-i}{\sqrt{2}}$	\cdot	\cdot
	$y \quad y$	$\frac{-1}{2}$	\cdot	$\frac{-1}{\sqrt{6}}$	\cdot	$\frac{-1}{2}$	\cdot	\cdot	\cdot	$\frac{-1}{\sqrt{3}}$
	$y \quad z$	\cdot	$\frac{-i}{2}$	\cdot	$\frac{-i}{2}$	\cdot	$\frac{-i}{2}$	\cdot	$\frac{i}{2}$	\cdot
	$z \quad x$	\cdot	$\frac{-1}{2}$	\cdot	$\frac{1}{2}$	\cdot	$\frac{1}{2}$	\cdot	$\frac{1}{2}$	\cdot
	$z \quad y$	\cdot	$\frac{-i}{2}$	\cdot	$\frac{-i}{2}$	\cdot	$\frac{i}{2}$	\cdot	$\frac{-i}{2}$	\cdot
	$z \quad z$	\cdot	\cdot	$\frac{2}{\sqrt{6}}$	\cdot	\cdot	\cdot	\cdot	\cdot	$\frac{-1}{\sqrt{3}}$

(24.2.9)

$$\left[\left[\left[A^1 \times B^1 \right]^2 \times C^1 \dots \right]^{k-1} \times K^1 \right]_q^k$$

$$= C_{q-1,1q}^{k-1,1k} \left[\left[[ABC \dots]_{q-1}^{k-1} K_1^1 + C_{q-1,0q}^{k-1,1k} \left[[ABC \dots]_q^{k-1} K_0^1 + C_{q+1-1q}^{k-1,1k} \left[[[ABC \dots]_{q+1}^{k-1} K_{-1}^1 \right. \right. \right. \right]$$
(24.2.10)

$$C_{q-1,1q}^{k-1,1k} = \sqrt{\frac{(k+q-1)(k+q)}{(2k-1)(2k)}}, \quad C_{q-1,0q}^{k-1,1k} = \sqrt{\frac{(k^2-q^2)}{k(2k-1)}}, \quad C_{q+1-1q}^{k-1,1k} = \sqrt{\frac{(k-q)(k-q-1)}{2k(2k-1)}}.$$
(24.2.11)

b. The general R₃ scalar coupling

One type of coupling coefficients should be memorized, the CGC that make scalars ($\ell = 0$).

$$C_{m_1 m_2 0}^{j_1 j_2 0} = \delta^{j_1 j_2} \delta_{m_1, -m_2} (-1)^{j_1 - m_1} / \sqrt{2j_1 + 1}.$$
(24.2.12)

We show below that the product of any two bases having the *same j* can be “scalarized” as follows.

$$\left| \begin{matrix} 0 \\ 0 \end{matrix} \right\rangle = \sum_m \frac{(-1)^{j-m}}{\sqrt{2j+1}} \left| \begin{matrix} j \\ m \end{matrix} \right\rangle \left| \begin{matrix} j \\ -m \end{matrix} \right\rangle,$$
(24.2.13)

So the result has zero total *J* and belongs to the scalar irrep $D^0(\mathbb{R}) \equiv 1$. Angular momentum scalar products are a little more difficult for complex bases than for real ones since the phase is variable.

Let us consider how we *D^j*-transform ket vectors versus how we do bras.

$$\begin{aligned} \left(R(a\beta\gamma) \left| \begin{matrix} j \\ m \end{matrix} \right\rangle \right)^\dagger &= \left(\sum_{m'} D_{m'm}^j(a\beta\gamma) \left| \begin{matrix} j \\ m' \end{matrix} \right\rangle \right)^\dagger \\ \left\langle \begin{matrix} j \\ m \end{matrix} \right| R^\dagger(a\beta\gamma) &= \sum_{m'} D_{m'm}^{j*}(a\beta\gamma) \left\langle \begin{matrix} j \\ m' \end{matrix} \right| \end{aligned} \quad (24.2.14)$$

Clearly the complex conjugate $(D^j)^*$ does the transformation of bra vectors. Note that the ket-bra product completeness relation is clearly a scalar. (Recall Axiom 4.)

$$\mathbf{1} = \sum_m \left| \begin{matrix} j \\ m \end{matrix} \right\rangle \left\langle \begin{matrix} j \\ m \end{matrix} \right| \quad (24.2.16)$$

One needs to find which combinations of bras $\left\langle \begin{matrix} j \\ m' \end{matrix} \right|$ transform like a given ket $\left| \begin{matrix} j \\ m \end{matrix} \right\rangle$. This will yield the coefficients that make scalars out of ket-ket products since bra-kets are ready-made scalars by Axiom 4.

To this end, let us examine the transpose conjugate of D^j and use the fact that it is unitary.

$$\left[D^j(\alpha\beta\gamma) \right]^\dagger = \left[D^j(\alpha\beta\gamma) \right]^{-1} = D^j(-\gamma, -\beta, -\alpha), \quad (24.2.17)$$

If D-formula (23.1.15) is relabeled by $\alpha \rightarrow -\gamma$, $\gamma \rightarrow -\alpha$, $m \rightarrow -m'$, $m' \rightarrow -m$, we find the following:

$$D_{m'm}^j(\alpha\beta\gamma) = D_{-m', -m}^j(-\gamma, \beta, -\alpha). \quad (24.2.18)$$

Also, by substituting $\beta \rightarrow -\beta$, one obtains

$$D_{m'm}^j(\alpha, -\beta, \gamma) = (-1)^{-m+m'} D_{m'm}^j(\alpha\beta\gamma). \quad (24.2.19)$$

Combining the last three equations in turn gives

$$\begin{aligned} D_{mm'}^{j\dagger}(\alpha\beta\gamma) &= D_{mm'}^j(-\gamma, -\beta - \alpha), \\ D_{m'm}^{j*}(\alpha\beta\gamma) &= D_{-m', -m}^j(\alpha, -\beta, \gamma) = D_{-m', -m}^j(\alpha\beta\gamma) (-1)^{-m+m'} \end{aligned} \quad (24.2.20a)$$

This is substituted into Eq. (24.2.15):

$$\begin{aligned} \left\langle \begin{matrix} j \\ m \end{matrix} \right| R^\dagger(\alpha\beta\gamma) &= \sum_{m'} D_{-m', -m}^j(\alpha\beta\gamma) (-1)^{-m+m'} \left\langle \begin{matrix} j \\ m' \end{matrix} \right| \\ (-1)^{-m} \left\langle \begin{matrix} j \\ -m \end{matrix} \right| R^\dagger(\alpha\beta\gamma) &= \sum_{m'} D_{m', m}^j(\alpha\beta\gamma) (-1)^{-m'} \left\langle \begin{matrix} j \\ -m' \end{matrix} \right| \end{aligned} \quad (24.2.20b)$$

This shows that ket bases $|j_m\rangle$ transform like the following bra bases, to within an overall phase.

$$(-1)^{-m} \langle -m |^j \quad \text{or} \quad (-1)^{j-m} \langle -m |^j$$

An extra overall phase factor $(-1)^j$ does not affect the transformation. It is conventional to choose $(-1)^{j-m}$ as the phase factor since it is real even when j is half-integral. This sets the scalar coupling CGC of (24.2.12).

c. CGC Definitions and Symmetry Relations: The Wigner $3j$ Coefficient

Clebsch-Gordan coefficients CGC are components of unitary-orthogonal transformation matrices.

$$\sum_{m_1=-j_1}^{j_1} \sum_{m_2=-j_2}^{j_2} C_{m_1 m_2 m_3}^{j_1 j_2 j_3} C_{m_1 m_2 m_3'}^{j_1 j_2 j_3'} = \delta_{j_3 j_3'} \delta_{m_3 m_3'} = \sum_{m_1=-j_1}^{j_1} \sum_{m_2=-j_2}^{j_2} \langle j_3 |^j_{m_3} | j_1 j_2 \rangle \langle j_1 j_2 |^j_{m_1 m_2} | j_3 \rangle \quad (24.2.21)$$

The CGC therefore satisfy completeness relations, too.

$$\sum_{j_3=|j_1-j_2|}^{j_1+j_2} \sum_{m_3=-j_3}^{j_3} C_{m_1 m_2 m_3}^{j_1 j_2 j_3} C_{m_1' m_2' m_3}^{j_1 j_2 j_3} = \delta_{m_1 m_1'} \delta_{m_2 m_2'} = \sum_{j_3=|j_1-j_2|}^{j_1+j_2} \sum_{m_3=-j_3}^{j_3} \langle j_1 j_2 |^j_{m_1 m_2} | j_3 \rangle \langle j_3 |^j_{m_3} | j_1' j_2' \rangle \quad (24.2.22)$$

We shall use these relations with the fundamental D -matrix orthogonality relation (15.1.30).

$$\int d(\alpha\beta\gamma) D_{m'n'}^{j'*}(\alpha\beta\gamma) D_{mn}^j(\alpha\beta\gamma) = \delta^{j'j} \delta_{m'm} \delta_{n'n} / (2j+1)$$

Also, we need the reduction equation for $D^j \otimes D^j$. This is the generic form of (24.1.6).

$$\sum_{m_1 m_2} \sum_{m_1' m_2'} C_{m_1 m_2 m_3}^{j_1 j_2 j_3} D_{m_1 m_1'}^{j_1}(\alpha\beta\gamma) D_{m_2 m_2'}^{j_2}(\alpha\beta\gamma) C_{m_1' m_2' m_3'}^{j_1 j_2 j_3'} = \delta^{j_3 j_3'} D_{m_3 m_3'}^{j_3}(\alpha\beta\gamma) \quad (24.2.23)$$

From Eq. (24.2.22), the inverse reduction equation has a block-diagonal matrix become un-diagonal.

$$D_{m_1 m_1'}^{j_1}(\alpha\beta\gamma) D_{m_2 m_2'}^{j_2}(\alpha\beta\gamma) = \sum_{j_3=|j_1-j_2|}^{j_1+j_2} \sum_{m_3=-j_3}^{j_3} \sum_{m_3'=-j_3}^{j_3} C_{m_1 m_2 m_3}^{j_1 j_2 j_3} D_{m_3 m_3'}^{j_3}(\alpha\beta\gamma) C_{m_1' m_2' m_3'}^{j_1 j_2 j_3} \quad (24.2.24)$$

Then, applying D -matrix orthogonality gives what is called a D -matrix *factorization lemma*.

$$\int d(\alpha\beta\gamma) D_{m_3 m_3'}^{j_3*}(\alpha\beta\gamma) D_{m_1 m_1'}^{j_1}(\alpha\beta\gamma) D_{m_2 m_2'}^{j_2}(\alpha\beta\gamma) = C_{m_1 m_2 m_3}^{j_1 j_2 j_3} C_{m_1' m_2' m_3'}^{j_1 j_2 j_3} / (2j_3+1) \quad (24.2.25)$$

Our first use of this equation will be to suggest a more symmetric form of coupling coefficient. We shall need the conjugation relation from Eq. (24.2.20a).

$$D_{m_3 m'_3}^{j_3*} = (-1)^{j_3 - m_3 - j_3 + m'_3} D_{-m_3 - m'_3}^{j_3} = (-1)^{-j_3 + m_3 - j_3 + m'_3} D_{-m_3 - m'_3}^{j_3} \quad (24.2.26)$$

We also need to become familiar with some of the tricks of phase arithmetic. For example, one can often use the fact that a phase factor is positive or negative unity even if j_3 is half-integral.

$$(\pm 1) = (-1)^{j_3 - m_3} = (-1)^{-j_3 + m_3} = 1 / (\pm 1) \quad (24.2.27)$$

Note that if j_3 is half-integral then so is m_3 . Thus, $j_3 \pm m_3$ is an integer. Also, for any $(j_1 j_2 j_3)$ in $C^{j_1 j_2 j_3}$

$$1 = (-1)^{2j_1 + 2j_2 + 2j_3} = (-1)^{2j_1 + 2j_2 - 2j_3} = (-1)^{2j_1 - 2j_2 + 2j_3} \text{ etc.} \quad (24.2.28)$$

This follows since the number of half-integral j 's in $C^{j_1 j_2 j_3}$ must be *even*. Finally, we obtain

$$\begin{aligned} & \int d(a\beta y) D_{m_3 m'_3}^{j_3} (a\beta y) D_{m_1 m'_1}^{j_1} (a\beta y) D_{m_2 m'_2}^{j_2} (a\beta y) \\ &= \left(\frac{(-1)^{-j_3 - m_3} C_{m_1 m_2 - m_3}^{j_1 j_2 j_3}}{\sqrt{2j_3 + 1}} \right) \left(\frac{(-1)^{-j_3 - m'_3} C_{m'_1 m'_2 - m'_3}^{j_1 j_2 j_3}}{\sqrt{2j_3 + 1}} \right) \\ &= \left(\frac{(-1)^{-j_1 - j_2 - m_3} C_{m_1 m_2 - m_3}^{j_1 j_2 j_3}}{\sqrt{2j_3 + 1}} \right) \left(\frac{(-1)^{-j_1 - j_2 - m'_3} C_{m'_1 m'_2 - m'_3}^{j_1 j_2 j_3}}{\sqrt{2j_3 + 1}} \right). \end{aligned} \quad (24.2.29)$$

The last line added a unit factor $1 = (-1)^{2j_1 - 2j_2 + 2j_3}$. This suggests the conventional *Wigner 3j coefficient*:

$$\begin{pmatrix} j_1 & j_2 & j_3 \\ m_1 & m_2 & m_3 \end{pmatrix} \equiv (-1)^{j_1 - j_2 - m_3} C_{m_1 m_2 - m_3}^{j_1 j_2 j_3} / \sqrt{2j_3 + 1} \quad (24.2.30a)$$

Wigner 3-j coefficients have a D -factorization relation that is symmetric to permutations of j_1, j_2 , and j_3 .

$$\int d(a\beta y) D_{m_1 m'_1}^{j_1} (a\beta y) D_{m_2 m'_2}^{j_2} (a\beta y) D_{m_3 m'_3}^{j_3} (a\beta y) = \begin{pmatrix} j_1 & j_2 & j_3 \\ m_1 & m_2 & m_3 \end{pmatrix} \begin{pmatrix} j_1 & j_2 & j_3 \\ m'_1 & m'_2 & m'_3 \end{pmatrix} \quad (24.2.30b)$$

From Eq. (24.2.30) a number of obvious symmetry relations follow.

However, the phase relations for the individual coefficients are not so obvious, since they depend on the detailed definition of $C_{m_1 m_2 m_3}^{j_1 j_2 j_3}$ for different products. Wigner's definition is made so the following permutation

properties hold.

$$\begin{aligned} \begin{pmatrix} j_1 & j_2 & j_3 \\ m_1 & m_2 & m_3 \end{pmatrix} &= (-1)^{j_1 + j_2 + j_3} \begin{pmatrix} j_2 & j_1 & j_3 \\ m_2 & m_1 & m_3 \end{pmatrix} = (-1)^{j_1 + j_2 + j_3} \begin{pmatrix} j_3 & j_2 & j_1 \\ m_3 & m_2 & m_1 \end{pmatrix} = (-1)^{j_1 + j_2 + j_3} \begin{pmatrix} j_1 & j_3 & j_2 \\ m_1 & m_3 & m_2 \end{pmatrix} \\ &= \begin{pmatrix} j_3 & j_1 & j_2 \\ m_3 & m_1 & m_2 \end{pmatrix} = \begin{pmatrix} j_2 & j_3 & j_1 \\ m_2 & m_3 & m_1 \end{pmatrix}. \end{aligned} \quad (24.2.31)$$

Also, we have from Eqs. (24.2.30) and (24.2.20b),

$$\begin{pmatrix} j_1 & j_2 & j_3 \\ m_1 & m_2 & m_3 \end{pmatrix} = (-1)^{j_1+j_2+j_3} \begin{pmatrix} j_1 & j_2 & j_3 \\ -m_1 & -m_2 & -m_3 \end{pmatrix}. \quad (24.2.32)$$

The 3- j coefficients have simple symmetries that quickly produce relations for CGC $C_{m_1 m_2 m_3}^{j_1 j_2 j_3}$. For example, transposing the first two factors of a CGC gives the following.

$$\begin{aligned} C_{m_2 m_1 m_3}^{j_2 j_1 j_3} &= (-1)^{j_2-j_1+m_3} \sqrt{2j_3+1} \begin{pmatrix} j_2 & j_1 & j_3 \\ m_2 & m_1 & -m_3 \end{pmatrix} \\ &= (-1)^{j_2-j_1+m_3} \sqrt{2j_3+1} (-1)^{j_1+j_2+j_3} \begin{pmatrix} j_3 & j_2 & j_1 \\ m_1 & m_2 & -m_3 \end{pmatrix} \\ &= (-1)^{j_1+j_2-j_3} C_{m_1 m_2 m_3}^{j_1 j_2 j_3} \end{aligned} \quad (24.2.33)$$

For $j_1 = j_2 = j$ this gives an important special case of this relation:

$$C_{m_2 m_1 m_3}^j = (-1)^{2j-j_3} C_{m_1 m_2 m_3}^j \quad (24.2.34)$$

This we use to apply the Pauli principle. Pairing integral momentum $j_1 = j_2 = n$ makes even- j_3 states symmetric and odd- j_3 states anti-symmetric to permutation, and *vice-versa* for half-integral $j_1 = j_2 = n/2$. Recall that singlet- ($S=0$) is anti-symmetric for a $(1/2 \otimes 1/2)$ -pair in Fig. 24.1.1, but scalar- ($L=0$) is symmetric for a $(1 \otimes 1)$ pair of a $(p)^2$ configuration in Fig. 24.1.3 or Fig. 24.1.5.

A permutation of the second two factors gives the following relation:

$$C_{m_1 m_3 m_2}^{j_1 j_3 j_2} = (-1)^{j_2-j_3+m_1} \sqrt{\frac{2j_2+1}{2j_3+1}} C_{-m_1 m_2 m_3}^{j_1 j_2 j_3} \quad (24.2.35)$$

The CGC are unitary matrix components. The Wigner 3- j are not unitary *per-se*, but do manifest their permutation symmetry, rather nicely.

Point symmetry group coupling coefficients

Every symmetry group has tensor or outer-product algebra with Clebsch-Gordan coefficients (CGC) for its irreducible representations (irreps). For Abelian groups like C_2 and C_3 the CGC are quite simple, and it is not too much trouble to derive CGC for non-Abelian groups like D_3 , D_4 , and D_6 discussed in Ch. 15.

Indeed, the process of developing CGC algebra of point symmetry is a recursive one based on first dealing with that of the subgroups. Like many things in life, there is a hierarchy that one does well to at least acknowledge. This was true of the $R(3)$ and $U(2)$ symmetry algebra that has the z -axial Abelian sub-group symmetry of $R(2)$ in its family tree. Without first diagonalizing the \mathbf{J}_z operator, where would we be?

For Abelian groups, all irreps are *1-by-1* matrices and so are their outer products, which are simple arithmetic products. For the z -angular momentum group $R(2)$, the irreps are the plain old plane wave exponential functions $e^{-im\phi}$ of polar angle ϕ . Their outer products are just arithmetic products of $e^{-im\phi}$.

$$D^{(m_1)}(\phi) \otimes D^{(m_2)}(\phi) = D^{(m_1)}(\phi) \cdot D^{(m_2)}(\phi) = e^{-im_1\phi} \cdot e^{-im_2\phi} = e^{-i(m_1+m_2)\phi} = D^{(m_1+m_2)}(\phi)$$

In this case, all products are summed up by quantum angular momentum conservation: $(m_3) = (m_1 + m_2)$.

The same is true for the cyclic point groups like C_2 , C_3 , and, in general, C_N . Their outer products reduce to arithmetic modulo- N that was introduced in Chapter 7. Examples C_2 and C_3 are given.

$$C_2 : \begin{array}{c|cc} (m)_2 \otimes (n)_2 & (0)_2 & (1)_2 \\ \hline (0)_2 & (0)_2 & (1)_2 \\ (1)_2 & (1)_2 & (0)_2 \end{array}$$

(24.2.36a)

$$C_3 : \begin{array}{c|ccc} (m)_3 \otimes (n)_3 & (0)_3 & (1)_3 & (2)_3 \\ \hline (0)_3 & (0)_3 & (1)_3 & (2)_3 \\ (1)_3 & (1)_3 & (2)_3 & (0)_3 \\ (2)_3 & (2)_3 & (0)_3 & (1)_3 \end{array}$$

(24.2.36b)

C_N -Outer product tables look like C_N -group product tables with label $(m)_N$ in place of operator \mathbf{r}^m of C_N . The C_2 case is the fundamental Boolean C_2 -algebra of *even* (A), (g), or (A_1) and *odd* (B), (u), or (A_2) states.

$$C_\sigma : \begin{array}{c|cc} & (A) & (B) \\ \hline (A) & (A) & (B) \\ (B) & (B) & (A) \end{array} \quad (24.1.36c)$$

$$C_I : \begin{array}{c|cc} & (g) & (u) \\ \hline (g) & (g) & (u) \\ (u) & (u) & (g) \end{array} \quad (24.1.36d)$$

$$C_R : \begin{array}{c|cc} & A_1 & A_2 \\ \hline A_1 & A_1 & A_2 \\ A_2 & A_2 & A_1 \end{array} \quad (24.1.36e)$$

The three different “flavors” of C_2 -symmetry indicated here are that of permutation or *reflection* (C_σ), *inversion* (C_I), and *180°-rotation* (C_R), but to a mathematician, all C_2 are the same, that is, *isomorphic*.

Simple C_N -operators are building blocks of greater symmetries D_N , O_h , or $U(m)$ that contain them. Since C_N is Abelian (mutually commuting), it may belong to a maximal set of commuting observables that are diagonal or “quantized” together. Thus, C_N quantum numbers, along with those in a hierarchy of higher symmetry

operators, help to define and construct irreps and CGC. Derivation of D_3 irreps using a C_2 or C_3 based MSOCO is described in Section 15.2. Here, D_3 subgroup hierarchy is used to derive its CGC.

Outer products of D_3 irreps have traces or characters that are arithmetic products of the irreducible characters (15.1.13) repeated below.

$$\begin{array}{c|ccc}
 D_3 \text{ characters } \mathbf{g} = & \mathbf{1} & \{\mathbf{r}, \mathbf{r}^2\} & \{\mathbf{i}_1, \mathbf{i}_2, \mathbf{i}_3\} \\
 \hline
 \text{Trace} D^{A_1}(\mathbf{g}) = \chi^{A_1}(\mathbf{g}) & 1 & 1 & 1 \\
 \text{Trace} D^{A_2}(\mathbf{g}) = \chi^{A_2}(\mathbf{g}) & 1 & 1 & -1 \\
 \text{Trace} D^{E_1}_{x_2, y_2}(\mathbf{g}) = \chi^{E_1}(\mathbf{g}) & 2 & -1 & 0
 \end{array} \quad (15.1.13)_{\text{repeated}}$$

The outer product $D^{E_1}(\mathbf{g}) \otimes D^{E_1}(\mathbf{g})$ has a character set that is product of $\chi^{E_1}(\mathbf{g})$ and $\chi^{E_1}(\mathbf{g})$ for each class.

$$\begin{array}{c|ccc}
 \mathbf{g} = & \mathbf{1} & \{\mathbf{r}, \mathbf{r}^2\} & \{\mathbf{i}_1, \mathbf{i}_2, \mathbf{i}_3\} \\
 \hline
 \text{Trace} D^{E_1} \otimes D^{E_1}(\mathbf{g}) = \chi^{E_1}(\mathbf{g}) \cdot \chi^{E_1}(\mathbf{g}) & 4 & 1 & 0
 \end{array} \quad (24.2.27)$$

The product character set is a sum of the irreducible characters for irreps $D^{A_1}(\mathbf{g})$, $D^{A_2}(\mathbf{g})$, and $D^{E_1}(\mathbf{g})$.

$$\begin{array}{c|ccc}
 \chi^{A_1}(\mathbf{g}) & 1 & 1 & 1 \\
 \chi^{A_2}(\mathbf{g}) & 1 & 1 & -1 \\
 \chi^{E_1}(\mathbf{g}) & 2 & -1 & 0 \\
 \hline
 \chi^{E_1}(\mathbf{g}) \cdot \chi^{E_1}(\mathbf{g}) & 4 & 1 & 0
 \end{array} \quad \begin{array}{l}
 \text{implies :} \\
 (CGC)^\dagger D^{E_1}(\mathbf{g}) \otimes D^{E_1}(\mathbf{g})(CGC) = D^{A_1}(\mathbf{g}) \oplus D^{A_2}(\mathbf{g}) \oplus D^{E_1}(\mathbf{g})
 \end{array} \quad (24.2.38a)$$

So, outer product $D^{E_1}(\mathbf{g}) \otimes D^{E_1}(\mathbf{g})$ reduces by CGC transformation to block sum $D^{A_1}(\mathbf{g}) \oplus D^{A_2}(\mathbf{g}) \oplus D^{E_1}(\mathbf{g})$. Also, there is a CGC transformation of product $D^{E_1}(\mathbf{g}) \otimes D^{A_2}(\mathbf{g})$ back to the irrep $D^{E_1}(\mathbf{g})$.

$$\begin{array}{c|ccc}
 \chi^{E_1}(\mathbf{g}) & 2 & -1 & 0 \\
 \hline
 \chi^{E_1}(\mathbf{g}) \cdot \chi^{A_2}(\mathbf{g}) & 2 & -1 & 0
 \end{array} \quad \begin{array}{l}
 \text{implies :} \\
 (CGC)^\dagger D^{E_1}(\mathbf{g}) \otimes D^{A_2}(\mathbf{g})(CGC) = D^{E_1}(\mathbf{g})
 \end{array} \quad (24.2.38b)$$

No CGC are needed to transform product $D^{E_1}(\mathbf{g}) \otimes D^{A_1}(\mathbf{g}) = D^{E_1}(\mathbf{g})$ to irrep $D^{E_1}(\mathbf{g})$ since $D^{A_1}(\mathbf{g}) \equiv 1$.

Derivation of CGC requires us to first pick a sub-group hierarchy or MSOCO. Two possibilities in Fig. 15.2.1 are a *standing C_2 -wave* choice $C_2 = \{\mathbf{1}, \mathbf{i}_3\}$ or the *moving C_3 -wave* choice $C_3 = \{\mathbf{1}, \mathbf{r}, \mathbf{r}^2\}$. CGC for $E_1 \otimes E_1$ and $E_1 \otimes A_2$ must have the forms given below according to subgroup products (24.2.36a-b).

$$\begin{array}{c|ccc}
 \begin{array}{c} |E_1\rangle \\ |m_2\rangle \end{array} \begin{array}{c} |E_1\rangle \\ |n_2\rangle \end{array} & A_1 & A_2 & E_1 & E_1 \\
 & A & B & A & B \\
 \hline
 \begin{array}{c} |E_1\rangle \\ |A\rangle \end{array} \begin{array}{c} |E_1\rangle \\ |A\rangle \end{array} & a & \cdot & e & \cdot \\
 \begin{array}{c} |E_1\rangle \\ |A\rangle \end{array} \begin{array}{c} |E_1\rangle \\ |B\rangle \end{array} & \cdot & c & \cdot & g \\
 \begin{array}{c} |E_1\rangle \\ |B\rangle \end{array} \begin{array}{c} |E_1\rangle \\ |A\rangle \end{array} & \cdot & d & \cdot & h \\
 \begin{array}{c} |E_1\rangle \\ |B\rangle \end{array} \begin{array}{c} |E_1\rangle \\ |B\rangle \end{array} & b & \cdot & f & \cdot
 \end{array} \quad (24.2.39b)$$

$$\begin{array}{c|ccc}
 \begin{array}{c} |E_1\rangle \\ |m_3\rangle \end{array} \begin{array}{c} |E_1\rangle \\ |n_3\rangle \end{array} & A_1 & A_2 & E_1 & E_1 \\
 & 0_3 & 0_3 & 1_3 & 2_3 \\
 \hline
 \begin{array}{c} |E_1\rangle \\ |1_3\rangle \end{array} \begin{array}{c} |E_1\rangle \\ |1_3\rangle \end{array} & \cdot & \cdot & \cdot & \phi \\
 \begin{array}{c} |E_1\rangle \\ |1_3\rangle \end{array} \begin{array}{c} |E_1\rangle \\ |2_3\rangle \end{array} & \alpha & \gamma & \cdot & \cdot \\
 \begin{array}{c} |E_1\rangle \\ |2_3\rangle \end{array} \begin{array}{c} |E_1\rangle \\ |1_3\rangle \end{array} & \beta & \delta & \cdot & \cdot \\
 \begin{array}{c} |E_1\rangle \\ |2_3\rangle \end{array} \begin{array}{c} |E_1\rangle \\ |2_3\rangle \end{array} & \cdot & \cdot & \varepsilon & \cdot
 \end{array} \quad (24.2.39b)$$

$$\begin{array}{c|cc}
 \begin{array}{c} |E_1\rangle \\ |m_2\rangle \end{array} \begin{array}{c} |A_2\rangle \\ |n_2\rangle \end{array} & E_1 & E_1 \\
 & A & B \\
 \hline
 \begin{array}{c} |E_1\rangle \\ |A\rangle \end{array} \begin{array}{c} |A_2\rangle \\ |B\rangle \end{array} & \cdot & x \\
 \begin{array}{c} |E_1\rangle \\ |B\rangle \end{array} \begin{array}{c} |A_2\rangle \\ |B\rangle \end{array} & y & \cdot
 \end{array} \quad (24.2.39c)$$

$$\begin{array}{c|cc}
 \begin{array}{c} |E_1\rangle \\ |m_3\rangle \end{array} \begin{array}{c} |A_2\rangle \\ |n_3\rangle \end{array} & E_1 & E_1 \\
 & 1_3 & 2_3 \\
 \hline
 \begin{array}{c} |E_1\rangle \\ |1_3\rangle \end{array} \begin{array}{c} |A_2\rangle \\ |0_3\rangle \end{array} & \kappa & \cdot \\
 \begin{array}{c} |E_1\rangle \\ |2_3\rangle \end{array} \begin{array}{c} |A_2\rangle \\ |0_3\rangle \end{array} & \cdot & \lambda
 \end{array} \quad (24.2.39d)$$

To find coefficients a, b, \dots we solve a CGC- D equation for one operator \mathbf{g} *not* in the MSOCO of the D .

$$(D^{E_1} \otimes D^{E_1}(\mathbf{g})) \cdot [CGC] = [CGC] \cdot (D^{A_1}(\mathbf{g}) \oplus D^{A_2}(\mathbf{g}) \oplus D^{E_1}(\mathbf{g}))$$

Standing wave $D_{m_2 n_2}^{E_1}$ may pick $\mathbf{r}, \mathbf{r}^2, \mathbf{i}_1$, or \mathbf{i}_2 , *i.e.*, any but diagonal $\mathbf{1}$ or \mathbf{i}_3 in a $D_{m_2 n_2}^{E_1}$ -MSOCO. Let's pick \mathbf{r} .

$$\begin{aligned}
 (D^{E_1} \otimes D^{E_1}(\mathbf{r})) \cdot [CGC] &= [CGC] \cdot (D^{A_1}(\mathbf{r}) \oplus D^{A_2}(\mathbf{r}) \oplus D^{E_1}(\mathbf{r})) \\
 \frac{1}{4} \begin{pmatrix} 1 & \sqrt{3} & \sqrt{3} & 3 \\ -\sqrt{3} & 1 & -3 & \sqrt{3} \\ -\sqrt{3} & -3 & 1 & \sqrt{3} \\ 3 & -\sqrt{3} & -\sqrt{3} & 1 \end{pmatrix} \begin{bmatrix} a & \cdot & e & \cdot \\ \cdot & c & \cdot & g \\ \cdot & d & \cdot & h \\ b & \cdot & f & \cdot \end{bmatrix} &= \begin{bmatrix} a & \cdot & e & \cdot \\ \cdot & c & \cdot & g \\ \cdot & d & \cdot & h \\ b & \cdot & f & \cdot \end{bmatrix} \begin{pmatrix} 1 & & & \\ & 1 & & \\ & & -1/2 & -\sqrt{3}/2 \\ & & -\sqrt{3}/2 & -1/2 \end{pmatrix} \\
 \frac{1}{4} \begin{pmatrix} a+3b & \sqrt{3}(c+d) & e+3f & \sqrt{3}(g+h) \\ \sqrt{3}(b-a) & c-3d & \sqrt{3}(f-e) & g-3h \end{pmatrix} &= \begin{pmatrix} a & 0 & -e/2 & -\sqrt{3}e/2 \\ 0 & c & \sqrt{3}e/2 & -g/2 \end{pmatrix} \quad \text{Solution: } \begin{cases} a=b \\ c=-d \\ e=-g=-f \\ h=g=f \end{cases}
 \end{aligned}$$

Moving wave $D_{m_3 n_3}^{E_1}$ may pick $\mathbf{i}_1, \mathbf{i}_2$, or \mathbf{i}_3 , *i.e.*, any but diagonal $\mathbf{1}, \mathbf{r}$, or \mathbf{r}^2 . Let's pick \mathbf{i}_3 .

$$\begin{aligned}
 (D^{E_1} \otimes D^{E_1}(\mathbf{i}_3)) \cdot [CGC] &= [CGC] \cdot (D^{A_1}(\mathbf{i}_3) \oplus D^{A_2}(\mathbf{i}_3) \oplus D^{E_1}(\mathbf{i}_3)) \\
 \begin{pmatrix} 0 & 0 & 0 & 1 \\ 0 & 0 & 1 & 0 \\ 0 & 1 & 0 & 0 \\ 1 & 0 & 0 & 0 \end{pmatrix} \begin{bmatrix} \cdot & \cdot & \cdot & \phi \\ \alpha & \gamma & \cdot & \cdot \\ \beta & \delta & \cdot & \cdot \\ \cdot & \cdot & \varepsilon & \cdot \end{bmatrix} &= \begin{bmatrix} \cdot & \cdot & \cdot & \phi \\ \alpha & \gamma & \cdot & \cdot \\ \beta & \delta & \cdot & \cdot \\ \cdot & \cdot & \varepsilon & \cdot \end{bmatrix} \begin{pmatrix} 1 & & & \\ & -1 & & \\ & & 0 & 1 \\ & & 1 & 0 \end{pmatrix} \\
 \begin{pmatrix} 0 & 0 & \varepsilon & 0 \\ \beta & \delta & 0 & 0 \\ \alpha & \gamma & 0 & 0 \\ 0 & 0 & 0 & \phi \end{pmatrix} &= \begin{pmatrix} 0 & 0 & \phi & 0 \\ \alpha & -\gamma & 0 & 0 \\ \beta & -\delta & 0 & 0 \\ 0 & 0 & 0 & \varepsilon \end{pmatrix} \quad \text{Solution: } \begin{cases} \alpha=\beta \\ \gamma=-\delta \\ \varepsilon=\phi \end{cases}
 \end{aligned}$$

Resolving unknowns x, y or κ, λ of product $D^{E_1} \otimes D^{A_2}$ is done the same way.

$$\begin{aligned}
 (D^{E_1} \otimes D^{A_2}(\mathbf{r})) \cdot [CGC] &= [CGC] \cdot (D^{E_1}(\mathbf{r})) & (D^{E_1} \otimes D^{A_2}(\mathbf{i}_3)) \cdot [CGC] &= [CGC] \cdot (D^{E_1}(\mathbf{i}_3)) \\
 \frac{1}{2} \begin{pmatrix} -1 & -\sqrt{3} \\ \sqrt{3} & -1 \end{pmatrix} \cdot \begin{bmatrix} \cdot & y \\ x & \cdot \end{bmatrix} &= \begin{bmatrix} \cdot & y \\ x & \cdot \end{bmatrix} \cdot \frac{1}{2} \begin{pmatrix} -1 & -\sqrt{3} \\ \sqrt{3} & -1 \end{pmatrix} & \begin{pmatrix} 0 & 1 \\ 1 & 0 \end{pmatrix} (-1) \cdot \begin{bmatrix} \kappa & \cdot \\ \cdot & \lambda \end{bmatrix} &= \begin{bmatrix} \kappa & \cdot \\ \cdot & \lambda \end{bmatrix} \cdot \begin{pmatrix} 0 & 1 \\ 1 & 0 \end{pmatrix} \\
 \begin{pmatrix} -\sqrt{3}x & -y \\ -x & \sqrt{3}y \end{pmatrix} = \begin{pmatrix} \sqrt{3}y & -y \\ -x & -\sqrt{3}x \end{pmatrix} & \text{Solution: } \{x = -y\} & \begin{pmatrix} 0 & -\lambda \\ -\kappa & 0 \end{pmatrix} = \begin{pmatrix} 0 & \kappa \\ \lambda & 0 \end{pmatrix} & \text{Solution: } \{\kappa = -\lambda\}
 \end{aligned}$$

The preceding solutions give “red” and “green” CGC up to an overall normalization and phase factor.

$ E_1\rangle E_1\rangle$	$ E_1\rangle E_1\rangle$	A_1	A_2	E_1	E_1	
$ m_2\rangle n_2\rangle$	$ A\rangle A\rangle$	A	B	A	B	
$ A\rangle A\rangle$	$ A\rangle A\rangle$	$\frac{1}{\sqrt{2}}$	\cdot	$\frac{1}{\sqrt{2}}$	\cdot	(24.2.40a)
$ A\rangle B\rangle$	$ B\rangle A\rangle$	\cdot	$\frac{1}{\sqrt{2}}$	\cdot	$\frac{-1}{\sqrt{2}}$	
$ B\rangle A\rangle$	$ A\rangle B\rangle$	\cdot	$\frac{-1}{\sqrt{2}}$	\cdot	$\frac{-1}{\sqrt{2}}$	
$ B\rangle B\rangle$	$ B\rangle B\rangle$	$\frac{1}{\sqrt{2}}$	\cdot	$\frac{-1}{\sqrt{2}}$	\cdot	

$ E_1\rangle E_1\rangle$	$ E_1\rangle E_1\rangle$	A_1	A_2	E_1	E_1	
$ m_3\rangle n_3\rangle$	$ 1_3\rangle 1_3\rangle$	0_3	0_3	1_3	2_3	
$ 1_3\rangle 1_3\rangle$	$ 1_3\rangle 1_3\rangle$	\cdot	\cdot	\cdot	1	(24.2.40b)
$ 1_3\rangle 2_3\rangle$	$ 2_3\rangle 1_3\rangle$	$\frac{1}{\sqrt{2}}$	$\frac{1}{\sqrt{2}}$	\cdot	\cdot	
$ 2_3\rangle 1_3\rangle$	$ 1_3\rangle 2_3\rangle$	$\frac{1}{\sqrt{2}}$	$\frac{-1}{\sqrt{2}}$	\cdot	\cdot	
$ 2_3\rangle 2_3\rangle$	$ 2_3\rangle 2_3\rangle$	\cdot	\cdot	1	\cdot	

$ E_1\rangle A_2\rangle$	$ E_1\rangle E_1\rangle$	E_1	E_1	
$ m_2\rangle n_2\rangle$	$ A\rangle B\rangle$	A	B	
$ A\rangle B\rangle$	$ B\rangle A\rangle$	\cdot	1	(24.2.40c)
$ B\rangle B\rangle$	$ B\rangle B\rangle$	-1	\cdot	

$ E_1\rangle A_2\rangle$	$ E_1\rangle E_1\rangle$	E_1	E_1	
$ m_3\rangle n_3\rangle$	$ 1_3\rangle 0_3\rangle$	1_3	2_3	
$ 1_3\rangle 0_3\rangle$	$ 0_3\rangle 1_3\rangle$	-1	\cdot	(24.2.40d)
$ 2_3\rangle 0_3\rangle$	$ 0_3\rangle 2_3\rangle$	\cdot	1	

As before, choice of CGC phases can be annoyingly arbitrary. CGC- D equations only fix *relative* phases *within* each irrep, but not *between* them. For example, the moving wave solution is quite explicit in that $\kappa = -\lambda$ and normalization requires $|\kappa|^2 = 1 = |-\lambda|^2$. But, *overall* phase allows either the (+)-real solution $\kappa = 1 = -\lambda$ or the (-)-one chosen in (24.2.40d) $\kappa = -1 = -\lambda$, or else, a continuum of complex choices.

The 1st and 2nd columns of (24.2.40b) used solutions $\alpha = \beta$ and $\gamma = -\delta$ each of which come with an implied orthonormality $|\alpha|^2 + |\beta|^2 = 1 = |\gamma|^2 + |\delta|^2$. The choice $\alpha = 1/\sqrt{2} = \beta$ could also have been its negative

$\alpha = -1/\sqrt{2} = \beta$, or it could be a complex CGC, $\alpha = e^{i\phi}/\sqrt{2} = \beta$, with no regard to the choice $\gamma = 1/\sqrt{2} = -\delta$ that is made in the 3rd and 4th columns of (24.2.40b). Again, overall phase of each irrep basis is arbitrary.

Because the 3rd and 4th columns of (24.2.40d) belong to the same irrep $D_{m_3 n_3}^{E_1}$ of D_3 , their *relative* phase (and norm) is linked by $\varepsilon = \phi$. No such linking occurs between the 1st and 2nd columns, which belong to different irreps $D_{0,0,3}^{A_1}$ and $D_{0,0,3}^{A_2}$ of D_3 . So CGC for the $E_1 \otimes E_1$ product has three undetermined overall phases, one for each of three irreps A_1 , A_2 , and E_1 yielded by $E_1 \otimes E_1 = A_1 \oplus A_2 \oplus E_1$.

Such “loose” overall phase factors get pinned down when they become internal and relative to those of components belonging to symmetry higher up in a sub-group hierarchy. When D_3 is a subgroup of a higher group like D_6 or O_h or $U(2)$ then its irreps are just components of a bigger irrep and have to obey whatever phase rules that super-symmetry demands. But, always the highest group in any chain gets to do whatever it pleases with its *overall* phases!

An important job for CGC analysis is to produce invariant or scalar functions. Those can be wave functions, potentials, or other kinds of operators. As an example, let us construct a third-degree scalar polynomial in Cartesian coordinates (x,y) that is invariant to D_3 symmetry operation.

This is done using CGC products of $x = x_1^E$ and $y = x_2^E$ which are the bases of the xy -standing wave irrep $D_{m_2 n_2}^{E_1}$ of D_3 . Before applying CGC, one must be certain that the objects used in the product, $x = x_1^E$ and $y = x_2^E$ in this case, do indeed belong to the $D_{m_2 n_2}^{E_1}$ and CGC that we think they do. As cautioned at the beginning of Sec. 2.2, one does well to begin with base vector definitions of symmetry operations. In this case that would involve Cartesian base vectors that transform under D_3 operations like $D_{m_2 n_2}^{E_1}$.

$$\begin{aligned} \mathbf{r} \cdot \hat{\mathbf{x}} = \mathbf{r} \cdot \mathbf{e}_x^E &= D_{x,x}^E(r) \mathbf{e}_x^E + D_{y,x}^E(r) \mathbf{e}_y^E = \frac{-1}{2} \mathbf{e}_x^E + \frac{\sqrt{3}}{2} \mathbf{e}_y^E & \mathbf{i}_3 \cdot \mathbf{e}_x^E &= D_{x,x}^E(i_3) \mathbf{e}_x^E + D_{y,x}^E(i_3) \mathbf{e}_y^E = (+1) \mathbf{e}_x^E + (0) \mathbf{e}_y^E \\ \mathbf{r} \cdot \hat{\mathbf{y}} = \mathbf{r} \cdot \mathbf{e}_y^E &= D_{x,y}^E(r) \mathbf{e}_x^E + D_{y,y}^E(r) \mathbf{e}_y^E = \frac{-\sqrt{3}}{2} \mathbf{e}_x^E + \frac{1}{2} \mathbf{e}_y^E & \mathbf{i}_3 \cdot \mathbf{e}_y^E &= D_{x,y}^E(i_3) \mathbf{e}_x^E + D_{y,y}^E(i_3) \mathbf{e}_y^E = (0) \mathbf{e}_x^E + (-1) \mathbf{e}_y^E \end{aligned}$$

This is the same definition (15.1.10) of $D_{m_2 n_2}^{E_1}$ as first used in Chapter 15 discussion of D_3 .

$$\begin{pmatrix} \mathbf{e}_x^E \cdot \mathbf{r} \cdot \mathbf{e}_x^E & \mathbf{e}_x^E \cdot \mathbf{r} \cdot \mathbf{e}_y^E \\ \mathbf{e}_y^E \cdot \mathbf{r} \cdot \mathbf{e}_x^E & \mathbf{e}_y^E \cdot \mathbf{r} \cdot \mathbf{e}_y^E \end{pmatrix} = \begin{pmatrix} \frac{-1}{2} & \frac{-\sqrt{3}}{2} \\ \frac{\sqrt{3}}{2} & \frac{-1}{2} \end{pmatrix} \quad (24.2.41a)$$

$$= \begin{pmatrix} D_{x,x}^E(r) & D_{x,y}^E(r) \\ D_{y,x}^E(r) & D_{y,y}^E(r) \end{pmatrix}$$

$$\begin{pmatrix} \mathbf{e}_x^E \cdot \mathbf{i}_3 \cdot \mathbf{e}_x^E & \mathbf{e}_x^E \cdot \mathbf{i}_3 \cdot \mathbf{e}_y^E \\ \mathbf{e}_y^E \cdot \mathbf{i}_3 \cdot \mathbf{e}_x^E & \mathbf{e}_y^E \cdot \mathbf{i}_3 \cdot \mathbf{e}_y^E \end{pmatrix} = \begin{pmatrix} 1 & 0 \\ 0 & -1 \end{pmatrix} \quad (24.2.41b)$$

$$= \begin{pmatrix} D_{x,x}^E(i_3) & D_{x,y}^E(i_3) \\ D_{y,x}^E(i_3) & D_{y,y}^E(i_3) \end{pmatrix}$$

We use the ‘‘alias’’ view so coordinates and bases transform to represent the *same* vector **P**.

$$\mathbf{P} = x_i \mathbf{e}_i^E = x_j(r) \mathbf{e}_j^E(r) = x_k(i) \mathbf{e}_k^E(i) = \dots \quad (24.2.42)$$

(Repeated indices imply sum.) In that view, real coordinates transform just as their base vectors do.

$$x_j(r) = \mathbf{P} \cdot \mathbf{e}_j^E(r) = x_i \mathbf{e}_i^E \cdot \mathbf{e}_j^E(r) = x_i \mathbf{e}_i^E \cdot \mathbf{r} \cdot \mathbf{e}_j^E = x_i D_{i,j}^E(r), \quad x_j(i_3) = x_i D_{i,j}^E(i_3), \dots \quad (24.2.43)$$

Then D_3 CGC (24.2.40a) give E and A -symmetry-defined quadratic and cubic polynomial functions.

$$\begin{aligned} [x^E \otimes x^E]_x^E &= C_{a b x}^{EEE} x_a^E x_b^E = \frac{x^2 - y^2}{\sqrt{2}} & [[x^E \otimes x^E]^E \otimes x^E]^{A_1} &= C_{a b A}^{EEA_1} [x^E \otimes x^E]_a^E x_b^E = \frac{x^3 - 3xy^2}{2} \\ [x^E \otimes x^E]_y^E &= C_{a b y}^{EEE} x_a^E x_b^E = \frac{-2xy}{\sqrt{2}} & [[x^E \otimes x^E]^E \otimes x^E]^{A_2} &= C_{a b B}^{EEA_2} [x^E \otimes x^E]_a^E x_b^E = \frac{3x^2y - y^3}{2} \end{aligned}$$

Scalar cubic A_1 is \mathbf{i}_3 -symmetric and pseudo-scalar A_2 is \mathbf{i}_3 -anti-symmetric as seen in Fig. 24.2.1.

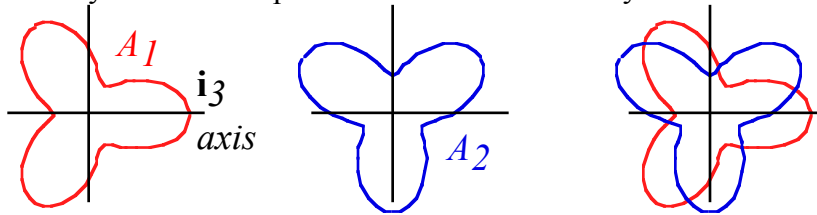


Fig. 24.2.1

24.3 Clebsch-Gordon and Wigner Coefficient Formulas

The connection between two-dimensional oscillator symmetry $U(2)$ and three-dimensional $R(3)$ -rotation begins in Ch. 10. Quantum two-dimensional oscillator states and three-dimensional angular momentum states are related in Section 21.2 and detailed in Sec. 23.1. [Recall (23.1.5).] Schwinger-Jordan boson creation operator algebra gives a formula (23.1.15) for $U(2)$ irreducible representation or irrep $D_{mm}^j(\alpha\beta\gamma)$. Here the same methods are used to

derive $C_{m_1 m_2 m_3}^{j_1 j_2 j_3}$ formulas for Clebsch-Gordan coefficients (CGC).

a. The A-and-B-Boson states

The product states $|j_1 m_1\rangle_A |j_2 m_2\rangle_B$ use two pairs of oscillator operators. One pair $\{a_\uparrow^\dagger \equiv a_1^\dagger, a_\downarrow^\dagger \equiv a_2^\dagger\}$ for boson- A ,

are spin-1/2 creation operators for momentum j_1 . The second pair $\{b_\uparrow^\dagger \equiv a_1^\dagger, b_\downarrow^\dagger \equiv a_2^\dagger\}$ for boson- B , are spin-1/2

creation operators for momentum j_2 . Note the change in notation. Creation operators a_i^j are indicated without the dagger (\dagger). Here we do more creating than destroying, and so it is silly to have to write a dagger \dagger over and over. For destruction operators $(a_i^j)^\dagger \equiv \bar{a}_i^j$ we replace the knife with a “lid” ($\bar{}$). (One wonders, “Why was a creation operation ever denoted by a murder weapon!”)

The product state consists of generalization of (23.1.4) in which the oscillator boson analogy is used once for the angular-momentum j_1 state of particle A and then again for the j_2 state of particle B .

$$\left| \begin{matrix} j_1 & j_2 \\ m_1 & m_2 \end{matrix} \right\rangle = \frac{(a_1^1)^{j_1+m_1} (a_2^1)^{j_1-m_1} (a_1^2)^{j_2+m_2} (a_2^2)^{j_2-m_2}}{\sqrt{(j_1+m_1)!(j_1-m_1)!} \sqrt{(j_2+m_2)!(j_2-m_2)!}} |00;00\rangle = |j_1+m_1, j_1-m_1; j_2+m_2, j_2-m_2\rangle. \quad (24.3.1)$$

The empty ket $|00,00\rangle$ denotes the vacuum zero angular momentum or “unoccupied” state.

We want to make states $\left| \begin{matrix} j \\ m \end{matrix} \right\rangle$ that are eigenvectors of definite total angular momentum using A and B pairs of creation-operators. Derivation of the D -matrix is based on the (a^\dagger) -operator formula (23.1.12b) for the fundamental $(D_{m,n}^{1/2} = u_{m,n})$ -transformation in terms of a -operators.

$$\begin{aligned} a_1'^k &= u_{11}a_1^k + u_{21}a_2^k \\ a_2'^k &= u_{12}a_1^k + u_{22}a_2^k \quad (j = 1, 2 \text{ or } A, B). \end{aligned} \quad (24.3.2)$$

Here, u_{ij} are components of a general *unitary* ($u^\dagger = u^{-1}$) *unimodular* ($\det |u| = 1$) two-by-two matrix where u is an element of $SU(2)$. The u -transformation of creation operators gives irrep $D^j(u)$ of $U(2)$ in (23.1.15a).

$$D_{mn}^j \begin{pmatrix} u_{11} & u_{12} \\ u_{21} & u_{22} \end{pmatrix} = \sum_k \frac{\sqrt{(j+n)!(j-n)!(j+m)!(j-m)!}}{(j-k+m)!(k-m+n)!k!(j-n-k)!} (u_{11})^{j-k+m} (u_{21})^{k-m+n} (u_{12})^k (u_{22})^{j-n-k} \quad (24.3.3)$$

A product of representations is a representation of products: $D^j(u)D^j(v) = D^j(uv) \equiv D^j(w)$.

$$\sum_n D_{mn}^j \begin{pmatrix} u_{11} & u_{12} \\ u_{21} & u_{22} \end{pmatrix} D_{nl}^j \begin{pmatrix} v_{11} & v_{12} \\ v_{21} & v_{22} \end{pmatrix} = D_{ml}^j \begin{pmatrix} w_{11} & w_{12} \\ w_{21} & w_{22} \end{pmatrix}, \quad (24.3.4a)$$

where

$$\sum_{j=1}^2 u_{ij}v_{jk} = w_{ik} \quad (24.3.4b)$$

Here is a *big* trick. Let each u_{ij} be replaced by creation operator a_i^j to define a *boson polynomial*.

$$B_{m,n}^j(a) = \sum_k \frac{\sqrt{(j+n)!(j-n)!(j+m)!(j-m)!/(2j)!}}{(j-k+m)!(k-m+n)!k!(j-n-k)!} (a_1^1)^{j-k+m} (a_2^1)^{k-m+n} (a_1^2)^k (a_2^2)^{j-n-k} \quad (24.3.5)$$

The boson polynomial $B_{m,n}^j$ is the same as $D_{mn}^j(a)$ with (a) replacing (u) . (A factor $\sqrt{1/(2j)!}$ normalizes $2j$ bosons.)

The result is a polynomial that has the correct transformation properties of a total angular-momentum state $|j_m\rangle$.

To see this, consider the polynomial made of transformed (a') operators given by (24.3.2). Here a' is written as a matrix product. The tilde (\sim) denotes a matrix transpose.

$$a' = \tilde{u} \cdot a, \quad \text{where: } \tilde{u}_{ij} = u_{ji}. \quad (24.3.6)$$

The representation equation $D^j(\tilde{u}a) = D^j(\tilde{u})D^j(a)$ is a transformation of the B^j -polynomial.

$$B_{mn}^j(\tilde{u}a) = \sum_{m'} D_{m'm}^j(\tilde{u}) B_{m'n}^j(a) \quad (24.3.7)$$

$$B_{mn}^j(a') = \sum_{m'} D_{m'm}^j(u) B_{m'n}^j(a), \quad (24.3.8)$$

Unitarity $D^j(u^\dagger) = D^j(u)^\dagger$ and conjugation $D^j(u^*) = D^j * (u)$ require $D_{m,n}^j(\tilde{u}) = D_{n,m}^j(u)$. A B^j -polynomial transforms

by D^j as spin components [$1 = \text{“up”}$ (\uparrow), $2 = \text{“down”}$ (\downarrow)] are mixed by the *same* u_{ij} according to (24.3.2) for *both* boson- A and boson- B . The fundamental spin-1/2 *up-down*-mixing then generates a rigid rotation of bosons A and B together in a coupled (j,m) -state of angular momentum.

The B^j -polynomial also transforms irreducibly under transformations that mix boson “ A -ness” and “ B -ness” of the two different particles in a transformation analogous to (24.3.2)

$$\begin{aligned} a_m'^1 &= v_{11}a_m^1 + v_{21}a_m^2, \\ a_m'^2 &= v_{12}a_m^1 + v_{22}a_m^2 \quad (m = 1, 2 \text{ or } \uparrow, \downarrow), \end{aligned} \quad (24.3.9a)$$

$$\text{In matrix notation this is:} \quad a' = a \cdot v. \quad (24.3.9b)$$

The representation multiplication rules (24.3.4) lead to the following transformation properties:

$$B_{mn}^j(a') = B_{mn}^j(a \cdot v) = \sum_{n'} B_{mn'}^j(a) D_{n'n}^j(v). \quad (24.3.10)$$

Thus, there are dual commuting groups of transformations for the system. The right-and-left-transformation laws (24.3.8) and (24.3.10) are analogous to “laboratory” and “body” transformations (23.1.20a-b). A transformation group $U(2) = \{\dots u \dots\}$ of states commutes with a transformation group $\bar{U}(2) = \{\dots v \dots\}$ of

particles, and together they are labeled $U_2 \times \bar{U}_2$ or $U_2 * \bar{U}_2$. The modified cross-product (*) notation is used to indicate that the two groups share a common irrep D^j .

A normalized j -state results if the boson creation operator (24.3.5) is applied to the vacuum:

$$\left| \begin{matrix} j \\ mn \end{matrix} \right\rangle = B_{mn}^j(a) |00,00\rangle = \sqrt{\frac{(j+m)!(j-m)!}{(2j)!}} \sum_k \sqrt{\frac{(j+n)!(j-n)!}{(n_1^1)!(n_2^1)!(n_1^2)!(n_2^2)!}} |n_1^1 n_2^1, n_1^2 n_2^2\rangle \quad (24.3.11a)$$

The occupation numbers $n_m^1 = n_m^A$ of “ A -ons” or $n_m^2 = n_m^B$ of “ B -ons” in state m are from (24.3.5).

$$n_1^1 = j + m - k, \quad n_2^1 = n - m + k, \quad n_1^2 = k, \quad n_2^2 = j - n - k. \quad (24.3.11b)$$

The following oscillator creation rules are used. [Recall Eqs. (21.1.15a) or (23.1.5e).]

$$(a_1^1)^{n_1^1} (a_2^1)^{n_2^1} (a_1^2)^{n_1^2} (a_2^2)^{n_2^2} |00,00\rangle = \sqrt{(n_1^1)!(n_2^1)!(n_1^2)!(n_2^2)!} |n_1^1 n_2^1, n_1^2 n_2^2\rangle$$

The normalization is verified by evaluating the j -state scalar product.

$$\left\langle \begin{matrix} j \\ mn \end{matrix} \middle| \begin{matrix} j \\ mn \end{matrix} \right\rangle = \frac{(j+m)!(j-m)!}{2j!} \sum_k \frac{(j+n)!}{(j+m-k)!(n-m+k)!} \frac{(j-n)!}{k!(j-n-k)!},$$

Orthonormality relations for oscillator eigenstates are assumed.

$$\langle a'b', c'd' | ab, cb \rangle = \delta_{a'a} \delta_{b'b} \delta_{c'c} \delta_{d'd}$$

A binomial coefficients relation $\binom{p}{m} = p! / m!(p-m)!$ is used to do the sum.

$$\sum_m \binom{p}{m} \binom{q}{s-m} = \binom{p+q}{s} \quad (24.3.12)$$

This relation is obtained by equating terms of binomial expansions:

$$(x+y)^{p+q} = \sum_x \binom{p+q}{s} x^s x^{p+q-s} = (x+y)^p (x+y)^q$$

The desired normalization is then proven.

$$\left\langle \begin{matrix} j \\ mn \end{matrix} \middle| \begin{matrix} j \\ mn \end{matrix} \right\rangle = \frac{(j+m)!(j-m)!}{(2j)!} \sum_k \binom{j+n}{j+m-k} \binom{j-n}{k} = \frac{(j+m)!(j-m)!}{(2j)!} \binom{2j}{j+m} = 1$$

The j -state (24.3.11) is made of exactly $(2j)$ bosons, the minimum number of spin-1/2 particles needed to make total angular momentum j . Each spin-1/2 counts toward the total, and so we call it an *all-count* state.

b. Scalar “no-count” states

The opposite of an all-count state is a *no-count* state that ends up with *zero* angular momentum. The smallest no-count state is an anti-symmetric singlet made by an $N=2$ boson determinant.

$$\det(a) \equiv D(a) \equiv a_1^1 a_2^2 - a_2^1 a_1^2. \quad (24.3.13)$$

$D(a)$ is invariant to transformations u and v in $SU_2 \times SU_2$, that is, unimodular ones $\det u = 1 = \det v$. We use elementary properties of determinants: $\det |A \cdot B| = \det |A| \cdot \det |B|$ and $\det |\tilde{A}| = \det |A|$.

$$\det(\tilde{u}av) = \det(\tilde{u}) \det(v) \det(a) = \det(a) \quad (24.3.14)$$

A “no-count” scalar ($j = 0$) state with ($N = 2d$) bosons is as follows.

$$\begin{aligned} \left| \begin{matrix} j=0 \\ 0,0 \end{matrix} \right\rangle_{N=2d} &= \frac{(a_1^2 a_2^2 - a_2^1 a_1^2)^{2d}}{\sqrt{(2d)!(2d+1)!}} |00;00\rangle = \sum_r \binom{2d}{r} \frac{(a_1^1 a_2^2)^r (-a_2^1 a_1^2)^{2d-r}}{\sqrt{(2d)!(2d+1)!}} |00;00\rangle \\ &= \sum_r (2d)! \frac{(-1)^r |r r; 2d-r \ 2d-r\rangle}{\sqrt{(2d)!(2d+1)!}} = \sum_r (-1)^r \frac{|r r; 2d-r \ 2d-r\rangle}{\sqrt{2d+1}} \end{aligned} \quad (24.3.15)$$

The sum over r contains $(2d + 1)$ terms, so the normalization of the scalar state is verified by having

$\langle j = 0 | j = 0 \rangle = 1$. No-count states are used to make general *N-boson j-coupled states* $\left| \begin{matrix} j_1 \ j_2 \\ m_1 \ m_2 \end{matrix} \right\rangle^{jN}$ by putting $(N-2j)$ no-count bosons (24.3.15) with $(2j)$ bosons in an all-count state (24.3.11) to satisfy three criteria.

First, the number n_\uparrow of spin-up minus the number n_\downarrow spin-down is the same for $\left| \begin{matrix} j_1 \ j_2 \\ m_1 \ m_2 \end{matrix} \right\rangle$ and $\left| \begin{matrix} j \ N \\ m \ n \end{matrix} \right\rangle$.

$$m_1 + m_2 = m = (n_\uparrow - n_\downarrow) / 2 \quad (24.3.16b)$$

That is total spin z -component m or J_z -eigenvalue is constant.

$$J_z \equiv J_z^A + J_z^B = (a_1^1 \bar{a}_1^1 - a_2^1 \bar{a}_2^1 + a_1^2 \bar{a}_1^2 - a_2^2 \bar{a}_2^2) / 2 = (n_\uparrow - n_\downarrow) / 2 \quad (24.3.16a)$$

Second, the number n^A of “*A-ons*” minus the number n^B of “*B-ons*” is the same for $\left| \begin{matrix} j_1 \ j_2 \\ m_1 \ m_2 \end{matrix} \right\rangle$ and $\left| \begin{matrix} j \ N \\ m \ n \end{matrix} \right\rangle$.

$$j_1 - j_2 = n = (n^A - n^B) / 2. \quad (24.3.17b)$$

The total “body- \bar{z} ”-component n or $J_{\bar{z}}$ -value is constant. (This is called *isospin* or *quasi-spin*.)

$$J_{\bar{z}} = (a_1^1 \bar{a}_1^1 + a_2^1 \bar{a}_2^1 - a_1^2 \bar{a}_1^2 - a_2^2 \bar{a}_2^2) / 2 = (n^A - n^B) / 2 \quad (24.3.17a)$$

Finally, the total number N of “*A-ons*” and “*B-ons*” is the same for the states $\left| \begin{matrix} j_1 \ j_2 \\ m_1 \ m_2 \end{matrix} \right\rangle$ and $\left| \begin{matrix} j \ N \\ m \ n \end{matrix} \right\rangle$.

$$N = 2(j_1 + j_2) = a_1^1 \bar{a}_1^1 + a_2^1 \bar{a}_2^1 + a_1^2 \bar{a}_1^2 + a_2^2 \bar{a}_2^2 = n_\uparrow^A + n_\downarrow^A + n_\uparrow^B + n_\downarrow^B = n^A + n^B = n_\uparrow + n_\downarrow \quad (24.3.18)$$

The grand total N counts each kind (A or B) of boson or each state (\uparrow or \downarrow) in which it may reside.

c. N-Boson coupled momentum states

To get a general N -boson j -coupled state $\left| \begin{matrix} j \ N \\ m \ n \end{matrix} \right\rangle$ an even number $(N - 2j)$ of bosons, in scalar determinant (no-count) combination (24.3.15), is added to an all-count state $\left| \begin{matrix} j \\ m \ n \end{matrix} \right\rangle = \left| \begin{matrix} j \ N-2j \\ m \ n \end{matrix} \right\rangle$ in (24.3.11)..

$$\left| \begin{matrix} j \ N \\ m \ n \end{matrix} \right\rangle = \sqrt{\frac{(2j+1)!(j+m)!(j-m)!}{(N/2-j)!(N/2+j+1)!}} \sum_k \left[\frac{(j+n)!}{(n_1^1)!(n_2^1)!} \frac{(j-n)!}{(n_1^2)!(n_2^2)!} \right] (a_1^1 a_2^2 - a_1^2 a_2^1)^{N/2-j} |n_1^1 n_2^1, n_1^2 n_2^2\rangle \quad (24.3.19a)$$

Here the occupation numbers n_j^u from (24.3.11b) are used. The normalization factors for this state are not so easy to prove. Expansion of the determinantal expression gives the following.

$$(a_1^1 a_2^2 - a_2^1 a_1^1)^{N/2-j} = \sum_r (-1)^r \frac{(N/2-j)!}{r! [N/2-j-r]!} (a_1^1 a_2^2)^{N/2-r} (a_2^1 a_1^1)^r. \quad (24.3.19b)$$

The no-count pairs (24.3.19b) are merged to make a coupled state.

$$\left| \begin{matrix} j & N \\ m, n \end{matrix} \right\rangle = \sqrt{\frac{(2j+1)!(j+m)!(j-m)!}{(N/2-j)!(N/2+j+1)!}} \sum_r (-1)^r \frac{\sqrt{(j+n)!(j-n)!(m_1^1)!(m_2^1)!(m_1^2)!(m_2^2)!}}{r!(N/2-j-r)!(n_1^1)!(n_2^1)!(n_1^2)!(n_2^2)!} \left(\frac{N}{2}-j\right)! |m_1^1 m_2^1, m_1^2 m_2^2\rangle \quad (24.3.19c)$$

Modified occupation numbers are found using quantum conservation relations (24.3.16) to (24.3.18).

$$\begin{aligned} m_1^1 &= n_1^1 + \frac{N}{2} - j - r &= j_1 + j_2 + m - k - r & (= j_1 + m_1) \\ m_2^1 &= n_2^1 + r &= j_1 - j_2 - m + k + r & (= j_1 - m_1) \\ m_1^2 &= n_1^2 + r &= k + r & (= j_2 + m_2) \\ m_2^2 &= n_2^2 + \frac{N}{2} - j - r &= 2j_2 - r - k & (= j_2 - m_2) \end{aligned} \quad (24.3.19d)$$

The equalities written in parentheses on the right must hold when this state is matched with (24.3.1) to derive the coupling coefficient. The r sum is eliminated then, since

$$r = j_2 - k + m - m_1 = j_2 + m_2 - k. \quad (24.3.19e)$$

The resulting coupling coefficient formula then has the conservation relations built into it.

$$\begin{aligned} C_{m_1 m_2 m_3}^{j_1 j_2 j_3} &= \left\langle \begin{matrix} j_1 & j_2 \\ m_1 & m_2 \end{matrix} \middle| \begin{matrix} j & N \\ m_3 n \end{matrix} \right\rangle \quad \text{with: } N = 2(j_1 + j_2), \quad \text{and: } n = j_1 - j_2, \\ &= (-1)^{j_2+m_2} \sqrt{\frac{(2j_3+1)(j_1+j_2-j_3)!(j_3+j_1-j_2)!(j_2+j_3-j_1)!}{(j_1+j_2+j_3+1)!}} \\ &\cdot \sum_k \frac{(-1)^k \cdot \sqrt{(j_1+m_1)!(j_1-m_1)!(j_2+m_2)!(j_2-m_2)!(j_3+m_3)!(j_3-m_3)!}}{(j_2+m_2-k)!(j_1-j_3-m_2+k)!(j_3+m_3-k)!(j_1-j_2-m_3+k)!k!(j_3-j_1+j_2-k)!} \end{aligned} \quad (24.3.20a)$$

The standard formula for the Wigner 3-j coefficient follows from (24.2.30) and is given below.

$$\begin{pmatrix} j_1 & j_2 & j_3 \\ m_1 & m_2 & m_3 \end{pmatrix} = (-1)^{j_1-j_2-m_3} C_{m_1 m_2 m_3}^{j_1 j_2 j_3} / (2j_3+1)^{\frac{1}{2}} \quad (24.3.20b)$$

The (j_1, j_2, j_3) -numbering has been reshuffled in the following to give a more standard formula.

$$\begin{aligned} \begin{pmatrix} j_1 & j_2 & j_3 \\ m_1 & m_2 & m_3 \end{pmatrix} &= (-1)^{j_1-j_2-n_3} \sqrt{\frac{(j_1+j_2-j_3)!(j_1-j_2+j_3)(-j_1+j_2+j_3)}{(j_1+j_2+j_3+1)!}} \\ &\sum_k \frac{(-1)^k}{k!} \frac{\sqrt{(j_1+m_1)!(j_1-m_1)!(j_2+m_2)!(j_2-m_2)!(j_3+m_3)!(j_3-m_3)!}}{(j_1-m_1-k)!(j_2-m_2-k)!(j_1+j_2-j_3-k)!(j_3-j_2-m_1+k)!(j_3-j_1-m_2+k)!} \end{aligned} \quad (24.3.20c)$$

Young tableau notation for N-spin-1/2

Building an N -spin-1/2 boson state is a complicated undertaking, but one of great utility in both quantum electronics and quantum optics as well as in atomic and molecular physics. It is directly applicable to N -photon

states since photons *are* Bose’s original bosons for the electromagnetic oscillators given in Chapter 22 or for the general 2D-quantum oscillator introduced in Chapter 21.

To help visualize an N -spin- $1/2$ state let us revisit the Young-tableau notation for symmetric oscillator states given at the end of Chapter 21. There in Fig. 21.3.2, symmetric N -boson oscillator states are indicated by horizontal rows of N -boxes with one box for each boson. Fig. 24.3.1 is similar but also has *vertical columns* of just two boxes denoting *anti*-symmetric singlet states made by determinant (24.3.13). Each N -box tableau for a spin- $(j=S)$ state has $(N-2j)$ column-boxes and an “overhang” of $(2j=2S)$ -horizontal boxes. Overhang-plus-one is *spin multiplicity* $(2S+1)$, the number of ways \uparrow and \downarrow can go in that tableau.

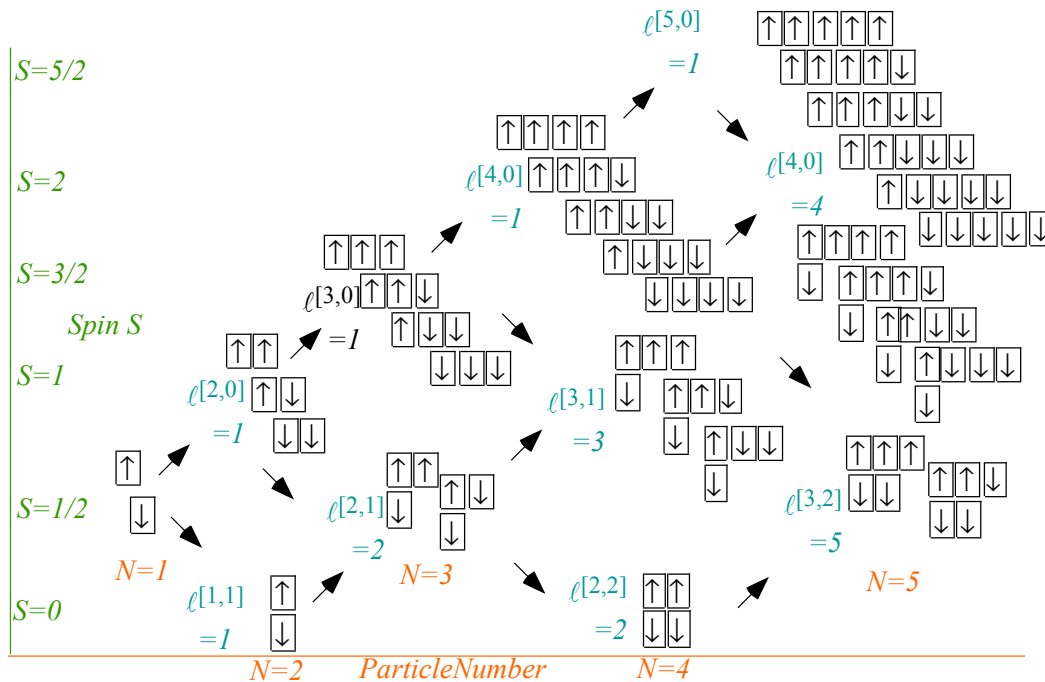


Fig. 24.3.1 N -Particle Spin- $1/2$ State Labeling by Young Tableaus.

Another kind of multiplicity is an *arrangement-multiplicity* or *permutation-degeneracy* $\ell^{[\mu]}$ discussed now.

The simplest tableau with 2-fold permutation multiplicity is a 3-particle case $\ell^{[2,1]} = 2$. It also happens to have a 2-fold spin-multiplicity $\ell^{[S]} = 2S+1=2$. But, do not confuse spin multiplicity $\ell^{[S]}$ with permutation multiplicity $\ell^{[\mu]}$. The spin multiplicity $\ell^{[S]}=2S+1$ is the number of spin states for a given S -tableau. Permutation multiplicity is the number $\ell^{[\mu_1, \mu_2]}$ of ways to make an S -multiplet from a product of N -spin- $1/2$. For example, the number of 5-particle $S=1/2$ doublets is $\ell^{[3,2]} = 5$ in Fig. 24.3.1. Another example is a 3-particle product $(1/2)^3$ that has two ($\ell^{[2,1]} = 2$) ways to make $S=1/2$ or tableau $[2,1]$.

$$\frac{1}{2} \otimes \frac{1}{2} \otimes \frac{1}{2} = (0 \oplus 1) \otimes \frac{1}{2} = \left(0 \otimes \frac{1}{2}\right) \oplus \left(1 \otimes \frac{1}{2}\right) = \frac{1}{2} \oplus \frac{1}{2} \oplus \frac{3}{2} = 2 \left(\frac{1}{2}\right) \oplus 1 \left(\frac{3}{2}\right) \quad (24.3.21)$$

But, a tableau $[3,0]$ or $S=3/2$ quartet appears in $(1/2)^3$ just once ($\ell^{[3,0]} = 1$). In all, $(1/2)^3$ has $2^3=8$ states.

To each column of (N) -particle tableaux in Fig. 24.3.1, one adds a single box in one of two ways to make an $(N+1)$ -particle tableau in the next column. One may add a box to the *first row* and *raise* total spin from S to $S + 1/2$, or one may add a box to the *second row* and *lower* total spin from S to $S - 1/2$. For example, an $(N=8)$ -box tableau of spin $(S=2)$ is the following combination of four $(N-1=7)$ -box tableaux.

$$\begin{aligned}
 & \left| \begin{array}{cccccc} \uparrow & \uparrow & \uparrow & \uparrow & \uparrow & \downarrow \\ \downarrow & \downarrow & & & & \end{array} \right. \left. \begin{array}{l} S = 2 \\ M_S = 1 \end{array} \right\rangle = \tag{24.3.22} \\
 & = C_{1/2 \ 1/2 \ 1/2 \ 1}^{5/2 \ 1/2 \ 2} \left| \begin{array}{cccccc} \uparrow & \uparrow & \uparrow & \uparrow & \downarrow & \downarrow \\ \downarrow & \dots & & & & \end{array} \right. \left. \begin{array}{l} 5/2 \\ 1/2 \end{array} \right\rangle \left| \begin{array}{l} \uparrow \\ 1/2 \end{array} \right\rangle + C_{3/2 \ -1/2 \ 1}^{5/2 \ 1/2 \ 2} \left| \begin{array}{cccccc} \uparrow & \uparrow & \uparrow & \uparrow & \uparrow & \downarrow \\ \downarrow & \dots & & & & \end{array} \right. \left. \begin{array}{l} 5/2 \\ 1/2 \end{array} \right\rangle \left| \begin{array}{l} \downarrow \\ -1/2 \end{array} \right\rangle \\
 & + C_{1/2 \ 1/2 \ 1}^{3/2 \ 1/2 \ 2} \left| \begin{array}{cccccc} \uparrow & \uparrow & \uparrow & \uparrow & \downarrow & \dots \\ \downarrow & \downarrow & & & & \end{array} \right. \left. \begin{array}{l} 3/2 \\ 1/2 \end{array} \right\rangle \left| \begin{array}{l} \uparrow \\ 1/2 \end{array} \right\rangle + C_{3/2 \ -1/2 \ 1}^{3/2 \ 1/2 \ 2} \left| \begin{array}{cccccc} \uparrow & \uparrow & \uparrow & \uparrow & \uparrow & \dots \\ \downarrow & \downarrow & & & & \end{array} \right. \left. \begin{array}{l} 3/2 \\ 1/2 \end{array} \right\rangle \left| \begin{array}{l} \downarrow \\ -1/2 \end{array} \right\rangle
 \end{aligned}$$

The first two have spin $(S=5/2)$ and add a box to their second row to *lower* total spin from $5/2$ to 2 . The next two have spin $(S=3/2)$ and add a box to their first row to *raise* total spin from $3/2$ to 2 . The CGC that are needed at each stage of “1-box-addition” have the following four general formulae and values for $j=3/2$.

$$\left(\begin{array}{cc} C_{m \ 1/2 \ m+1/2}^{j \ 1/2 \ j+1/2} = \sqrt{\frac{j+m+1}{2j+1}} & C_{m+1 \ -1/2 \ m+1/2}^j = \sqrt{\frac{j-m}{2j+1}} \\ C_m^{j+1 \ 1/2 \ j+1/2} = -\sqrt{\frac{j-m+1}{2j+3}} & C_{m+1}^{j+1 \ 1/2 \ j+1/2} = \sqrt{\frac{j+m+2}{2j+3}} \end{array} \right) \text{ example: } \left(\begin{array}{cc} C_{1/2 \ 1/2 \ 1}^{3/2 \ 1/2 \ 2} = \sqrt{\frac{2}{3}} & C_{1/2 \ 1/2 \ 1}^{3/2 \ 1/2 \ 2} = \sqrt{\frac{1}{3}} \\ C_{1/2 \ 1/2 \ 1}^{5/2 \ 1/2 \ 2} = -\sqrt{\frac{1}{3}} & C_{1/2 \ 1/2 \ 1}^{5/2 \ 1/2 \ 2} = \sqrt{\frac{2}{3}} \end{array} \right) \tag{24.3.23}$$

A box-addition diagram of $\ell^{[\mu]}$ in Fig. 24.3.2(a) reminds one of the Pascal’s triangles in Fig. 21.3.2(a). Each $\ell^{[\mu]}$ entry in the N^{th} column ($N > 1$) is a sum of one or two numbers located diagonally to its left in the preceding $(N-1)^{\text{th}}$ column. Fig. 24.3.2(b) shows spin degeneracy ($\ell^{[S]} = 2S+1$) for each entry. Fig. 24.3.2(c) shows both $\ell^{[S]}$ and permutation $\ell^{[\mu]}$ -multiplicity. The N^{th} -column sum of their products $\ell^{[S]}\ell^{[\mu]}$ is 2^N .

$$2^N = \sum_S^{N/2} \ell^{[S]} \ell^{[\mu_1, \mu_2]} = \sum_S^{N/2} (2S+1) \ell^{\left[\frac{N+2S}{2}, \frac{N-2S}{2} \right]} \tag{24.3.24}$$

Clebsch-Gordan coefficients (CGC) of $U(2)$ give N -particle states with total spin S . Fig. 24.1.1 shows the simplest 2-particle ($N=2$) case involving spin- $1/2$ -particle states. The CGC give a singlet ($S=0$) and a triplet ($S=1$) listed in the $(N=2)$ -column of Fig. 24.3.2 and makes the singlet anti-symmetric ($\left[\begin{array}{c} \uparrow \\ \downarrow \end{array} \right]$) and triplets ($\left[\begin{array}{c} \uparrow\uparrow \\ \uparrow\downarrow \\ \downarrow\downarrow \end{array} \right]$) symmetric. But for $N > 2$, CGC schemes like (24.3.23) give ill-defined permutation symmetry. Section 25.3 shows a more natural and elegant way to couple three or more particles.

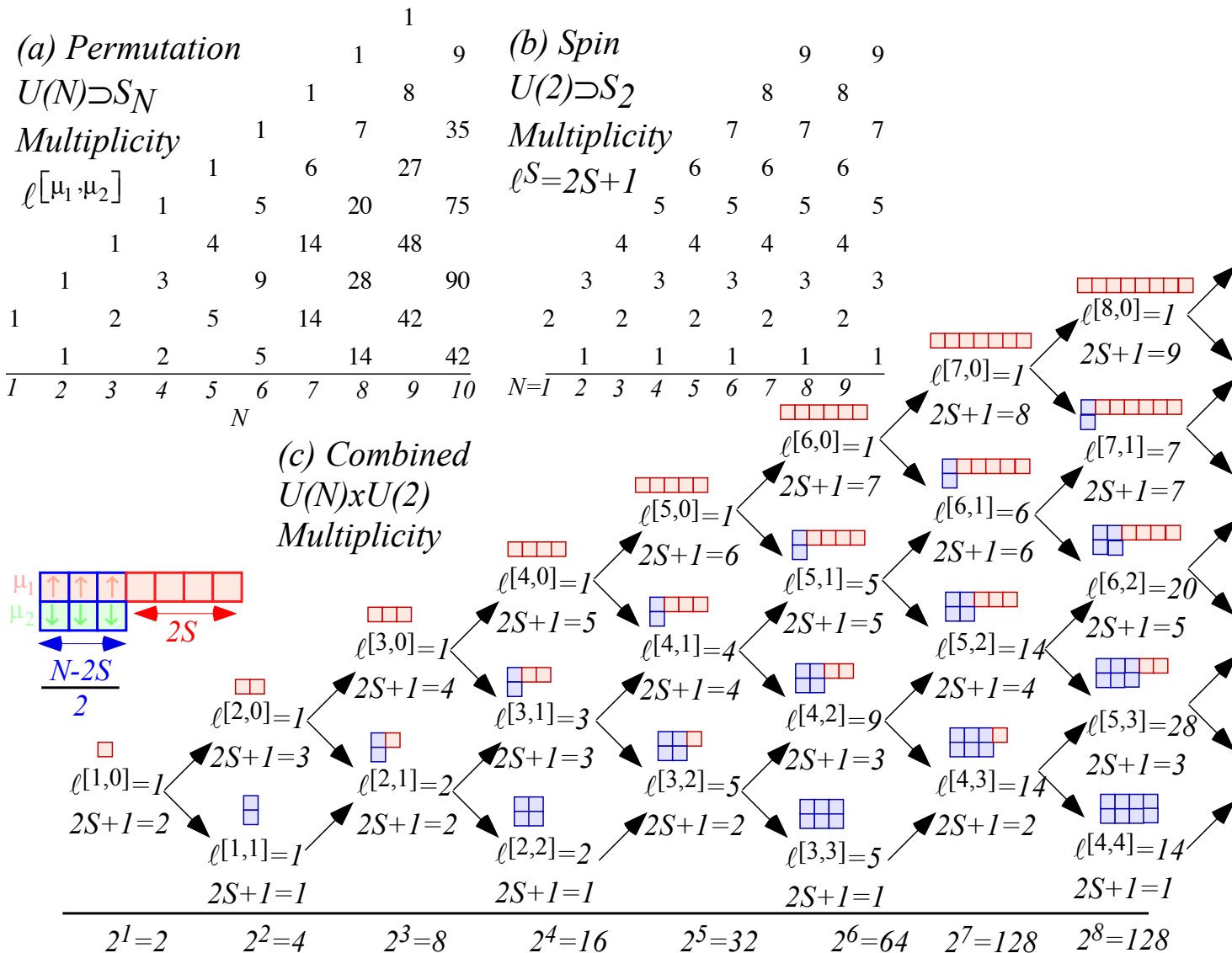


Fig. 23.3.2 Spin-1/2 and U(2) Tableau branching diagrams

Appendix 24A Classical theory for spin-interactions and fine structure

Classical models for spin and orbit interactions in fields and their resulting spectral fine structure is based upon the $\mathbf{A} \cdot \mathbf{p}$ interaction of the pondermotive–electromagnetic Hamiltonian (17.1.10) and is given as follows in the first chapter 17 of Unit 6 for a mass m charge e in a vector potential field \mathbf{A} .

$$H = \frac{1}{2m}(\mathbf{p} - e\mathbf{A}) \cdot (\mathbf{p} - e\mathbf{A}) + eV(\mathbf{r}) = \frac{p^2}{2m} - \frac{e}{m} \mathbf{A} \cdot \mathbf{p} + \frac{e^2}{2m} \mathbf{A} \cdot \mathbf{A} + eV(\mathbf{r}) \quad (24A.1a)$$

Electron momentum \mathbf{p} , charge $e = -|e| = 1.60218 \cdot 10^{-19} \text{C}$, and mass $m = 9.10939 \cdot 10^{-31} \text{kg}$ (or *reduced mass* $m_{eM} = mM / (M + m) = 9.10443 \cdot 10^{-31}$) appear in the electron-nucleon-field interaction term that is used.

$$H_{eM} = -\frac{e}{m_{eM}} \mathbf{A} \cdot \mathbf{p} \quad (24A.1b)$$

Nuclear vector potential \mathbf{A} and mass $M = 1.67262 \cdot 10^{-27} \text{kg}$ of a single proton are assumed above. Here we assume the non-relativistic “Coulomb gauge” requirement ($\nabla \cdot \mathbf{A} = 0$) so that $(\mathbf{p} \cdot \mathbf{A})\psi = (\mathbf{A} \cdot \mathbf{p})\psi$.

The vector potential is expressed using a multipole expansion as developed in Chapter 23.

$$\frac{1}{|\mathbf{r} - \mathbf{r}'|} = \sum_k \sum_{m=-k}^k \frac{4\pi}{2k+1} \frac{r'^k}{r^{k+1}} Y_m^k(\theta\varphi) Y_m^{k*}(\theta'\varphi') = \frac{1}{|\mathbf{r}|} - \frac{\mathbf{r} \cdot \mathbf{r}'}{|\mathbf{r}|^3} + \dots$$

The first two far-field ($r \gg r'$) multipole expansion terms of internal nuclear currents near origin are here.

$$\begin{aligned} \mathbf{A}(\mathbf{r}) &= \frac{\mu_0}{4\pi} \iiint d^3r' \frac{\mathbf{j}(\mathbf{r}')}{|\mathbf{r} - \mathbf{r}'|} = \frac{\mu_0}{4\pi|\mathbf{r}|} \iiint d^3r' \mathbf{j}(\mathbf{r}') + \frac{\mu_0}{4\pi|\mathbf{r}|^3} \iiint d^3r' (\mathbf{r} \cdot \mathbf{r}') \mathbf{j}(\mathbf{r}') \\ &= 0 + \frac{\mu_0}{4\pi|\mathbf{r}|^3} \iiint d^3r' \frac{\mathbf{r}' \times \mathbf{j}(\mathbf{r}')}{2} \times \mathbf{r} \end{aligned} \quad (24A.3)$$

Only the second *magnetic dipole* term survives if nuclear currents are assumed localized with no net flow. (For now we ignore the quadrupole and higher order moments.) Moreover, the dipole integrand separates into symmetric (S) and anti-symmetric (A) parts. Only the latter survive for zero net flow. ($\nabla \cdot \mathbf{j} = 0$)

$$(\mathbf{r} \cdot \mathbf{r}') \mathbf{j}_b = (r_a r'_a) j_b = \frac{1}{2} r_a (r'_a j_b + r'_b j_a) + \frac{1}{2} r_a (r'_a j_b - r'_b j_a) = \frac{1}{2} r_a (S_{ab} + A_{ab}) \quad (24A.4)$$

Levi-Civita cross-product analysis and identity $\varepsilon_{abc} \varepsilon_{efc} = \delta_{ae} \delta_{bf} - \delta_{be} \delta_{af}$ gives a triple-cross identity.

$$\begin{aligned} |(\mathbf{r}' \times \mathbf{j}) \times \mathbf{r}|_b &= \varepsilon_{bca} (\mathbf{r}' \times \mathbf{j})_c r_a = \varepsilon_{abc} (\varepsilon_{cef} r'_e j_f) r_a = (\varepsilon_{abc} \varepsilon_{efc} = \delta_{ae} \delta_{bf} - \delta_{be} \delta_{af}) r'_e j_f r_a \\ &= r'_a j_b r_a - r'_b j_a r_a = (r_a (r'_a j_b - r'_b j_a)) = |(\mathbf{r} \cdot \mathbf{r}') \mathbf{j} - (\mathbf{r} \cdot \mathbf{j}) \mathbf{r}'|_b \end{aligned}$$

The volume integral of term $S_{ab} = r'_a j_b(\mathbf{r}') + r'_b j_a(\mathbf{r}')$ is zero if $\nabla \cdot \mathbf{j} = 0$ since S is a divergence $\nabla \cdot (r'_a r'_b \mathbf{j}(\mathbf{r}'))$.

$$\nabla \cdot (r'_a r'_b \mathbf{j}(\mathbf{r}')) = \frac{\partial}{\partial r'_c} (r'_a r'_b j_c) = r'_b j_a + r'_a j_b + r'_a r'_b \frac{\partial j_c}{\partial r'_c} = r'_b j_a + r'_a j_b$$

Then the divergence theorem reduces the volume integral to one over a large surface that has no current.

$$\iiint d^3r' (r'_b j_a + r'_a j_b) = \iiint d^3r' \nabla \cdot (r'_a r'_b \mathbf{j}(\mathbf{r}')) = \oint dS (r'_a r'_b \mathbf{j}(\mathbf{r}')) \rightarrow 0$$

Continuity equation $\nabla \cdot \mathbf{j} = -\frac{\partial \rho}{\partial t}$ precludes time-dependent charge if $\nabla \cdot \mathbf{j} = 0$, which like $\nabla \cdot \mathbf{A} = 0$ is strictly a *non-relativistic* approximation. This gives then the static *magnetic dipole* vector potential.

$$\mathbf{A}(\mathbf{r}) = \frac{\mu_0}{4\pi|\mathbf{r}|^3} \mathbf{M} \times \mathbf{r} = \frac{\mu_0}{4\pi} \mathbf{M} \times \nabla \left(\frac{1}{r} \right) \quad \text{where:} \quad \mathbf{M} = \iiint d^3r' \frac{\mathbf{r}' \times \mathbf{j}(\mathbf{r}')}{2} \quad (24A.5a)$$

The nuclear *magnetic moment* \mathbf{M} is defined above. The magnetic field due to such a moment is

$$\mathbf{B}(\mathbf{r}) = \nabla \times \mathbf{A}(\mathbf{r}) = \frac{\mu_0}{4\pi} \nabla \times \left(\frac{\mathbf{M} \times \mathbf{r}}{|\mathbf{r}|^3} \right) = \frac{\mu_0}{4\pi} \nabla \times \left(\mathbf{M} \times \nabla \left(\frac{1}{r} \right) \right) \quad (24A.5b)$$

Electronic-nuclear-orbit-spin interaction

The Hamiltonian for nuclear moment \mathbf{M} coupled to electronic orbital momentum $\mathbf{L} = \mathbf{r} \times \mathbf{p}$ is here.

$$\begin{aligned} H_{eM} &= -\frac{e}{m} \mathbf{A} \cdot \mathbf{p} = -\frac{e}{m} \frac{\mu_0}{4\pi|\mathbf{r}|^3} \mathbf{M} \times \mathbf{r} \cdot \mathbf{p} = -\frac{e}{m} \frac{\mu_0}{4\pi|\mathbf{r}|^3} \mathbf{M} \cdot \mathbf{r} \times \mathbf{p} \\ &= -\frac{e}{m} \frac{\mu_0}{4\pi} \frac{\mathbf{M} \cdot \mathbf{L}}{|\mathbf{r}|^3} = -\mathbf{M} \cdot \mathbf{B} \quad \text{where:} \quad \mathbf{B}(\text{at } M \text{ due to } e) = \frac{\mu_0}{4\pi} \frac{e}{m} \frac{\mathbf{L}}{|\mathbf{r}|^3} \end{aligned} \quad (24A.6a)$$

The B-field at the nucleus due to electronic charge $e = -|e|$ Bohr-orbiting with $L = \ell\hbar = mvr$ is

$$\begin{aligned} B(\text{at } r=0) &= \frac{\mu_0}{4\pi} \frac{e}{m} \frac{mvr}{r^3} = -\frac{\mu_0}{4\pi} \frac{|e|v}{r^2} \\ &= \frac{\mu_0}{4\pi} \frac{e\hbar}{m} \frac{\ell}{r^3} = -\frac{\mu_0}{4\pi} \frac{|j|}{r^2} \end{aligned} \quad (24A.6b)$$

This relates a classical loop current $j = ev$ to the orbital quantum number $\ell = 0, 1, 2, \dots$

$$j \cdot r = \frac{e\hbar}{m} \ell = g \cdot \mu_e \cdot \ell, \quad \text{where:} \quad \mu_e = \frac{e\hbar}{2m} \quad (\text{Bohr magneton}) \quad \text{and:} \quad g = 2 \quad (24A.6c)$$

The *Bohr magneton* $\mu_e = 9.27401 \cdot 10^{-24} (J \cdot T^{-1} \text{ or } A \cdot m)$ was first given after (24.1.18). For $\ell = 1$ the magnetic moment is $j \cdot r / 2 = e\hbar / 2m = \mu_e$. For $\ell = 1/2$ we have that $j \cdot r = \mu_e$. But, this is just numerology like earlier numerology (5.6.5) in Chapter 5. Instead, Dirac's spin theory is the current standard we will use.

Electronic-nuclear spin-spin interaction

First approximation Dirac theory of electron spin magnetic moment is $m_e = -2\mu_e$. Using this we derive the energy of the electron spin moment in the B-field (24A.5) of the proton spin moment.

$$H_{e\text{-spin-p-spin}} = -\mathbf{m}_e \cdot \mathbf{B}_p = -\mathbf{m}_e \cdot \nabla \times \mathbf{A}(\mathbf{r}) \quad (24A.7)$$

The proton spin B-field is reduced using the Levi-Civita algebra. $\varepsilon_{bca} \varepsilon_{bdf} = \delta_{cd} \delta_{af} - \delta_{cf} \delta_{ad}$.

$$\frac{4\pi}{\mu_0} \mathbf{B} = \nabla \times \left(\frac{\mathbf{M}_p \times \mathbf{r}}{|\mathbf{r}|^3} \right) = -\nabla \times \left(\mathbf{M}_p \times \nabla r^{-1} \right) \quad (24A.8a)$$

$$\begin{aligned} -\frac{4\pi}{\mu_0} B_c &= \varepsilon_{abc} \partial_a \left(\mathbf{M} \times \nabla r^{-1} \right)_b = \varepsilon_{abc} \partial_a \left(\varepsilon_{bdf} M_d \partial_f r^{-1} \right) \\ &= \varepsilon_{bca} \varepsilon_{bdf} M_d \partial_a \partial_f r^{-1} = \left(\delta_{cd} \delta_{af} - \delta_{cf} \delta_{ad} \right) M_d \partial_a \partial_f r^{-1} = M_c \partial_a \partial_a r^{-1} - M_a \partial_a \partial_c r^{-1} \end{aligned} \quad (24A.8b)$$

Monopole derivatives $\nabla(1/r) = \partial_a r^{-1}$ use ∂_a to denote derivatives $\partial/\partial r_a$ of coordinates $(r_1, r_2, r_3) = (x, y, z)$. Repeated indices are summed as in the Pythagorean radial square $r_b r_b = r_1 r_1 + r_2 r_2 + r_3 r_3 = x^2 + y^2 + z^2 = r^2$.

$$\partial_a r^{-1} = \partial_a (r_b r_b)^{-1/2} = -r_a (r_b r_b)^{-3/2} = -r_a r^{-3} \quad (24A.9a)$$

$$\partial_a \partial_c r^{-1} = -\partial_a r_c (r_b r_b)^{-3/2} - r_c \partial_a (r_b r_b)^{-3/2} = -\delta_{ac} r^{-3} + 3r_a r_c r^{-5} \quad (24A.9b)$$

This translates back to Gibbs-vector notation for dipole-dipole interactions.

$$\begin{aligned} -\frac{4\pi}{\mu_0} \mathbf{m} \cdot \mathbf{B} &= -\frac{4\pi}{\mu_0} m_c B_c \\ &= -m_c M_c \partial_a \partial_a r^{-1} + M_a \partial_a m_c \partial_c r^{-1} = -m_c M_c \partial_a \partial_a r^{-1} + M_a m_c (\delta_{ac} r^{-3} - 3r_a r_c r^{-5}) \\ &= -\mathbf{m} \cdot \mathbf{M} \nabla^2 \left(\frac{1}{r} \right) + (\mathbf{m} \cdot \nabla)(\mathbf{M} \cdot \nabla) \left(\frac{1}{r} \right) = -\mathbf{m} \cdot \mathbf{M} \nabla^2 \left(\frac{1}{r} \right) + \frac{\mathbf{m} \cdot \mathbf{M}}{r^3} - \frac{3(\mathbf{m} \cdot \mathbf{r})(\mathbf{M} \cdot \mathbf{r})}{r^5} \end{aligned}$$

We put in the standard definitions $\mathbf{m}_e = -|g_e \mu_e| \mathbf{J}^e$ and $\mathbf{M}_p = +|g_p \mu_p| \mathbf{J}^p$ for electron and proton moments.

$$H_{e-spin-p-spin} = \frac{\mu_0}{4\pi} \left[-\mathbf{m} \cdot \mathbf{M} \nabla^2 \left(\frac{1}{r} \right) + \frac{\mathbf{m} \cdot \mathbf{M}}{r^3} - \frac{3(\mathbf{m} \cdot \mathbf{r})(\mathbf{M} \cdot \mathbf{r})}{r^5} \right] \quad (24A.10a)$$

$$= \frac{\mu_0 |g_e \mu_e g_p \mu_p|}{4\pi} \left[\mathbf{J}^e \cdot \mathbf{J}^p \nabla^2 \left(\frac{1}{r} \right) - \frac{\mathbf{J}^e \cdot \mathbf{J}^p}{r^3} + \frac{3(\mathbf{J}^e \cdot \mathbf{r})(\mathbf{J}^p \cdot \mathbf{r})}{r^5} \right] \quad (24A.10b)$$

We now see a way to derive from this the Fermi contact interaction $a_{ep} \mathbf{J}^{proton} \cdot \mathbf{J}^{electron}$ stated in (24.1.12). (The first term $\mathbf{J}^e \cdot \mathbf{J}^p \nabla^2(r^{-1}) = 4\pi \delta(\mathbf{0}) \mathbf{J}^e \cdot \mathbf{J}^p$ is wrong since the other terms contribute.)

Gauss hyper-theorem analysis of Fermi-contact term

Freshman electromagnetism students are drilled on the divergence theorem and Gauss law.

$$\iiint d^3 r \rho(\mathbf{r}) / \epsilon_0 = \iiint d^3 r \nabla \cdot \mathbf{E}(\mathbf{r}) = \oiint d\mathbf{S} \cdot \mathbf{E}(\mathbf{r}) = \iint d\Omega R^2 \mathbf{n} \cdot \mathbf{E}(R) \quad (24A.11)$$

Not as well known are two \mathbf{E} and \mathbf{B} -vector integration relations that sum fields as do the following.

$$\iiint d^3 r \mathbf{E}(\mathbf{r}) = -\iiint d^3 r \nabla \varphi(\mathbf{r}) = -\oiint d\mathbf{S} \varphi(\mathbf{r}) = -\iint d\Omega R^2 \mathbf{n} \varphi(\mathbf{r}) \quad (24A.12a)$$

$$\iiint d^3 r \mathbf{B}(\mathbf{r}) = \iiint d^3 r \nabla \times \mathbf{A}(\mathbf{r}) = \oiint d\mathbf{S} \times \mathbf{A}(\mathbf{r}) = \iint d\Omega R^2 \mathbf{n} \times \mathbf{A}(\mathbf{r}) \quad (24A.12b)$$

Volume sums of fields involve some charge $\rho(\mathbf{r})$, current $\mathbf{j}(\mathbf{r})$, and scalar or vector potentials $\varphi(\mathbf{r})$ or $\mathbf{A}(\mathbf{r})$.

$$\varphi(\mathbf{r}) = \frac{1}{4\pi\epsilon_0} \iiint d^3 r' \frac{\rho(\mathbf{r}')}{|\mathbf{r} - \mathbf{r}'|} \quad (24A.13a) \quad \mathbf{A}(\mathbf{r}) = \frac{\mu_0}{4\pi} \iiint d^3 r' \frac{\mathbf{j}(\mathbf{r}')}{|\mathbf{r} - \mathbf{r}'|} \quad (24A.13b)$$

The sum over B-field observer position \mathbf{r} can be reversed with the sum over source position \mathbf{r}' if the R -surface is beyond current carrying points so that $\mathbf{j}(\mathbf{r}') = \mathbf{0}$ where $|\mathbf{r}'| \geq R$ to avoid a $1/|\mathbf{r} - \mathbf{r}'|$ blowup.

$$\iiint d^3r \mathbf{B}(\mathbf{r}) = \iint d\Omega R^2 \mathbf{n} \times \frac{\mu_0}{4\pi} \iiint d^3r' \frac{\mathbf{j}(\mathbf{r}')}{|\mathbf{r}-\mathbf{r}'|} = -\frac{\mu_0}{4\pi} \iiint d^3r' \mathbf{j}(\mathbf{r}') \times \iint d\Omega \frac{\mathbf{n}R^2}{|\mathbf{r}-\mathbf{r}'|}$$

The solid angle integral is easily evaluated using the addition theorem expansion (23.4.9) of $1/|\mathbf{r}-\mathbf{r}'|$.

$$\iint d\Omega \frac{\mathbf{n}R^2}{|\mathbf{r}-\mathbf{r}'|} = \iint d\Omega \mathbf{n} \sum_{\ell=0}^{\infty} \sum_{m=-\ell}^{\ell} \frac{4\pi R^2}{(2\ell+1)} \frac{r'^{\ell}}{R^{\ell+1}} Y_m^{\ell*}(\phi, \theta) Y_m^{\ell}(\phi', \theta')$$

Sum and integral switch and unit normal in vector or dipole coordinates is $\mathbf{n} = \sum \mathbf{n}_n^1 Y_n^1(\phi, \theta)$

$$\begin{aligned} \iint d\Omega \frac{\mathbf{n}R^2}{|\mathbf{r}-\mathbf{r}'|} &= \sum_{\ell=0}^{\infty} \sum_{m=-\ell}^{\ell} \iint d\Omega \sum_{n=-1}^{n=1} \mathbf{n}_n^1 Y_n^1(\phi, \theta) Y_m^{\ell*}(\phi, \theta) Y_m^{\ell}(\phi', \theta') \frac{4\pi R^2}{(2\ell+1)} \frac{r'^{\ell}}{R^{\ell+1}} \\ &= \sum_{\ell=0}^{\infty} \sum_{m=-\ell}^{\ell} \sum_{n=-1}^{n=1} \mathbf{n}_n^1 \iint d\Omega Y_n^1(\phi, \theta) Y_m^{\ell*}(\phi, \theta) Y_m^{\ell}(\phi', \theta') \frac{4\pi R^2}{(2\ell+1)} \frac{r'^{\ell}}{R^{\ell+1}} \\ &= \sum_{\ell=0}^{\infty} \sum_{m=-\ell}^{\ell} \sum_{n=-1}^{n=1} \mathbf{n}_n^1 \delta^{\ell,1} \delta_{m,n} Y_m^{\ell}(\phi', \theta') \frac{4\pi R^2}{(2\ell+1)} \frac{r'^{\ell}}{R^{\ell+1}} \end{aligned}$$

Orthonormality of Y_n^1 and Y_m^{ℓ} reduces the result to the source radius times $4\pi/3$.

$$\iint d\Omega \frac{\mathbf{n}R^2}{|\mathbf{r}-\mathbf{r}'|} = \sum_{m=-1}^1 \mathbf{n}_m^1 Y_m^1(\phi', \theta') \frac{4\pi R^2}{(3)} \frac{r'}{R^2} = \mathbf{n}' r' \frac{4\pi}{3} = \frac{4\pi}{3} \mathbf{r}' \tag{24A.14}$$

Finally, the magnetic field-sum reduces to the source current's total magnetic dipole \mathbf{M} times $8\pi/3$.

$$\iiint d^3r \mathbf{B}(\mathbf{r}) = -\frac{\mu_0}{4\pi} \iiint d^3r' \mathbf{j}(\mathbf{r}') \times \mathbf{r}' \frac{4\pi}{3} = \frac{\mu_0}{4\pi} \iiint d^3r' \frac{\mathbf{r}' \times \mathbf{j}(\mathbf{r}')}{2} \frac{8\pi}{3} = \frac{\mu_0}{4\pi} \mathbf{M} \frac{8\pi}{3} \tag{24A.15a}$$

In contrast an electric field-sum is the electric source charge's total dipole \mathbf{p} times $-4\pi/3$.

$$\iiint d^3r \mathbf{E}(\mathbf{r}) = -\iiint d^3r' \nabla \varphi = \frac{-1}{4\pi\epsilon_0} \iiint d^3r' \rho(\mathbf{r}') \frac{4\pi}{3} = \frac{1}{4\pi\epsilon_0} \mathbf{p} \frac{-4\pi}{3} \tag{24A.15b}$$

Fig. 25A.1 suggests the difference in sign and magnitude is due to different field geometry at the “heart” of each dipole type where the field intensity is greatest. The magnetic B-field flux is continuous through the origin as shown in Fig. 24A.1(b) while the electric dipole has a huge E-field reversal in between the (+) and (-) charges that are the presumed sources for a dipole. Yet, the far-field geometry is the same for each.

An electron at $r=0$, the “heart” of the proton, tends to strongly align its moment \mathbf{m} with the moment \mathbf{M} of the proton. (Like currents *attract*.) An electric dipole at $r=0$ tends to strongly anti-align its moment \mathbf{p} with the \mathbf{P} at the “heart” of its source. (Like charges *repel*.)

Electron spin \mathbf{J}^e is opposite to \mathbf{m} , The electron moment \mathbf{m} tends to align with whatever \mathbf{B} -field it finds as the \mathbf{J}^e does the opposite as shown in Fig. 24A.1(b). At the origin $r=0$ and on z -axis, electron \mathbf{m} and minus- \mathbf{J}^e tend to align with \mathbf{M} and proton spin \mathbf{J}^p . Hence, the coefficient of the Fermi-contact interaction operator $\delta(\mathbf{0})\mathbf{J}^e \cdot \mathbf{J}^p$ should be positive so state $|\uparrow^p\rangle|\downarrow^e\rangle$ is the lowest s -configuration.

But, in the xy -plane normal to z with $r \neq 0$, electron \mathbf{m} and minus- \mathbf{J}^e tend to anti-align with \mathbf{M} and proton spin \mathbf{J}^p . Hence, the coefficient of the dipole-dipole interaction operator $\mathbf{J}^e \cdot \mathbf{J}^p / r^3$ should be negative. At intermediate angles, the other dipole-dipole term $3(\mathbf{J}^e \cdot \mathbf{r})(\mathbf{J}^p \cdot \mathbf{r}) / r^5$ becomes non-zero and, close to the z -axis, it tends to anti-align \mathbf{J}^e to proton \mathbf{J}^p and \mathbf{M} like the Fermi contact term does.

The full electron-nuclear-spin-moment Hamiltonian is now collected in one place.

$$H_{e-p-spin} = \frac{\mu_0 |g_e \mu_e g_p \mu_p|}{4\pi} \left[\frac{8\pi}{3} \delta(\mathbf{0}) \mathbf{J}^e \cdot \mathbf{J}^p + \frac{\mathbf{L}^e \cdot \mathbf{J}^p}{r^3} - \frac{\mathbf{J}^e \cdot \mathbf{J}^p}{r^3} + \frac{3(\mathbf{J}^e \cdot \mathbf{r})(\mathbf{J}^p \cdot \mathbf{r})}{r^5} \right] \quad (25A.16)$$

First is the Fermi-contact term using (24A.15a) and then *e-orbit-p-spin* from (24A.6a). The final terms give the *anisotropic* or *tensor spin-spin interaction* with its quadratic (or quadrupole) $\mathbf{J}^e \cdot \mathbf{r} \mathbf{r} \cdot \mathbf{J}^p$ form.

Electronic-spin -orbit interaction

The interaction of an electron spin with its own electronic orbital momentum $\mathbf{L} = \mathbf{r} \times \mathbf{p}$ is, perhaps, the single interaction most in need of a relativistic theory. Without considering the effects of relativistic velocity and acceleration by rotation, it comes out wrong by a factor of two or worse. Dirac algebra gives directly the following operator for spin-orbit-in-potential- $V(r)$ as will be shown later.

$$H_{e-spin-orbit} = \frac{\partial V}{\partial r} \frac{\mathbf{L}^e \cdot \mathbf{S}^e}{2rm^2c^2} = \frac{e^2Z}{2r^3} \frac{\mathbf{L}^e \cdot \mathbf{S}^e}{4\pi\epsilon_0 m^2 c^2} = \frac{\mu_0}{4\pi} \frac{e^2Z}{2m^2 r^3} \mathbf{L}^e \cdot \mathbf{S}^e \quad \text{for potential: } V(r) = \frac{1}{4\pi\epsilon_0} \frac{Ze^2}{r} \quad (24A.$$

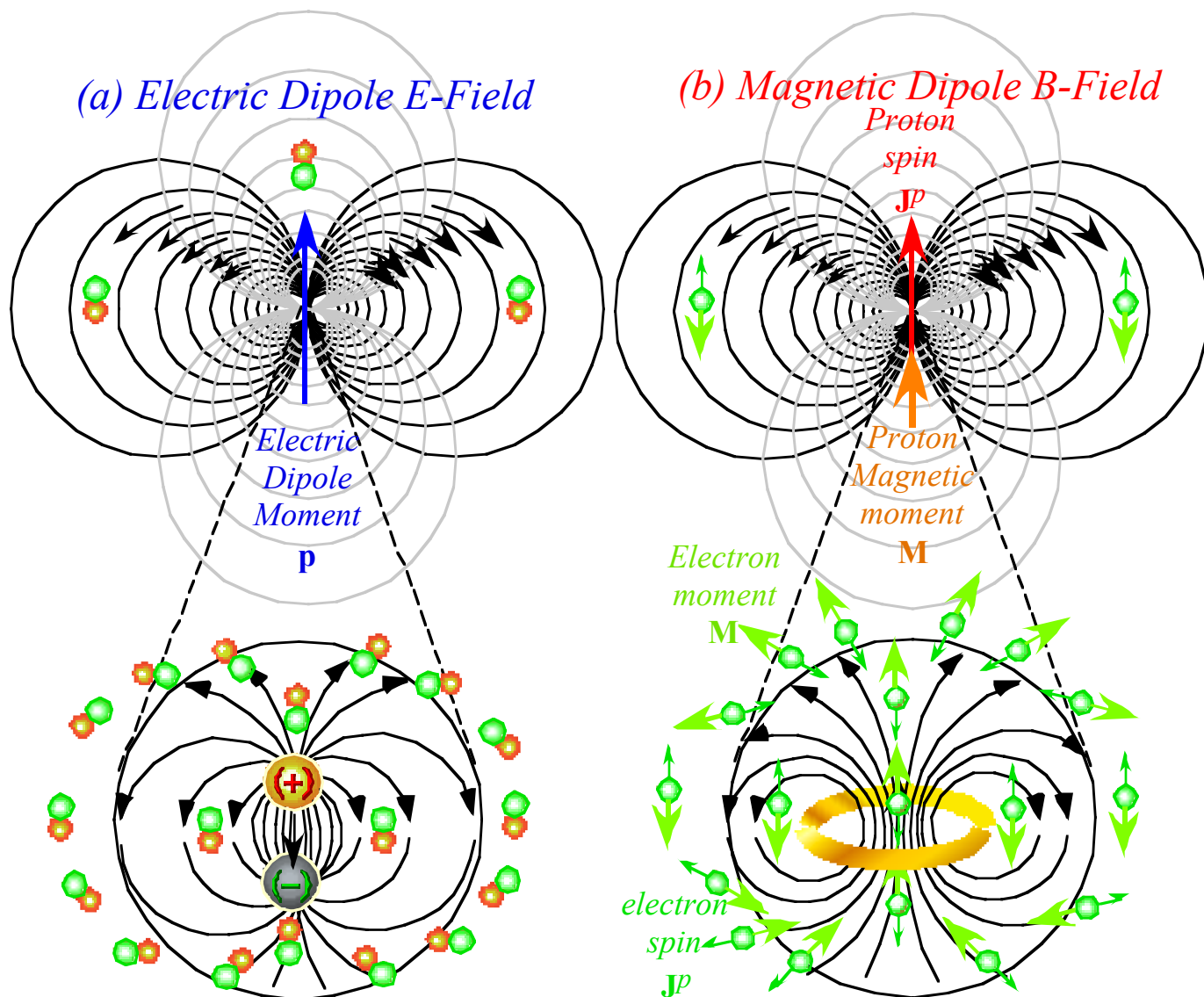


Fig. 25A Comparing near-source fields and interacting dipoles (a) Electric dipole and (b) Magnetic dipole.

